NASA CR-66406

FINAL REPORT
BUOYANT VENUS STATION FEASIBILITY STUDY

Volume III - Instrumentation Study

By A. R. Barger and J. F. Baxter

Prepared under Contract NAS1-6607 by
MARTIN MARIETTA CORPORATION
PO Box 179
Denver, Colorado 80201
for
NATIONAL AERONAUTICS AND SPACE ADMINISTRATION

FOREWORD

This final report on the Buoyant Venus Station Feasibility Study is submitted by the Martin Marietta Corporation, Denver Division, in accordance with Contract NAS1-6607.

The report is submitted in six volumes as follows:

Volume I - Summary and Problem Identification;

Volume II - Mode Mobility Studies;

Volume III - Instrumentation Study;

Volume IV - Communication and Power;

Volume V - Technical Analysis of a 200-lb BVS;

Volume VI - Technical Analysis of a 2000- and 5000-lb BVS.

CONTENTS

TABLES

FIGURES

FINAL REPORT

BUOYANT VENUS STATION FEASIBILITY STUDY

VOLUME III - INSTRUMENTATION STUDY

By A. R. Barger and J. F. Baxter
Martin Marietta Corporation

INSTRUMENTATION STUDIES - TASK 4.2

The contractor shall establish the scientific objectives and investigate various scientific experiments to determine their possible use on the buoyant station. The contractor shall establish a reference coordinate system and investigate the measurements required to determine the station position.

SUMMARY

The present knowledge of Venus is appraised and the general scientific objectives of an early Venus mission are defined. More specific objectives or measurements are given and priorities assigned. Experiments that relate to these objectives and that are compatible with the buoyant Venus station (BVS) concept are examined and arranged into payloads for a 200- and a 2000-lb BVS.

The detailed characteristics of the experiments, several drop sonde configurations, the atmospheric circulation pattern, possible BVS missions and trajectories, and tracking instrumentation are discussed in the Appendixes A thru E.

The engineering instrumentation determination task, which was originally part of this task, is discussed in Volume II of this report.

INTRODUCTION

The three broad, general objectives of all planetary science are: (1) an understanding of the origin and evolution of the solar system, (2) an understanding of the origin and evolution of life, and (3) an understanding of the dynamic processes that shape the planetary environment (ref. 1). Each planet has associated with it a certain body of knowledge, gained over the years from observational and theoretical investigations. For each planet there is also a set of uncertainties and limitations to our knowledge. It is the basic objective of the buoyant Venus station (BVS) to eliminate as many of these uncertainties as possible while attacking problems of greatest relevance to the three objectives stated above.

Although Venus is closer to Earth than Mars, and is more like Earth in mass, size, and density, our present knowledge of Venus lags behind that of Mars. There are several reasons for this. Most of our information on planetary characteristics is derived from remote sensing. Because Venus apparently has a complete and constant cloud cover in its atmosphere, remote sensing of the surface and atmosphere below the cloud is impeded. Thus, we have relatively little information on subcloud conditions. The presence of the cloud cover also makes interpretation of any remote sensing observations extremely difficult. With a lack of good observational data, accurate theoretical deductions are limited. In addition, the apparent differences between Earth and Venus in rotation rate, cloudiness, atmospheric pressures, temperatures, and compositions preclude extending our knowledge by arguments based on analogy.

The major scientific questions and uncertainties associated with Venus revolve around the surface and subsurface, the cloud layer, the atmosphere, and the presence or absence of life on the planet. Microwave observations suggest an extremely hot surface -- 600°K. However, recent suggestions that the microwave emission may be in large part not surface radiation but rather some form of electrical discharges in the atmosphere would indicate a much lower average surface temperature. Thus, at present it appears our knowledge of the average surface temperature of Venus may be uncertain by a factor of two. Our knowledge of the horizontal temperature gradient at the surface -- from subsolar point to antisolar point, or subsolar point to pole -- is even more uncertain. The current estimate of the atmospheric pressure at the surface, about 10 atm, is probably uncertain by a factor of five. The nature of the surface and subsurface is almost completely in the realm of theoretical speculation.

The cloud layer, the only thing on Venus that we see, is not understood at all. Although recent spectroscopic observations indicate an ice crystal composition, not all scientists agree with this interpretation. Thus, the nature of the cloud layer must be considered uncertain. Aside from the uncertainty in the cloud layer's composition, its thickness and height, horizontal extent and temporal variations, and forming and sustaining mechanisms are unknown.

Our present knowledge of the Venusian atmosphere is also meager. Carbon dioxide is definitely present, and there are indications of small amounts of water vapor, HCR, and HF. However, we do not know whether the atmosphere is 5 or 90% carbon dioxide or what the other major constituents are, but we do know that oxygen is not present in any significant amount. With regard to state and structure parameters such as pressure, density, and temperature and their variations with height, location, and time, we have only a few indications based on inferences from remote sensing. Temperatures in the vicinity of the cloud level appear to be about 235°K on both sunlit and dark sides of the planet and the atmospheric pressures in the vicinity of the cloud level appear to be about 1 atm. Our knowledge of the winds and atmospheric circulation pattern is limited to some theoretical estimates based on wind systems on a nonrotating planet. No observations, even remote, of Venusian winds are available.

With regard to the possibility of life on the planet, only indirect observational inferences can be made. If the surface is really hot, chances for life on the surface are remote. But biologists would still cling to the possibility of life floating in the atmosphere, or on mountains or in cold spots on the planet. If the surface temperature is not really so high, the case for life on the planet would be enhanced.

The specific scientific objective of the BVS should be the conduct of experiments aimed at removing the present uncertainties in our knowledge of the surface and subsurface, clouds, atmosphere, and life on Venus, as described above. The BVS concept has the great advantage of allowing (1) direct in situ observations, (2) sampling both vertically and horizontally, and (3) reprograming of the experiment format to permit investigations based on the initial observations. The experiments suggested should be designed to answer as many as possible of the questions raised above and to fully use the inherent vertical and horizontal sampling capabilities of the BVS.

Appendix E of this volume was written by J. D. Pettus, M. L. Salis, and E. P. Friend, Martin Marietta Corporation, Denver Division.

SYMBOLS

a	radius of Venus, km
AU	astronomical unit
B	ballistic coefficient, $slug/ft^2$
B_o	temperature difference between surface and top of atmosphere, °C
BVS	buoyant Venus station
C	coefficient of eddy viscosity
C_D	drag coefficient
c_p	specific heat at constant pressure
D	amplitude of the heating function
g	gravitational acceleration, cm/sec^2
GC	gas chromatograph
IR	infrared
JPL	Jet Propulsion Laboratory
k	coefficient of friction, sec^{-1}
LRC	Langley Research Center
$\bar{M}$	mean molecular weight
MBL	minimum biological laboratory
MS	mass spectrometer
P	pressure, mb
p_o	surface pressure, atm
R	gas constant, erg $°K^{-1}$ mol^{-1}; radius of reference sphere, km

RADVS	radar-altitude-Doppler-velocity system
S	incident solar radiation at subsolar point, $cal/cm^2/min$
T	absolute gas temperature, °K
T_e	infrared brightness temperature, °K
T_2	temperature at middle of atmosphere, °K
V	velocity, m/sec
vlf	very low frequency
w	outgoing longwave radiation, $cal/cm^2/min$
a	difference in rate of temperature change between subsolar and antisolar points,. °K/sec
β	= 1.916
γ	vertical temperature gradient °K/km
$\gamma = c_p/C_V$	specific heat ratio, dimensionless
γ_d	adiabatic temperature gradient, °K/km
Δp	pressure difference between surface and top of troposphere, mb
δ	latitude measured from orbital plane on reference sphere, deg
θ_o	initial latitude of BVS with respect to the subsolar point, deg
A	$= \frac{p_o\ a}{B_o\ c_p}$
μ	$= \frac{\alpha^2\ c^2\ a^2}{RB_\theta}$
ρ	density, gm/cm^3

σ Stefan-Boltzmann constant, erg $/cm^2$ sec $°K^4$

τ temperature difference between subsolar and antisolar points, °C

φ_o initial longitude of BVS with respect to the subsolar point, deg

PRESENT KNOWLEDGE OF VENUS

The first task of the instrumentation study was to appraise present knowledge of Venus and to identify those problems that appear most amenable to solution with the technology at hand or likely to be at hand by the mid-1970s. Although a comprehensive survey and critique of the present knowledge of Venus was beyond the scope of this study, a survey was made of several existing review articles and of earlier studies performed for NASA (ref. 2 thru 19). To paraphrase a recent speaker on the subject, "We know a little more than we did several years ago, much less than we should, and understand much, much less than we know."

Observations and Interpretations

General planetary data. - The relative positions of Earth and Venus as they will be during 1972 are shown in figure 1. Other general characteristics are summarized in table 1. The orbital elements are well known and the rotation rate has recently been determined by radar methods at the JPL Goldstone facility. The rotation rate given by Goldstein is about that required by Venus to present the same face to Earth at each inferior conjunction (243.16 days, sidereal). This appears to be a manifestation of a resonance effect between Earth and Venus.

Venus appears to be completely cloud covered and, hence, the diameter of the solid globe is not known. However, radio interometry techniques indicate that the surface (or the radio emitting layer) lies about 50 to 60 km below the top of the visible cloud layer.

This cloud layer, which is presumably opaque to all but microwave and longer wavelengths, is the main cause of our lack of knowledge of the atmosphere and surface of Venus.

Atmospheric temperature. - The atmospheric temperatures have been inferred from infrared radiometry at 8 to 14 μ and from the vibration-rotation bands of CO_2 in the near infrared (e.g., 7820 to 8600Å). The temperatures given by IR radiometry (~234°K) refer to levels in the vicinity of the cloud tops, while the temperatures given by the CO_2 bands range from 300 to 700°K and presumably refer to different levels in the atmosphere seen through breaks in the clouds. The levels to which the measured temperatures correspond cannot be specified to greater precision than

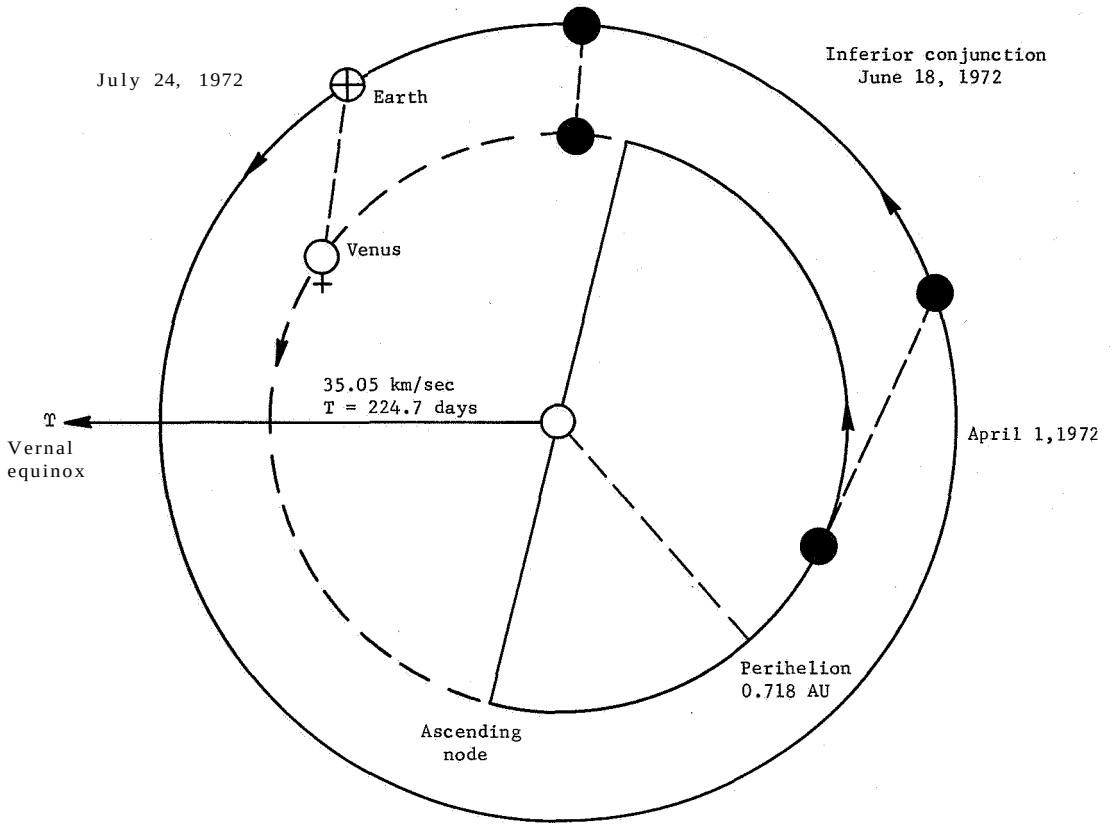

Figure 1. - Relative Positions of Earth and Venus, 1972

Distance from sun Aphelion Perihelion Mean	 108.9×10^6 km, .728 AU 107.5×10^6 km, .718 AU 108.0×10^6 km, .723 AU
Orbital eccentricity	.00679
Orbital inclination	3°24'
Sidereal period of revolution (about sun)	$224^d\ 16^h\ 48^m$ (1.6 deg/day)
Longitude of ascending node	76°.35
Longitude of perihelion	131°.05
Sidereal period of rotation (about polar axis)	-243 days (retrograde) (1.48 deg/day) (a)
Axis orientation	98" ± 5" (right ascension) -69" ± 2° (declination) (a)
Mass	408 300 reciprocal solar mass .81485 Earth mass 4.869×10^{27} g (a)
Visible diameter	12 228 ± 14 km (deVaucouleurs, ref. 20) 12 310 km (Smith, ref. 21) (a)
Radio diameter	12 114 ± 110 km (ref. 22)
Oblateness	None detected
Mean density	About 5 g/cm^3 (a)

"in the vicinity of the cloud tops," "within the cloud layer," or "deep in the atmosphere." As a result, no conclusive temperature profiles can be produced.

The temperature profiles given for the various model atmospheres that have been published are derived by assuming various lapse rates for the temperature gradient between the cloud tops and the surface (whose temperature is derived from microwave radiometric measurements, see below). This gives the cloud top height above the surface. Several of the model atmosphere temperature profiles are shown in figure 2. Note the isothermal cloud layer postulated by Jones (ref. 23) to explain the Mariner II data.

Surface temperatures. - The surface temperatures have been inferred from the microwave radiometric brightness temperature of Venus (see fig. 3) by assuming that all of the emission arises from a hot surface maintained by a greenhouse effect. Sagan (ref. 7) has reviewed the data and gives the surface temperatures in figure 4(a). This raises the question as to what causes the tremendous atmospheric opacity required to maintain such surface temperatures. Several sources (e.g., pressure-broadened CO_2, CO_2 and H_2O, the clouds) have been suggested, but none seem to be completely adequate.

Recently, a number of workers, notably Plummer and Strong refs. 24 thru 26), have ascribed part of the observed microwave emission as being caused by nonthermal sources in the lower atmosphere or clouds. The surface temperatures that result by assuming that 30% of the emission is caused by nonthermal sources (of an unspecified nature) are shown in figure 4(b). Note that this model gives temperatures below freezing (-13°C) at the poles; therefore, temperate zones where life might exist should be found.

At present, neither of the two extreme models can be ruled out. The observations of Clark and Kuz'min (ref. 22), which show that the radio diameter of Venus is fairly compact and is about 100 to 120 km smaller than the visible diameter, and the Mariner II observations of limb darkening definitely rule out a "hot" ionosphere as being the source of high microwave emission, but do not, as has been proposed recently, rule out the lower atmosphere or clouds as a source of nonthermal emission.

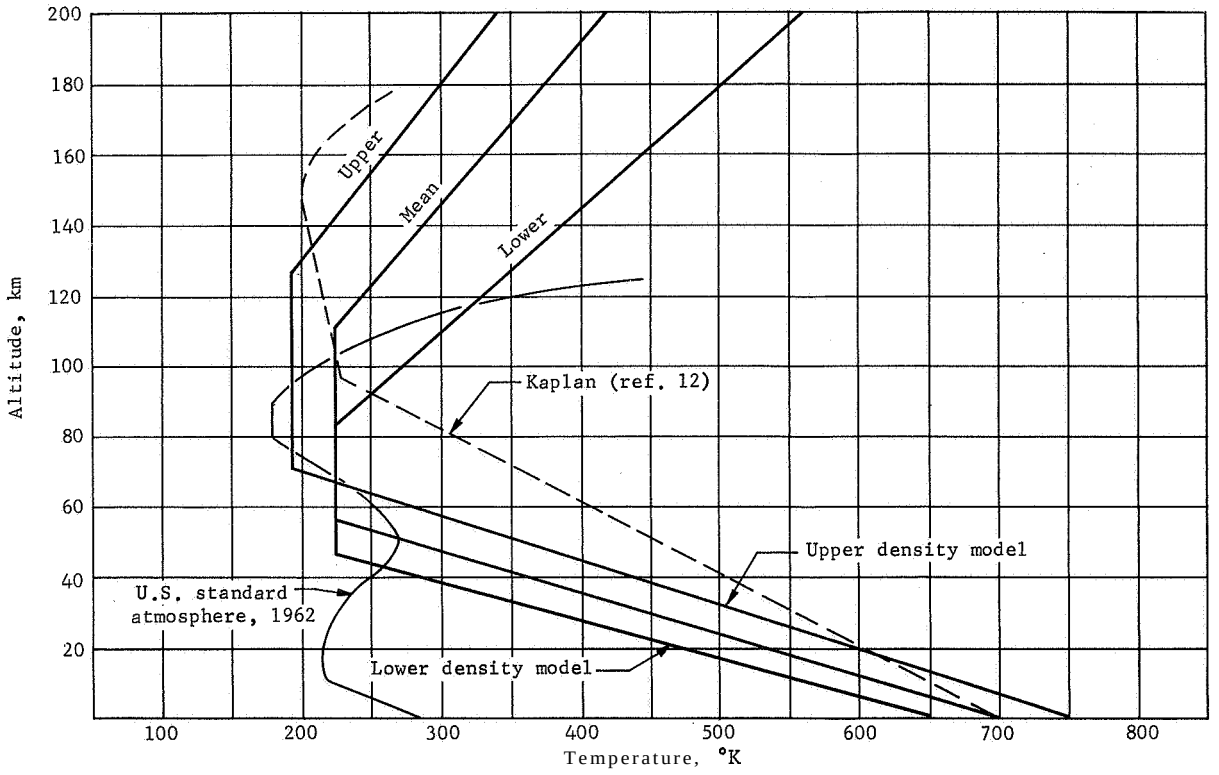

(a) NASA SP-3016 Data

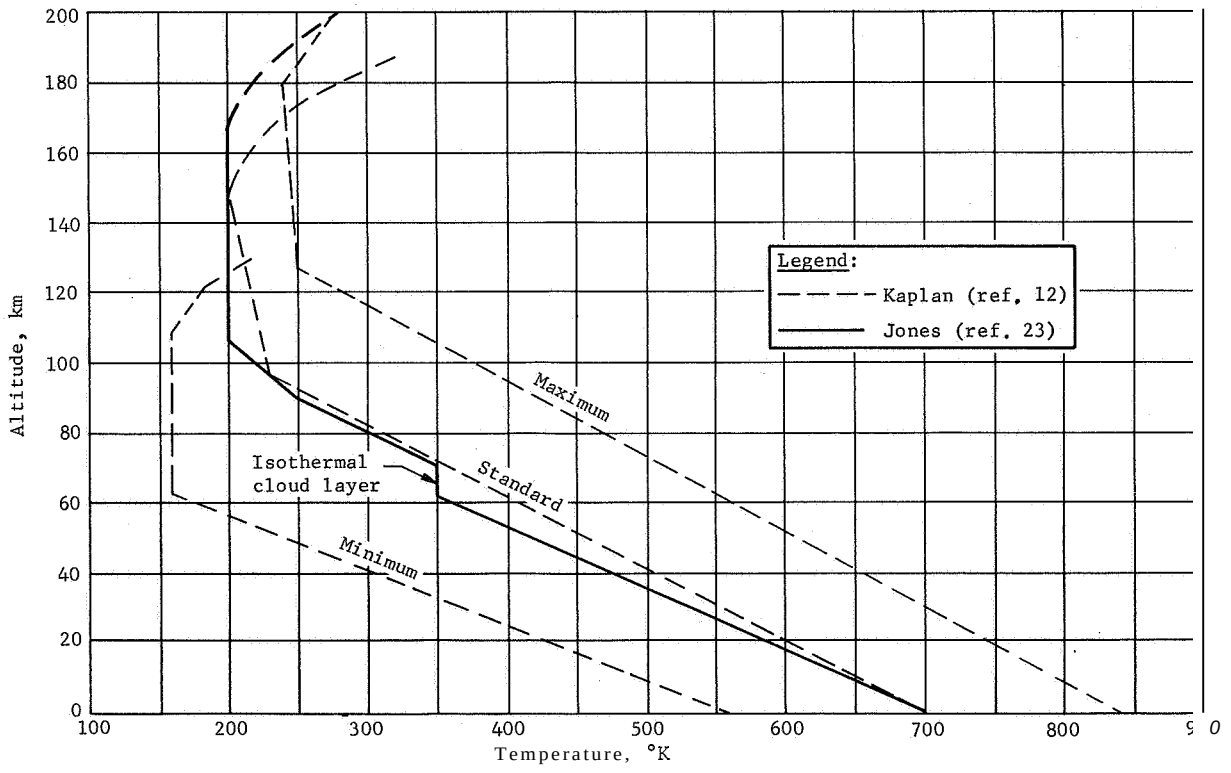

(b) Kaplan and Jones Data

Figure 2. - Venus Temperature Profiles

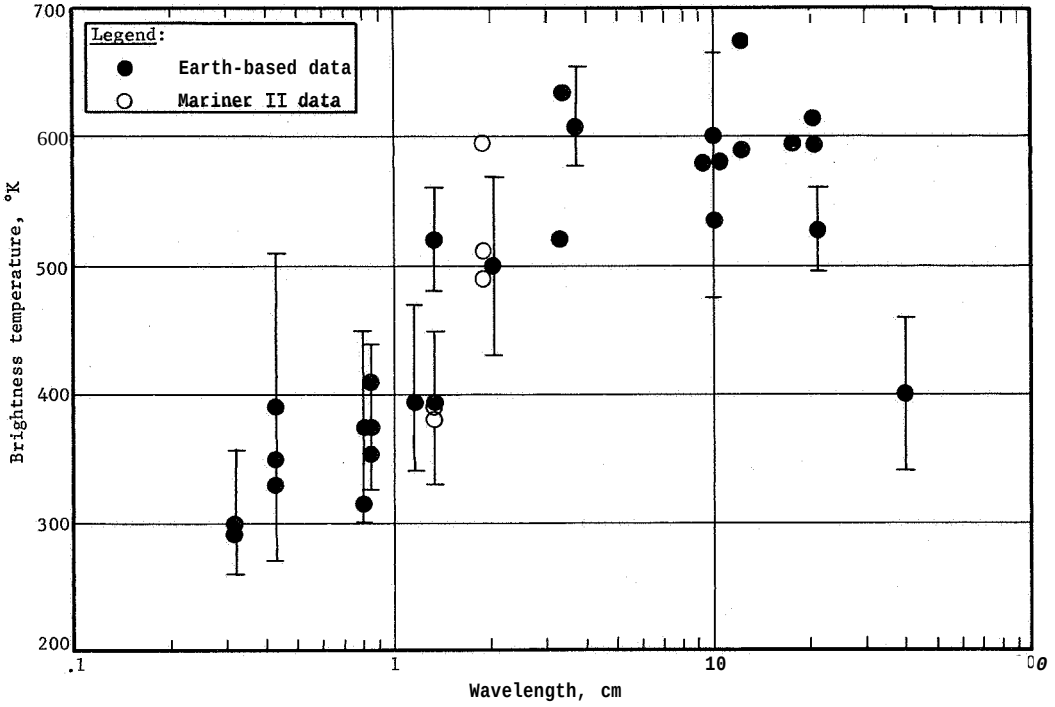

Figure 3. - Microwave Observations of Venus

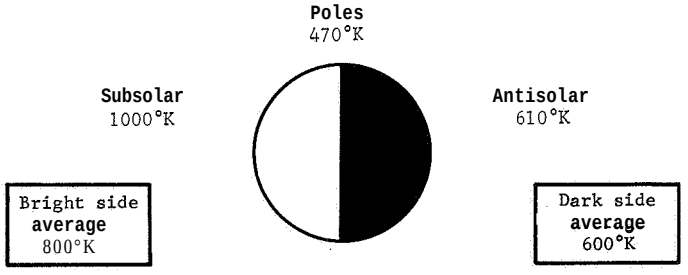

(a) Sagan (ref. 7) Hot-Surface Model

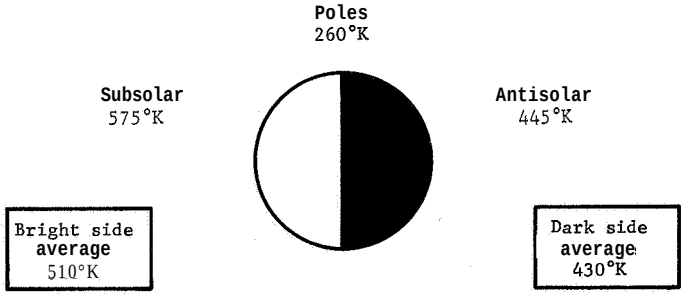

(b) Plummer and Strong (ref. 24) Emitting Cloud Model

Figure 4. - Surface Temperatures

Atmospheric pressure. - Since the temperature lapse rate between the cloud tops and the surface is, at most, adiabatic, the high thermal gradient (~450°K) implies a very thick atmosphere and a high surface pressure ranging from about 5 to as much as 100 Earth atmospheres depending on the cloud top pressure. This is generally substantiated by the 7820Å CO_2 band pressures, which range from 1 atm at 300°K to 5.6 atm at 700°K (refs. 27 and 28).

Sagan (ref. 29) gives the cloud top pressures as 90 mb on the dark side and 0.6 atm on the light side; the surface pressure is greater than 30 atm and possibly as high as 200 atm.

The occultation of Regulus by Venus in 1959 gave data on the scale height (H = 6.8 km) at about 60 km above the visible cloud layer from which a pressure (at 60 km above clouds) of 2.6×10^{-3} mb was inferred (ref. 30). However, these data are not of much use for the lower atmosphere.

Pressure profiles for the NASA SP-3016 model atmospheres are shown in figure 5(a). The disparity of the various estimates for the surface pressure is shown in figure 5(b).

Atmospheric density. - The density is calculated from the equation of state for the various model atmospheres. There are no direct observations of the density. Figure 6 shows the NASA SP-3016 model atmosphere density profiles.

Atmospheric composition. - Until recently, CO_2 was the only gas identified conclusively as a constituent of the Venus atmosphere. The presence of H_2O has been confirmed by Belton and Hunten (ref. 31) and other investigators (refs. 32 and 33) and trace amounts of HCR and HF have been observed (ref. 34) in the interferometric spectra of Venus. The estimated amount of CO_2 present is between 5 and 20%. The amount of H_2O present is not known, but is a very minor constituent above the clouds. The estimated partial pressures of HCR and HF are 10^{-4} and 10^{-6} torr near the cloud tops.

Tentative identifications have been made of CO, N_2, O_2, but attempts to confirm these identifications have been unsuccessful.

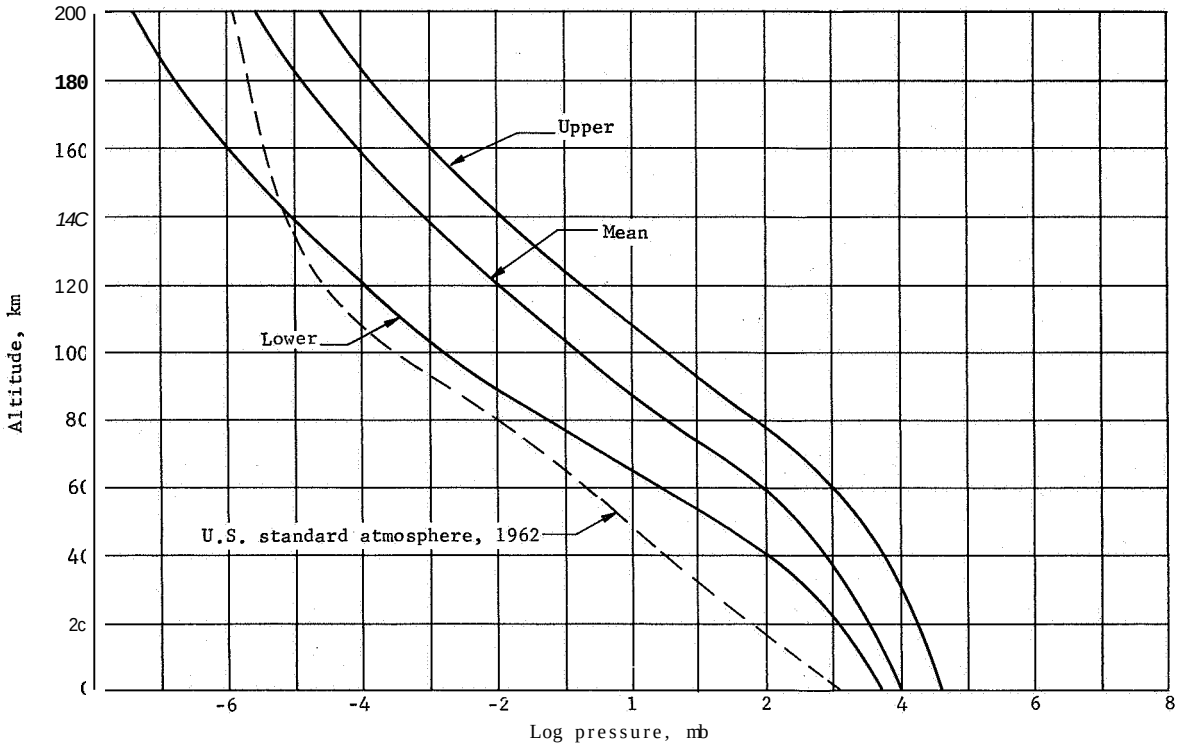

(a) **NASA** SP-3016 Data

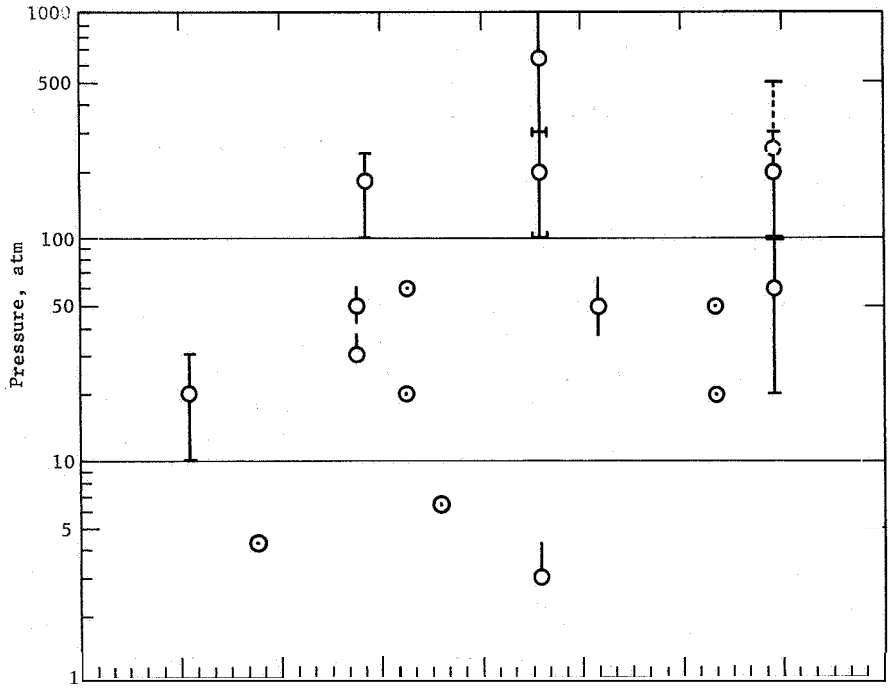

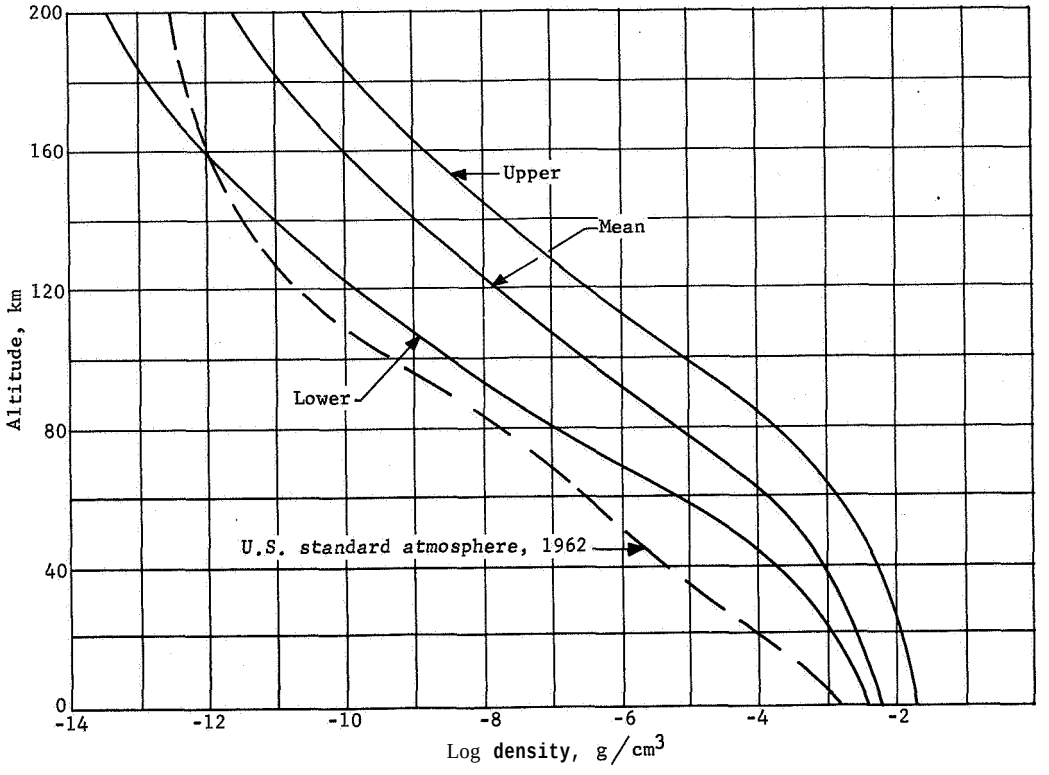

Figure 6. - Venus Density Profiles, NASA SP-3016 Data

Nothing is known of the composition below the clouds, although it is clear that CO_2 is a constituent. Nitrogen is generally accepted as the major constituent with trace amounts of argon present by analogy with Earth. However, Suess (ref. 35) suggests that Venus has retained a much larger fraction of the solar nebula than the Earth and that it appears quite probable that the atmosphere of Venus contains more than 50% and possibly as much as 85% neon.

It may also be argued that because of the considerable amounts of CO_2 present, the exospheric temperature of Venus may be reduced by radiative cooling of CO_2 in the upper atmosphere. The low exospheric temperatures would reduce the rate at which gravitational escape of light gases takes place, permitting Venus to retain its helium content. Thus, helium, rather than neon or nitrogen, may be the predominant atmospheric gas.

Winds. - Very little is known about the winds and atmospheric circulation on Venus. There are only two observations that may be related to the circulation. The first is the time-variable character of the 7820Å GO, bands, which has been interpreted as an indication that the cloud tops are in a state of turbulence.

The other is the observation of dark patches or bands that have been interpreted as circulation patterns. Dollfus (ref. *36)* reports a visible radial pattern centered on the subsolar point whereas Ross reports straight, parallel bands in the ultraviolet. The difference in appearance may result from the fact that different levels are being observed. However, these interpretations are subject to debate and the nature of the circulation on Venus remains uncertain.

GCA, Inc, was requested to review the present theories of circulation on Venus and to compute wind velocities and directions likely to be encountered by the buoyant station. Appendix C is the result of their review. It should be stressed that the conclusions reached are based on theoretical models and are supported by very meager (and even questionable) observational data.

Particles and haze above main cloud. - The extension of the cusps when Venus is near inferior conjunction indicates the existence of high cloud or haze layers above the opaque cloud. A relatively bright haze layer extends several kilometers above the cloud tops; a weaker layer extends approximately 10 km and there is some indication of a very weak scattering layer at heights as great as *30* km above the opaque cloud. Most of the aerosol seems to be confined to a layer about 5 km thick.

Clouds. - From Earth, Venus appears to be completely cloud covered. The infrared brightness temperature maps (see fig. *7)* obtained by Murray (ref. *37)* show a very uniform temperature distribution over both light and dark hemispheres with a slightly greater limb darkening at the poles. The hot spot near the south pole is presumably a storm. Both of these observations, that the planet is apparently completely cloud covered and the temperature (at cloud tops) is the same in both hemispheres, are rather puzzling. The apparently complete cloud cover may be caused by the low resolution of Earth-based telescopes, and clear spots may exist below the resolution limit. For example, the Lunar Orbiter pictures show Earth as almost completely cloud covered.

The existence of water vapor and ice clouds (refs. *31, 32,* and *38)* offer an explanation for the constant temperature of the clouds in both hemispheres (ref. *38,* pp. *147-148).* The failure of the dark hemisphere to cool is due to the release of latent heat of H_2O vapor, (about *620* cal/g) as the vapor condenses. This is in agreement with the observed temperature (234°K) below which saturated water vapor cannot be cooled without spontaneous crystallization. This temperature is observed in many high-altitude cumulus clouds on Earth.

That the clouds, or at least the upper layers, are composed of ice crystals is substantiated by both observation and theory. The observed reflection spectrum of the Venus cloud layer is in excellent agreement with the reflection spectrum of a laboratory ice cloud at 234°K (ref. 38, pp. 147-148). Sagan (ref. 38) has confirmed, on a theoretical basis, Strong's identification of ice as the constituent of the clouds and estimates the mean radius of the cloud particles to be between 7.5 and 10 μ.

The nature of the clouds below the opaque upper layers is unknown. Jones (ref. 23) has postulated the presence of an isothermal cloud layer at 350°K (see fig. 3) to explain the Mariner II microwave radiometer data.

Estimates of the cloud top heights vary from 35 km to greater than 100 km above the surface. Radio interferemetry (ref. 22) indicates that the radio diameter of Venus is about 100 to 120 km smaller than the visible diameter. This gives cloud top heights between 50 and 60 km.

Figure 8 shows the phase diagram for H_2O and the range of pressures and temperatures for the NASA SP-3016 model atmospheres. As can be seen, ice clouds or water clouds are possible in certain regions of the atmosphere while only water vapor can exist near the surface. Thus the atmosphere near the surface may be clear -- if water is the only cloud forming substance on Venus. However because of the extremely high pressures and temperatures postulated, other types of clouds may form.

Surface characteristics. - The surface of Venus appears to be generally smoother than the moon's at radar wavelengths. However, five localized areas appear rougher than the surrounding terrain at radar wavelengths. Two of the most prominent of these areas (ref. 38, pp. 164-171) are shown in figure 9. These areas have been described as either mountain ranges or boulder strewn fields. However, their exact nature is not known.

Electromagnetic fields. - No fields attributable to Venus were observed during the Mariner II flyby. The magnetic dipole moment of Venus, if it exists, must be less than 1/10 to 1/20 that of Earth (see section on Mariner 11).

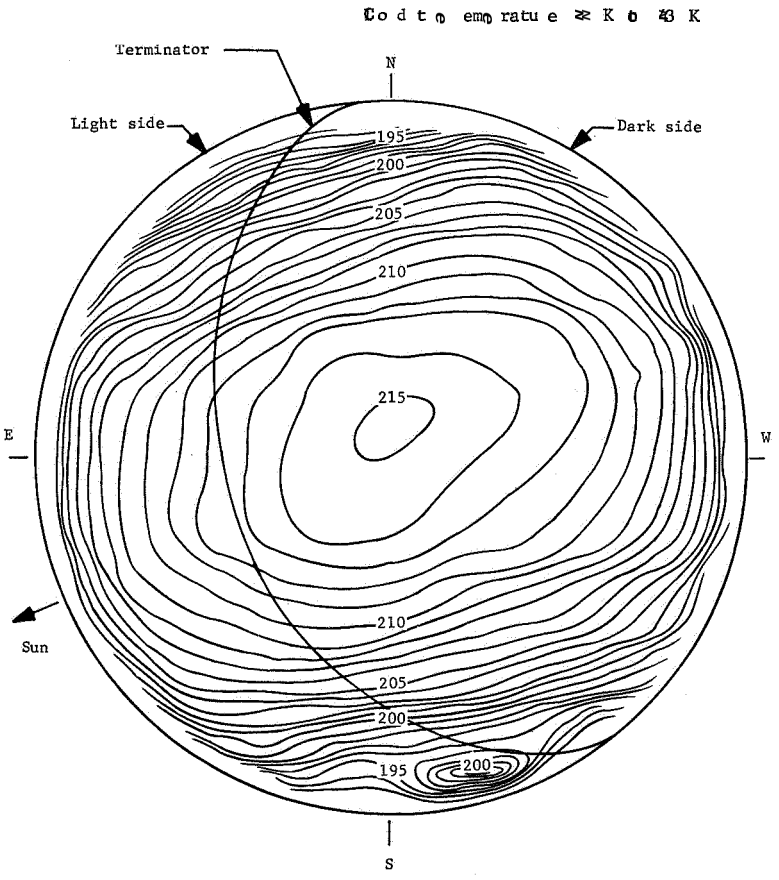

Figure 7. - Brightness Temperature of Venus

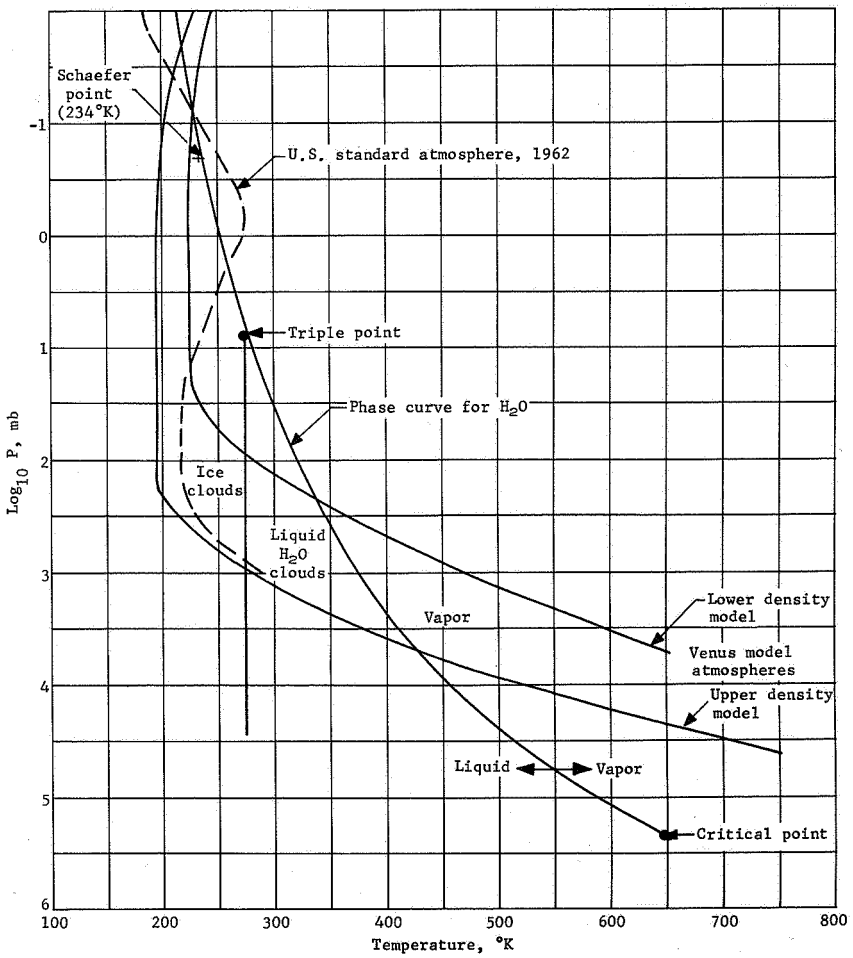

Figure 8. - Phase Diagram for H_2O and Range of Model Atmospheres

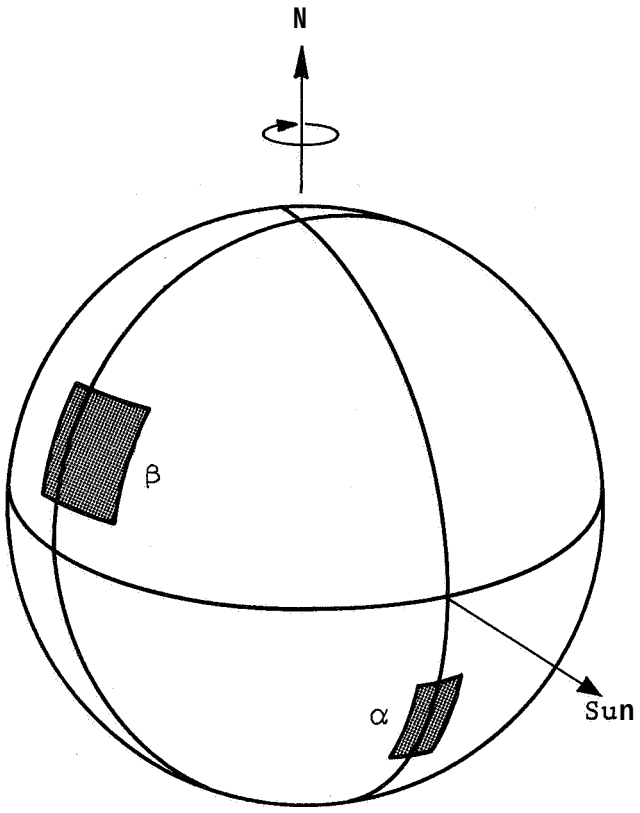

Figure 9. - Radar Surface features

Radiation. - The experiments on Mariner II did not detect the presence of trapped radiation belts about Venus. Due to the low magnetic field of Venus, radiation belts, if they exist, will be found close to the planet and should be detected by Mariner-Venus 67 (See section on Mariner-Venus 67).

Table 2 summarizes present knowledge of Venus.

TABLE 2. - SUMMARY OF PRESENT KNOWLEDGE OF VENUS

Parameter	Relevant observations/techniques	Major results and interpretations
Surface temperature	Microwave radiometry from Earth and Mariner II at wavelengths between 3 mm and 70 cm detects high-intensity radiation from Venus. Phase effect observed (refs. 39 thru 43)	See fig. 3 for inferred brightness temperatures and next section for Mariner II data. Two extremes (fig. 4) are given by: 1) Plummer & Strong (refs. 24, 25, and 39): 30% of emission is nonthermal arising from deep clouds, 70% thermal from surface; implies cold areas may exist. 2) Sagan (ref. 7): All emission is thermal arising from surface insulated by greenhouse effect; implies very hot surface. Phase effect gives ~ 70°K difference between light and dark side.
	Distribution of polarization of emitted radiation measured by interferometry near λ = 10 cm (refs. 22, 39, and 44)	Polarization distribution consistent with thermal radiation from a solid dielectric sphere ($\varepsilon \approx 2.5$) with the poles about 25% cooler than the equator. Sagen (ref. 7) and Plummer and Strong (ref. 24) interpret as in frg. 3.
Atmospheric temperature	Infrared radiometry and thermal mapping of Venus from Earth in 8- to 14-μ wavelength interval and from Mariner II at 8.4- and 10.4 μ	General limb darkening (~ 30°K) and isolated cool spots observed. See fig. 7 for typical thermal map. Inferred temperatures of ≈234°K in bath light and dark hemispheres - emission arises from vicinity of cloud tops. Temporary variations attributed to breaks in cloud layer Figs 4 and 5 show several model temperature profiles. (refs. 37 and 45 thru 48). See next section for Mariner II data.
	Radiometry in 17.5- to 25-μ interval	Inferred temperatures of 248 ± 10°K at 20 μ - probably from levels within clouds (ref. 49).
	Spectroscopy of rotational fine structure in CO_2 bands	Band at 7820 Å shows variable temperatures and pressures; pressures and temperatures at effective scattering levels range from 1 atm, 300°K to 5.6 atm, 700°K. Implies high temperature and pressures at surface. Bands at 8600 Å indicate 285°K (refs. 27, 28, and 50 thru 52).
Atmospheric pressure	Pressure broadened spectral line profile measurements in CO_2 bands (refs. 27 and 28)	Pressures computed from line width and effective rotational temperatures of CO_2 bands range from 1 atm at 300°K near cloud tops to 5 atm at 700°K deep within atmosphere. Latter probably seen through breaks in cloud layer.
	Occultation of Regulus (ref. 30)	Pressure scale height, H = 6.8 km at 60 km above visible cloud layer and $dH/dz \approx 10^{-2}$; estimated pressure at occulting level, P = 2.6 x 10^{-3} mb.
	Polarimetry	Cloud top pressure on sunlit side .1 to 1 atm. Estimates of surface pressure range from 5 atm to greater than 200 atm. See fig. 5 for some model atmosphere pressure profiles.
Atmospheric density	No direct observations	Calculated from equation of state for various model atmospheres. See fig. 6 far models.
Atmospheric composition	Observations of absorption and emission spectra of atmosphere above clouds	CO_2 definitely present in significant quantities (~ 10 to 20%) (ref. 53). Detection of H_2O recently verified (refs. 26 and 31 thru 33); present in small but uncertain amounts. HCℓ and HF lines detected by Fourier spectroscopy (ref. 34). Disputed identification of CO, N_2^+, O_2, N_2O_4. Unsuccessful searches for N_2O, CH_4, C_2H_4, NH_3. Nothing known of composition below clouds other than CO_2 must be major constituent. Argon and N_2 presumably present by analogy to Earth (refs. 54 and 55).
Winds	No observations except possibly wheel-spoke markings emanating from subsolar point	Markings may be due to high altitude wind streams. Observations of variable 7820 Å temperatures seem to indicate that cloud tops are turbulent.
Particles, haze above main cloud	Visual and photographic observations of cusps and polarization (refs. 2, 20, and 21).	Thin layers of small particles at higher altitudes with most of aerosol confined to layer 5- to 30-km thick above top of opaque cloud layer.
Electromagnetic fields	Mariner II measurement of magnetic fields as close as 35 000 km to Venus	No fields attributable to Venus were detected. Implies magnetic dipole moment less than 1/10 to 1/20 of Earth's.
Radiation	Photometric and visual observations	Albedos: W, .5; visual, .8; integrated bolometric, .75. See refs. 20, 57, and 58 for details and fig. 10.
	See above for measurements in various spectral regions.	
	Mariner II measurements of charged particles and ionizing radiation near Venus (ref. 56)	No phenomena attributable to Venus.
Radiation from surface	Microwave radiometry from Earth and Mariner II	See surface temperature above and fig. 3.
Surface characteristics	Radar from Earth, analysis of pulse delay time, pulse length, frequency shift and spread, intensity (refs. 39, 59)	Reflectivity from 12.5 to 68 cm wavelength = 0.1; dielectric constant = 4. Reflectivity drops to .01 at 3.6 cm, rises to 1.5 of that expected from smooth conducting sphere at 6-7 meters. Surface generally smoother than moon's. some areas reflect more effectively indicating rough or mountainous areas. At least 5 rough regions located (see fig. 9).
Cloud top heights	Radio interferometry at 10 cm (ref. 22, 39)	Radio diameter of Venus about 60 km smaller than diameter of visible cloud surface. Other values given are estimated from model atmospheres and "reasonable" assumptions, range from 35 to 100 km above surface.
Cloud particles	Spectroscopy and polarimetry from Earth.	Appear to be ice crystals about 10 μ, (refs. 24 thru 26, 32, and 38) although the identification is disputed. Other proposals include quartz dust, formaldehyde, carbon suboxide polymers.

Mariner II Results and Interpretations

On August 27, 1962, the Mariner II spacecraft was launched from Cape Kennedy and injected into a trajectory that carried it past Venus on December 14, 1962. It carried six scientific instruments, of which three were directly concerned with measuring properties of Venus, Table 3 lists the instruments and observations (refs. 60 thru 65).

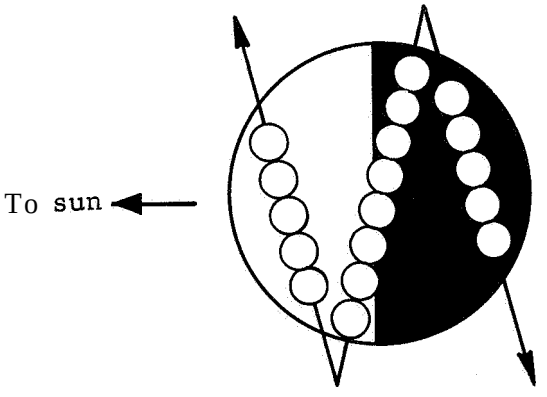

Figure 10. - Mariner II (1962) Radiometer Scans

Both radiometers scanned the planetary disk as shown in figure 10 to give 18 measurements of the emitted radiation at each of the four wavelengths (λ = 8.4μ, 10.4μ, 1.35 cm, and 1.9 cm). The microwave radiometer confirmed the high intensity of radiation seen from Earth. The limb darkening seen in the 1.9-cm channel discounted the theory that the high microwave brightness was caused by a hot ionosphere. Limb darkening was also observed with the IR radiometer, but the equality of the radiation temperatures at both wavelengths indicates that the limb darkening comes from a cloud structure rather than the atmosphere, The anomaly detected by both radiometers near the end of the second scan was also observed from Earth at 8 to 14μ (see fig. 7) and was variously interpreted to be caused by a marked increase in cloud opacity, a true cloud temperature variation, or a hidden surface feature. The magnetometer did not detect any fields attributable to Venus, nor did the trapped radiation and solar plasma instruments detect any changes while near Venus. The details and analyses of the results of the experiments can be found in the references cited in Table 3.

Mariner-Venus 1967 Flyby

The Mariner-Venus 1967 Flyby spacecraft will be a converted Mariner-Mars 1964 spare spacecraft. It is scheduled for launch during a 14-day period starting June 12, 1967 (ref. 76). The spacecraft will be injected into a 120-day transit trajectory and will pass behind Venus about 3000 miles above the surface as shown in fig 11.

TABLE 3. - II EXPERIMENTS

Experiment	Purpose	Results and interpretations
Microwave radiometer	To establish the place of origin of, and the radiation responsible for, the observed centimeter- and millimeter - wavelength radiation. To investigate the variations in intensity from different positions of the planetary disk, including the daylight and dark hemispheres and the region of the terminator (refs 23 and 66).	Strong limb darkening at 1.9 cm discounts theory of "hot" ionosphere. No definite limb darkening at 1.35 cm. Anomalous cool spot detected near end of second scan. Difference of signals at the two wavelengths indicate line absorption at 1.35 cm (H_2O?). Surface dielectric constant estimated between 3 and 4 and upper limit of ~100 atm surface pressure indicated for 20% CO_2. High brightness temperatures observed from Earth confirmed supporting theory of hot surface and/or low atmosphere as source. See fig. 2(b) for temperature profile of model atmosphere (refs 23 and 67 thru 69).
Infrared radiometer	To measure the IR emission from small areas of Venus at 8.4- and 10.4-μ wavelengths. To search for and identify breaks in the cloud structure.	Inferred radiation temperatures agreed with Earth-based measurements in same wavelength region ($T_B \sim 235°K$). Light and dark side temperatures equal. Definite limb darkening in both channels. Equality of temperatures at 8.4 and 10.4 μ indicates emission is from cloud structure. Anomaly detected by microwave radiometer and by Earth-based IR radiometer also seen in both channels; due to either cloud break or temperature variation (ref 70).
Three-axis magnetometer	Measure planetary and interplanetary fields. Capable of detecting up to 320 gammas near Venus and 64 gammas interplanetary.	No magnetic field attributable to Venus detected. Supports theory that Venus is rotating very slowly. Indicates dipole moment of Venus is less than 1/20 that of Earth (ref. 71).
Ion chamber, Geiger-Muller tubes, and Anton special-purpose tube	Detect protons above 10 MeV, electrons above .5 MeV, alpha particles above 40 MeV. Directional tube counts protons above .5 MeV, electrons above .04 MeV.	Flux almost constant throughout trip, no change near Venus. Consistent with magnetic measurements (ref. 72).
Micrometeoroid detector	Measure flux of cosmic dust, particles as small as 1.3×10^{-9} g.	Only two particles detected during mission; malfunction near Venus (ref 65).
Solar plasma spectrometer	Measure spectrum of low energy protons from sun between 0.24 and 8.4 keV.	Solar wind constant, varies in temperature and intensity. Mariner did not enter magnetosphere or cross shock front associated with Venus (refs. 73 and 74).
Radio tracking	Measure astronomical unit, masses of moon and Venus by tracking.	Mass of Venus = 0.81485 mass of Earth ± 0.015% (ref. 60) $\frac{M_\odot}{M_\varphi}$ = 408 533.5 ± 30 (ref. 75).

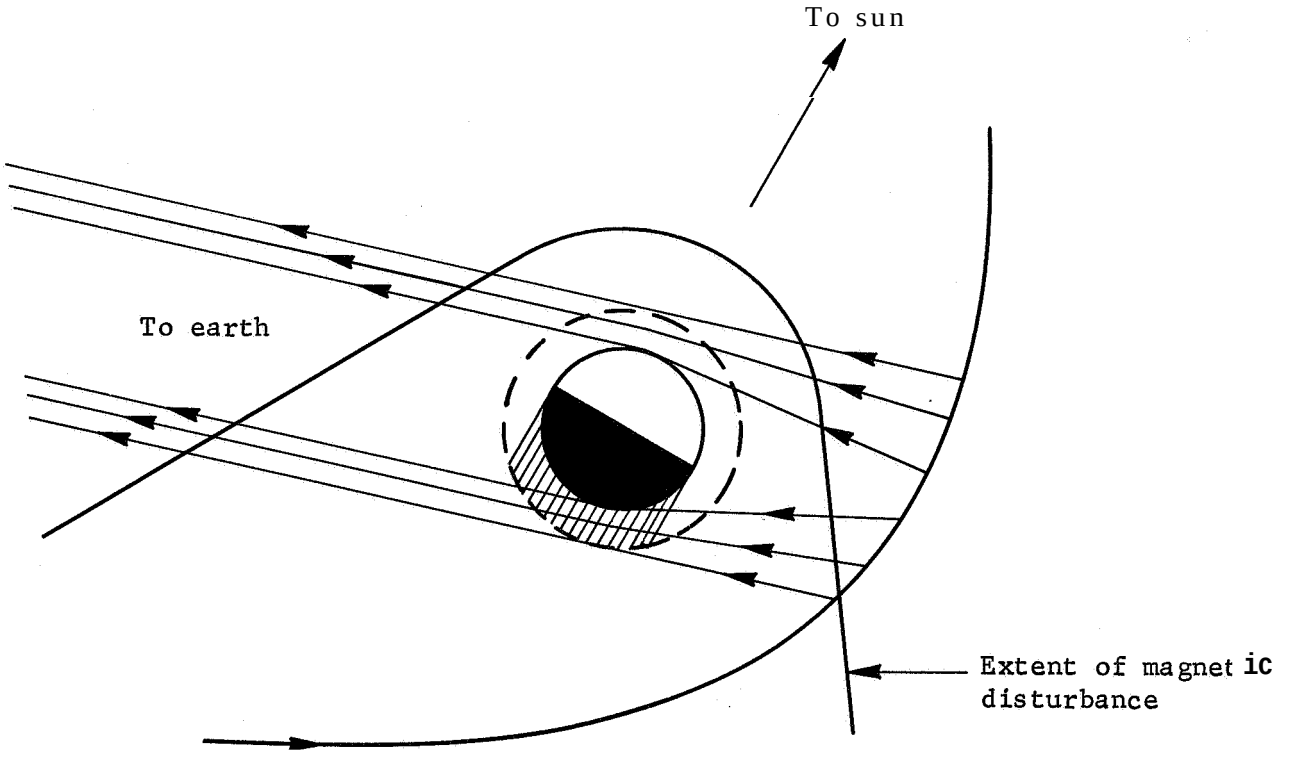

Figure 11. - Proposed Mariner 67 Flyby (JPL Drawing, ref. 76)

The mission objectives are as follows:

1) The primary objective of the Mariner-Venus 67 Project is to conduct a flyby mission to Venus in 1967 to obtain scientific information that will complement and extend the results obtained by Mariner II relevant to determining the origin and nature of Venus and its environment;

2) Secondary objectives are to acquire engineering experience in converting and operating a spacecraft designed for flight to Mars into one flown to Venus, and to obtain information on the interplanetary environment during a period of increasing solar activity,

The seven scientific experiments selected to satisfy these objectives are listed in Table 4. Of these seven, two require no instrumentation other than the transmitter, four are to be accomplished with existing instrumentation, and only one, the Stanford dual-frequency experiment, requires new scientific instrumentation.

TABLE 4. - MARINER-VENUS 1967 EXPERIMENTS

Experiment	Observations
UV photometers	Measure ultraviolet radiation from atomic hydrogen (λ = 1216 Å) and atomic oxygen (A = 1300 Å). Determine distribution and and density of H and O and temperature profile in upper atmosphere.
S-band radio occultation	Observe change in frequency, phase, and amplitude of 2300 mHz telemetry signal as spacecraft passes behind Venus. Gives refractivity of the atmosphere as a function of altitude. Can infer ionospheric electron density and atmospheric scale height, density.
Dual-frequency radio propagation	Similar to above but spacecraft receives signals from Stanford 210-ft antenna, which are processed on the spacecraft.
Helium vapor magnetometer	Measure strength, multipolarity, and direction of Venus magnetic field.
Trapped radiation detector	Observe particles of various energies to search for trapped radiation belts near Venus and energetic particle emissions from the sun.
Solar plasma probe	Faraday cup detector for low-energy protons measures density, velocities, temperature; and direction in solar wind.
Celestial mechanics	Spacecraft tracking by DSIF to refine the astronomical unit, the masses of Venus and the moon, and the ephemerides of Earth and Venus,

The radio occultation experiments are expected to provide information on the lower atmosphere and surface -- if the atmospheric density is not too great. If the density is high enough, the radio beams may either be "captured" by refraction, or be occulted before reaching the surface.

In any event, the refractive index of the atmosphere as a function of altitude above some occulting level will be determined from the change in frequency, phase, and amplitude of the signals passing through the atmosphere (ref. 77 and 78). From this, the local scale height, the electron density of the ionosphere, and the number density of the neutral atmosphere can be obtained. If the temperature profile is known, the local scale height yields the mean molecular weight, thus allowing the calculation of pressure and mass density,

The ultraviolet photometers will measure the intensity of the resonance reradiation from atomic hydrogen (1216 A) and atomic oxygen (1302, 1304, and 1306 Å) in the upper atmosphere.

While these expected measurements will significantly increase our knowledge of Venus, they will not be sufficient to define the atmosphere of Venus. Unambiguous information on the atmosphere and surface can only be obtained from a vehicle that enters the atmosphere and makes direct measurements.

SCIENTIFIC OBJECTIVES FOR A BUOYANT VENUS STATION

As can be seen from the preceding sections, there is at best a large uncertainty in the knowledge of some parameters and no knowledge other than theoretical estimates for others; for still others, there is merely speculation. This paucity of definitive data on the Cytherean environment below the clouds allows the data to be interpreted nonuniquely. In fact, almost any theory or model atmosphere can claim the support of the observational data if one or two pieces of data can be judiciously ignored. While the different models may not be able to explain all of the observations and are somewhat exclusive of one another, they serve the very useful purpose of allowing experiments to be postulated to test their predictions and validity. Thus, one of the objectives of the BVS should be to make measurements critical to the validity of the various models.

However, scientific interest is far from being limited to that of testing the various model atmospheres. In June and July of 1965, the Space Science Board of the National Academy of Sciences convened to "develop a program of planetary exploration and to recommend priority within it" (ref. 1). They recommended that "... , the prime goals of the nation's space program should be the elucidation of the ... three central scientific problems of our time:

1) The origin and evolution of life;

2) The origin and evolution of the Earth, Sun, and Planets;

3) The dynamic processes that shape man's terrestrial environment."

Their remarks on Venus are also of interest here: "Venus, in spite of an allegedly high surface temperature, nevertheless retains some limited biological interest, for the following reasons: the lack of complete certainty regarding the interpretation of the radio emission as thermal radiation from the surface, the possibility of elevated topography at lower temperature, and the possibility of development of life-forms suspended in the atmosphere. Furthermore, as a sister planet to the Earth, with a dense atmosphere of considerable meteorological interest, Venus ranks high in its relevance to terrestrial problems. Finally, the interior of Venus and its rotational and dynamical characteristics are of great interest in connection with the evolution of the solar system."

While the search for life should be accorded the highest priority in the overall exploration of the planets, it cannot be conducted intelligently on Venus until more is known of the environmental conditions existing below the clouds. A similar statement can be made concerning geological investigations, Therefore, for the purposes of this study, the investigation of the Cytherean atmosphere, its composition, structure, and physical and chemical dynamics will be the primary object of the the mission. The investigation of surface and body characteristics will be accorded second priority. The search for life through direct life detection methods is given the lowest priority. However, the search for life through the investigation of environmental constraints is given priority equal to and is essentially synonomous with the investigation of the atmosphere.

More specific objectives and experiments to satisfy them are presented in the next section.

Desired Measurements

Table 5, based on the general scientific objectives and the present knowledge of Venus, lists the desirable measurements for an early Venus mission. In creating this list, the following ground rules were used:

TABLE 5. - DESIRED MEASUREMENTS FOR EARLY VENUS MISSIONS

Atmosphere and clouds	Atmospheric pressure Altitude profiles Spatial and temporal variations Atmospheric temperature Altitude profiles Spatial and temporal variations Atmospheric density Altitude profiles Spatial and temporal variations Atmospheric composition Identity and quantity of major constituents Concentrations of major constituents as function of altitude Identity and quantity of trace constituents Concentrations of trace constituents as function of altitude Particles (aerosols, haze, etc., above cloud layer) Particle concentrations and spatial distribution Shape and size distribution Refractive indices Chemical composition Winds General circulation pattern Magnitudes, shears, turbulence Spatial and temporal variations Radiation fluxes Incoming fluxes as a function of altitude and wavelength in the UV, visible, and IR regions Outgoing fluxes as a function of altitude and wavelength in the IR and microwave regions Spatial and spectral distribution of outgoing IR and microwave radiation as function of altitude Altitude variation of incoming ionizing radiation and energetic charged particles Clouds Extent of cover, texture, breaks Cloud top altitudes, spatial, and temporal variations Cloud layers, thicknesses, and altitudes Cloud particle shape and size distributions, refractive indices, as function of altitude Cloud composition as function of altitude Precipitation as function of altitude Electrical discharges, altitude variations Occurrence of nonthermal microwave radiation	Surface and body characteristics	Surface temperatures Magnitudes and Cythereagraphical variations, especially at subsolar and antisolar points and poles Surface composition Liquid vs solid Sandy, rocky, dust, mud, etc. Cythereagraphical variations Chemical composition Surface features and topography Large-scale roughness; mountains, chains, etc., and locations High-resolution radar mapping High-resolution thermal mapping Seismicity Volcanic activity Surface radioactivity Gravitational field Gravitational acceleration Horizontal variations and anomalies Distribution over planet Shape of planet Magnetic field Field strength Direction and configuration Multipolarity, pole locations Variations due to surface features and anomalies Rotation Refinement of rate and direction
		Exobiology	Environmental measurements Organic compounds In atmosphere In dust and cloud particles Life detection experiments

1) The measurements will be made during the early stages of exploration, i.e., the mission is either the first to enter the atmosphere or has been preceded only by a simple atmosphere entry probe or flyby vehicle such as Mariner 67;

2) Emphasis will be placed on measurements of the ambient environment and the environment below and slight above station altitude; i.e., from about 150 km down to the surface. Ionospheric measurements, for example, are neglected;

3) Measurements of questionable feasibility have been included to avoid making a priori decisions.

Priorities

No single observing system could hope to accomplish the measurement of all of the parameters listed in table 5. Therefore, it is necessary that some form of priority ordering on the basis of scientific merit be applied to this list. A numerical ordering of each measurement in the list is not meaningful. However, a breakdown into three or four general categories into which all measurements might be arranged is feasible. As a result of discussions with Dr. G. Ohring of GCA, it was decided that both Martin Marietta and GCA would make parallel attempts at such a grouping and to make the final ordering after an analysis of both lists. A list of priorities was also compiled by Mr. R. Henry of LRC. In general all three groupings were similar to within ±1 category.

The priorities are based mainly on the contribution to increased knowledge that the measurement of a particular parameter would make. In our approach to the assignment of ratings we have assumed that the most important parts of the Venus environment are the surface and lower atmosphere. By defining these parts of the environment, other parts, such as the upper atmosphere and hard body of the planet could be inferred. The reverse is not necessarily true. Thus, emphasis has been placed on lower atmosphere and surface parameters, and such parameters generally received high ratings.

The four groupings of possible experiments, arranged according to priorities, are listed in table 6. The Priority 1 grouping contains measurements that would answer the most important of the presently outstanding problems concerning the Venus environment. The measurement of these six parameters alone would constitute an enormous increase in our knowledge of the planet.

TABLE 6. - PRIORITY ORDERING OF MEASUREMENTS

Priority 1	Atmospheric pressure profile to surface	Priority 3	Albedo -- large-scale horizontal variations of total planetary albedo and spectral distribution of albedo at top of clouds
	Atmospheric temperature profile to surface		Outgoing thermal radiation -- large-scale horizontal variations of outgoing thermal radiation and spectral distribution at top of clouds
	Major atmospheric constituents - mean molecular weight		Insolation within atmosphere -- vertical and large-scale horizontal variations of total, and spectral distribution of solar radiation
	Surface temperature		Thermal radiation within atmosphere - vertical and large-scale horizontal variations of total upward and downward, and spectral distribution of, thermal radiation.
	Cloud composition - several altitudes		Magnetic field -- field strength and orientation
	General circulation pattern - vertical and large scale horizontal variations		Gravitational variations -- large-scale horizontal variations and anomalies
Priority 2	Cloud structure - vertical extent, height above surface, and horizontal variations		Winds - small- scale temperatures
	Atmospheric temperature - large-scale horizontal variations		Precipitation --
	Source of microwave emission - nonthermal component (if any) of microwave emission, electrical discharge		Surface topography - mapping by microwave or IR imaging devices
	Atmospheric pressure - large-scale horizontal variations	Priority 4	Seismic activity
	Water vapor and other trace constituents - vertical and horizontal variations		Volcanic activity
	Nature of surface - general topography and composition		Surface radioactivity
	Atmospheric particulates - vertical and large-scale horizontal variations of concentration and size distribution, nature of particles		Direct life detection experiments
	Insolation at surface - total and spectral distribution		TV photographs of clouds and surface
			Incoming ionizing radiation etc.

Note that although only six parameters are listed, the number of experiments required to determine these parameters may be greater than six. For example, determination of atmospheric composition and cloud composition may each require several experiments, This may also apply to the determination of other properties of the Venus environment.

The second group of measurements are those that define the dynamics, thermodynamics, and structure of the atmosphere as well as the spatial variations of important lower atmosphere parameters, The term large-scale horizontal variations in these listings is meant to represent the variation from subsolar to antisolar points and from subsolar to polar points on the planet. Successful accomplishment of the measurements in Priority 1 and 2 groups would provide us with a good picture of the overall climatology of the Venus atmosphere and some important information on surface characteristics,

The Priority 3 measurements include parameters associated with the upper atmosphere, various radiation fluxes, and fields. Measurement of the radiation fluxes, aside from providing information on the heat balance of the planet and its atmosphere, would be useful for inferring such characteristics of the environment as atmospheric, cloud, and surface composition; surface and atmospheric temperatures; and scattering properties of the atmosphere and clouds.

The Priority 4 measurements include hard-core geophysics observations, life-detection experiments, and television photographs of the clouds and surface. Both life detection and television experiments are considered premature at this time, but for different reasons. With our present uncertain knowledge of the Venusian environment, the existence of life seems improbable. Television photographs of the clouds would probably not furnish as much additional information on the Venusian clouds as would direct in situ cloud composition observations. Television photographs of the surface, however, would furnish a great deal of new information. Unfortunately, our knowledge of the lower atmosphere is so meager that we do not know how much solar radiation penetrates the cloud layer, and hence, whether there is sufficient illumination in the lower atmosphere for obtaining television photographs.

Experiments

In the previous section, a priority list was given in which several key parameters whose measurements would answer the most important of the present questions concerning Venus were given top priority. The choice of those key parameters was based on an analysis of our present understanding of Venus. In defining possible experiments to measure these key parameters, another criterion was adopted in addition to the scientific value of a particular experiment. This criterion is the compatibility of a particular experiment with the BVS concept. In general, the buoyant station has the important capabilities of (1) direct in situ sampling, (2) direct sampling of vertical and horizontal variations, and (3) long experiment life.

In selecting experiments for the BVS, it has been assumed that the station floats at an equilibrium altitude above the cloud tops and has the capability to release several drop sondes.

The starting point for selecting the experiments was a "shopping list" of experiments for each of the desired measurements in table 6. This list is shown in table 7. The experiments were then examined to determine their detailed characteristics (Anpendix B) and compatibility with the BVS concept. Suitable experiments were arranged into payloads for each of the five basic BVS configurations used in the mode mobility studies and the payloads analyzed to determine the requirements they place on the other station subsystems.

The two most promising configurations, namely the small, noncyclic station and the medium-weight Voyager-class station, were selected for further study and their scientific payloads reiterated. The experiment complements selected for these two configurations are shown in tables 8 thru 11. The experiments and the scientific missions are discussed further in appendix B and in the volumes on the 200 lb and 2000 lb stations (vol V and VI),

No claim is made that these experiment complements are the ultimate; however, they are considered typical and appropriate for this study in that they provide the detail necessary for determining the feasibility and general scientific value of the BVS concept.

TABLE 7. - CANDIDATE EXPERIMENTS FOR THE BVS

Measurement	Experiments
Priority 1	
Pressure - atmospheric	Pressure sensors on BVS and drop sondes
Temperature - atmospheric	Temperature sensors on BVS and drop sondes
Composition - atmospheric	Mass spectrometer Gas chromatograph Single gas detectors
Acoustic transmission line	Absorption spectrophotometers
Temperature - surface	IR radiometers and temperature sensors on drop sondes Microwave radiometer on sondes and BVS
Cloud composition	Pyrolysis/gas chromatograph/ mass spectrometer combination Pyrolysis/GC on drop sonde
Circulation	Tracking of BVS from special drop sondes or RADVS on BVS
Atmospheric density	Calculate from above Acoustic transmission line Radiation backscatter densitometer
Priority 2	
Cloud structure	Photometers, spectral detector on drop sondes IR imager TV camera Lidar (laser ranging)
Temperature variations Pressure variations	Temperature and pressure sensors on drop sondes
Microwave emission	Microwave radiometer on drop sonde Sferics detector, electrometer
Trace constituents	Same as for atmosphere composition
Nature of surface	Penetrometer drop sonde Radar scatterometer
Particulates	Aerosol detector Vidicon microscope
Surface insolation	Pyranometers on drop sondes

Measurement	Experiments
Priority 3	
Albedo	Filter photometers on BVS
Outgoing thermal radiation	IR and microwave radiometers on BVS
Atmospheric insolation	Filter photometers on drop sondes and BVS
Atmospheric thermal radiation	IR radiometers on drop sondes
Magnetic fields	Magnetometers
Gravity	Gravimeter on BVS
Wind - small scale	Special drop sonde model meters on BVS
Precipitation	Measurements
Topography	Radar scatterometer, Microwave scanning radiometer on BVS IR scanning radiometer on drop sonde
Priority 4	
Seismic activity	Seismometer on drop sonde
Volcanic activity	Thermal mapping, seismometer
Sea surface activity	Geiger tube on drop sonde
Life detection	Minimum biolaboratory Vidicon microscope
Incoming ionizing radiation	Ion chamber Geiger tube

TABLE 8. - SCIENCE INSTRUMENTS FOR 200-LB BVS

	Weight, lb	Power, W	Data per measurement, bits	Range of measurements	Data acquisition
4 platinum resistance temperature sensors	1.0	.8	14	200-500°K 450-800°K	Three times per orbit; every 1.25 hr except during acquisition of drop sonde data Measure every 13.3 sec during decent
6 pressure sensors	3.0	.6	14	6 ranges: $1\text{-}10^4$ mb	
Composition:					
H_2O	1.5	1.0	7	.01% vol	
N_2	1.0	1.0	7	1%	
O_2	1.5	1.0	7	.01%	
A	1.5	1.0	7	.01%	
CO_2	1.0	1.0	7	1%	
Acoustic transmission line (ρ, $\bar{\gamma}$, $\bar{M}$)	3.0	4.0	28	$10^{-2}\text{-}10^{-5}$ g/cm^3	
Drop sondes (2) measure P, T. H_2O	LO (5 each)	5 5	28 (3192 total)	Station to surface	On command
Total Weight:	23.5 (including two 5-lb drop sondes)				

TABLE 9. - FIVE-POUND DROP SONDE EXPERIMENTS

	Weight, lb	Power, W	Data
Platinum resistance temperature sensor	.25	.2	7 bits every 30 sec
Pressure sensors (2) (wide range)	.75	.2	14 bits every 30 sec
Water vapor detector (Al_2O_3 electrolytic	.5	.5	7 bits every 30 sec
Totals	1.5	.9	28

TABLE 10. - 2000-POUND BVS EXPERIMENTS

No.	Experiment	eight, lb	Power, W	Data acquisition
1	Temperature sensors (4)	2	0.8	Two 7-bit words/measurement (range switched electronically)
2	Pressure sensors (10)	5	1.0	Four 7-bit words/measurement (2 ranges - 2 sensors/range)
3	Acoustic transmission	3	4	Four 7-bit words/reading Three readings/sample = 84 bits
4	Mass spectrometer (atmospheric gases)	10	10	4000 bits/analysis 60 sec/analysis
5	Pyrolysis/gas chromatograph/ MS (cloud, dust composition]	15	15	10 000 bits/analysis 1 hr/analysis
6	Dust/cloud particle collector for 5	2	10 peak 1.0 Cont.	Status only
7	Vidicon microscope (dust & biota)	15	8	255 000 bits/picture 20 pictures/sample = 5.1 x 10^6 bits
8	Minimum biolaboratory	20	10 peak	100 hr/analysis 13 500 bits/analysis
9	Dust collector for experiments 7 & 8	2	0.5	Status only
10	Ion chamber and Geiger tube	3	0.5	14 bits - ion chamber 21 bits - GM tube every 10 sec for 60 sec
11	Ultraviolet radiation flux	2	1.5	Six 7-bit words/measurement
12	Visible/near-IR flux	3	2.3	25 7-bit words/measurement
13	Altimeter/radar scatterometer	15	30	10 000 bits/10 sec scan 14 bits - altitude
14	Microwave scanner/spectrometer	25		100 000 bits/image 10 000 bits/scan, 4 wavelengths
15	IR scanner/spectrometer	10	4	255 000 bits/image 10 000 bits/scan, 4 wavelengths
16	Light backscatter from aerosols	5	5	10 7-bit words/sec
	Weight	137		

TABLE 11 - LARGE SONDE EXPERIMENT COMPLEMENT

Experiment/instrument	Range of measurement	Weight, lb	Power, W	Bits/measurement	Data acquisition
Temperature sensing, A_1	200 to 500°K	.25	.2	7	One measurement every 10 sec
Temperature sensing, A_2	200 to 500°K	.25	.2	7	One measurement every 10 sec
Temperature sensing, B_1	450 to 800°K	.25	.2	7	One measurement every 10 sec
Temperature sensing, B_2	450 to 800°K	.25	.2	7	One measurement every 10 sec
Pressure-static, A	0 to 10 mb	.5	.1	7	One measurement every 10 sec (only two ranges read out)
Pressure-static, B	0 to 10^2 mb	.5	.1	7	
Pressure-static, C	0 to 10^3 mb	.5	.1	7	
Pressure-static, D	0 to 10^4 mb	.5	.1	7	
Pressure-impact Pitot Tube	0 to 20 mb	.5 .5	.1	7	One measurement every 10 sec
Impactometer		.5	5	2-sec pulses on carrier frequency	At impact only
Photometers and filters looking up	CO_2, H_2O absorption bands	20	30	Six 7-bit word	One measurement every 10 sec
Mass spectrometer (MS)	H_2O, N_2, O_2, A, CO_2 gases or scan 10 to 50 a mu	10.0	10.0	4E7	One measurement every 6 minutes 1 minute/analysis First measurement at 1 minute
Cloud sampler for MS	Heat cloud sample	2.0	2.0	497	Present vaporized cloud to MS One analysis every 6 minutes 1 minute/analysis First measurement at 4 minutes
Totals		22.5	16.8		

CONCLUSIONS

Table 12 compares the two experiment payloads on the basis of their contributing to the desired objectives. As can be seen, both payloads contribute to all of the Priority 1 measurements. (with the exception of cloud composition in the small BVS) and many of the Priority 2 measurements. Thus, the small station answers the most important questions about the Venus atmosphere while the large station answers those and most of the other questions we can intelligently ask about Venus. In fact, since we know so little at present about Venus, it becomes difficult to use the full capability of the larger station in an optimum manner and the selection of one experiment over another becomes somewhat fanciful for the early missions.

We conclude that an early BVS mission of the Atlas/Centaur launch vehicle class can answer the most important scientific questions we have about Venus while the larger, Voyager-class BVS (cyclic or with drop sondes) appears to have the capability for answering all of the questions that might be asked about the Venus atmosphere and general surface characteristics. The investigation of the body and detailed surface characteristics will, of course, require a vehicle to be landed on the surface. The design of such a vehicle, however, will require a detailed investigation of the surface and near surface conditions that only a large BVS can conduct.

The drop sondes are a necessary adjunct to any BVS, cyclic or noncyclic. Indeed, their versatility makes the concept of cycling the station somewhat questionable from the scientific point of view.

TABLE 12. - COMPARISON OF 200- AND 2000-LB BVS

Measurement	200-lb BVS	2000-lb BVS
Priority 1		
Pressure	X	X
Temperature	X	X
Composition	X	X
Surface Temperature	X	X
Cloud Composition		X
Circulation	X	X
Priority 2		
Cloud structure		X
Temperature variations	X	X
Pressure variation	X	X
Microwave emission		X
Trace Constituents	X	X
Nature of surface		X
Particulates		X
Surface insolation		X
Priority 3		
Albedo		X
Outgoing thermal radiation		X
Atmospheric insolation		X
Atmospheric thermal radiation		X
Magnetic fields		
Gravity		
Winds - small scale		
Precipitation		
Topography		X
Priority 4		
Seismic activity		
Volcanic activity		
Surface radioactivity		
Life detection		X
Ionizing radiation, etc.		X

Martin Marietta Corporation
Denver, Colorado
April 28, 1967

APPENDIX A

DROP SONDES

DROP SONDE OBJECTIVES

One of the advantages of a buoyant station floating high in the Cytherean atmosphere is its ability to conduct multilocation investigations of the lower atmosphere through the use of small probes without exposing itself to the hostile near-surface environment. The determination of atmospheric pressure, temperature, density, and composition at several widely spaced locations is of prime importance to an understanding of the Cytherean meteorology, atmospheric physics and chemistry, surface chemistry, and the optimum design of future exploratory missions. These lower atmosphere parameters could be measured from small probes or drop sondes and telemetered to the station. By employing thermal insulation techniques and phase change heat sinks, the sonde might even survive the high surface temperatures long enough to gather detailed data on the surface characteristics. However, the intelligent design of such a sonde requires a much better knowledge of the surface conditions than presently exists so it should probably be relegated to a later mission.

The three general objectives such devices could satisfy are:

1) To eliminate the need for vertical cycling by a station not designed to descend below the clouds;

2) To perform experiments beyond the capability of a station with a degree of vertical mobility such as determining near-surface conditions;

3) To be used before a station descent to ascertain whether below station conditions will allow a safe descent.

There are three general classes of drop sondes that could perform such missions. They are:

1) Slowly falling sondes to accurately determine atmospheric and cloud structure;

2) Rapidly falling sondes to determine near-surface and surface conditions;

3) Small, constant-level balloons floating at about 30 km to determine wind and circulation patterns.

APPENDIX A

TRAJECTORIES

To bring the drop sonde concept into focus, trajectories were calculated for sondes with a range of ballistic coefficients $B = 5, 1, 0.5$, and 0.1 slug/ft^2 in each of the three model atmospheres given in NASA SP-3016. This range of ballistic coefficients was chosen to give fast, short duration flights at one end $(B = 5)$ and slow, long-duration flights at the other $(B = 0.1)$. The initial conditions assumed were the same in all cases, namely, the initial altitude was 70 km and the initial velocity was zero. The effects of winds were neglected. The calculated parameters given at 30-sec time-of-flight intervals were:

1) Radius from planet center, km;
2) Altitude above surface, km;
3) Vertical velocity, mlsec;
4) Dynamic pressure, lb/ft^2;
5) Mach number;
6) Drag acceleration, Earth g;
7) Time of flight, sec.

Figures 12 thru 17 show the altitude-time and altitude-velocity profiles for the three model atmospheres. Figure 18 shows the altitude-Mach number profile for the mean density model atmosphere. The method of calculation assumed a constant drag coefficient for all Mach numbers. This is a valid assumption for Mach numbers less than about 0.9, but the drag coefficient generally increases rapidly between $0.9 < M < 1.1$ to a value that may be a factor of 2 or 3 greater than the low-speed value. Consequently, figures 16 and 17 show higher velocities for longer periods than will actually be obtained with the high ballistic coefficients.

BALLISTIC COEFFICIENTS

These trajectories allow limits to be set on the choice of ballistic coefficients for a class of sonde or objective. The lower limit on B is dictated by communication range and thermal control considerations. It is desirable that the sonde reach the

surface or perform its mission before either the communication range or the operating temperature limit of the sonde instruments are exceeded. Reasonable thermal control and communication systems allow about 30 to 40 minutes of useful sonde life. If the mean density model atmosphere is used as the design environment, figure 13 shows that $B \geq 0.5$ allows the sonde to reach the surface within this time limit. Thus, a lower limit on the ballistic coefficient for most classes of sondes is $B_L = 0.5$. No strong requirement has been identified for a sonde life greater than 30 to 40 minutes (with the exception of the small, constant-level balloons; however, the above remarks do not apply in this case since it is envisioned that the balloons would float at a temperate altitude and would communicate with the orbiter). If such a requirement does present itself, stringent, but perhaps not impossible, demands will be placed on the thermal control and communications systems.

In the event that the upper density model atmosphere were encountered, a sonde with $B = 0.5$ would require 75 minutes to reach the surface. This predicament could be remedied by changing the ballistic coefficient in flight. As will be seen later a ballistic coefficient of $B = 0.5$ is obtained with drag devices such as parachutes or flared afterbodies. A timer or temperature sensor could be employed to initiate the release of the drag device after a given time or temperature were exceeded, thereby increasing the ballistic coefficient and allowing broader altitude coverage.

If the station is not designed to descend, it will be desirable to use a sonde that descends very slowly through the clouds. A ballistic coefficient of 0.1 will allow this, but the station will drift out of range before the sonde reaches the lower atmosphere. In this case, a timer or pressure switch could be used to initiate release of the parachute.

Thus, the limits on the ballistic coefficient depend on the scientific mission or objective of the sonde. If the mission of the sonde is to investigate atmospheric or cloud structure, it is desirable to keep the sonde velocity well below the speed of sound to facilitate accurate and simple measurements. While the accurate measurement of pressure, temperature, etc., at velocities near the speed of sound is not too difficult, it does require more complex instrumentation and knowledge of other parameters such as Mach number and specific heat ratio. Figure 18 shows that

a sonde with $B = 1$ is below Mach 1 during its entire flight, and a sonde with $B = 5$ is below Mach 1 for all but 50 sec or 15 km of its flight. However, to allow for the contingency of encountering the lower density model atmosphere, an upper limit of $B = 1$ should be selected.

If it is desired to reach the surface quickly or to reach the lower atmosphere (~20 km) quickly and proceed more slowly from there by deploying a parachute, a ballistic coefficient of $B \geq 5$ would be the logical selection.

In conclusion, it is seen that ballistic coefficients in the range $0.1 \leq B \lesssim 10$ can be used to advantage with the choice of B depending on the scientific objectives of the particular sonde.

DROP SONDE SHAPE

The drag coefficient C_D for slender, dart-shaped missiles is generally between 0.1 and 0.3 (ref. 79), depending on the exact shape. For the purposes of this study it is assumed that dart-shaped sondes can be designed with a drag coefficient of 0.3.

To keep a sonde from tumbling, the length should be about three times the diameter. The weight of the sonde is given by:

$$mg = \rho \frac{\pi}{4} d^2 \ell \geq \rho \frac{3\pi}{4} d^3 \tag{A1}$$

or, since $B = m/C_D A$,

$$mg = \frac{\pi}{4} g B C_D d^2 \tag{A2}$$

Equating (A1) and (A2), we get the lower limit on B:

$$B \geq 10 \frac{\rho}{g} d \tag{A3}$$

Figure 19 shows this minimum ballistic coefficient for packaging densities of 25, 50, 75, and 100 lb/cu ft. If it is desired to use this type of sonde with a low ballistic coefficient ($\lesssim 1$) low packaging densities result.

APPENDIX A

The high drag coefficients required to get low ballistic coefficients can be obtained with small parachutes or flared afterbodies as shown in figure 20. Another possibility would be counterrotating propellers to supply both drag and electrical power. These configurations can be designed with $0.4 \lesssim C_D \lesssim 0.8$ for the flared afterbodies or propellers and with $0.7 \gtrsim C_D$ for parachutes.

DROP SONDE CONFIGURATIONS

Speculation on the different types of sondes and experiments that could be performed from such sondes can be almost limitless. Two configurations were defined to restrict the study to that of determining the feasibility, or rather the degree of feasibility of various sizes of sondes. They are essentially sondes at two ends of the weight scale. The smaller is defined by the minimum complement of experiments required to make it scientifically meaningful. The larger was chosen to be representative of a heavy sonde with complex experiments. Table 13 lists these as Configurations A and E, with B, C, and D being typical gradations between the two.

Many other experiments and combinations of experiments could be defined to give an almost continuous spectrum from the smaller sonde up to perhaps a sonde of twice the size of Configuration E. The intent here is to investigate the difference in requirements of the two sondes.

A ballistic coefficient of 1 was assumed to be desirable for both sondes, giving a time of flight from station to surface of *1440* sec or *24* minutes in the mean density model atmosphere. If an extreme atmosphere is encountered, the times of flight become 56 and 15 minutes, respectively, for the upper and lower density model atmospheres. The mean atmosphere will be assumed for purposes of discussion.

The starting point for each configuration was the list of experiments as shown in table 13. Using these lists, data rates were established, the telemetry system and batteries sized, and an average payload packaging density computed. The average density was used to define the dimensions of a cylindrical sonde and thermal control weights were calculated. Finally, a drag device

was chosen to give a ballistic coefficient of 1, and the total weight and dimensions were computed. The battery and thermal control weights were computed for a 1 hr drop time in the upper density atmosphere.

TABLE 13. - DROP SONDE EXPERIMENT COMPLEMENTS

Experiment/instrument	Weight, lb	Power, W	Configuration				
			A	B	C	D	E
Temperature sensors (2)	.5	.4	X	X	X	X	XX
Pressure (static) (4)	2.0	.4	X	X			
(impact) (1)	.5	.1	X	X			
Combination Pitot tube/ impactometer (4 static, 1 impact pressure sensors)	3.0	1.0			X	X	X
Photometers/filters (3)	3.0	1.5		X		X	
(6)	6.0	3.0					X
Acoustic transmission 1ine	3.0	4.0		X	X		
Mass spectrometer (MS)	10.0	10.0				X	X
Cloud sampler for MS	2.0	2.0					X
Simple gas detectors:							
H_2O	1.5	1.0			X		
CO_2	1.0	1.0			X		
O_2	1.5	1.0			X		
A	1.5	1.0			X		
N2	1.0	1.0			X		
Total weight			3.0	9.0	13.0	16.5	22.0
Total power			.8	6.3	10.4	12.9	16.8

SMALL SONDE

The minimum complement of experiments that would make a drop sonde meaningful would be one that measured pressure and temperature as a function of time. Pressure and temperature measured at

lcnown time intervals can be used to determine density, altitude, and mean molecular weight, and to give an estimate of the composition (ref. 80).

After the sonde has reached terminal velocity and begins to decelerate (–10 km free-fall for the mean atmosphere), the gravitational and aerodynamic forces balance,

$$mg = 1/2\ \rho V^2\ C_D A \tag{A4}$$

The hydrostatic equation,

$$dP = -g\rho dz \tag{A5}$$

gives the velocity,

$$V = \frac{dz}{dt} = -\frac{1}{g\rho}\frac{dP}{dt} \tag{A6}$$

and hence, the density,

$$\rho = \frac{C_D A}{2\ mg^3}\left(\frac{dP}{dt}\right)^2 \tag{A7}$$

The altitude change is given by equation (A5). The gas law gives the mean molecular weight:

$$\overline{M} = \rho\frac{RT}{P} = \frac{C_D A\ RT}{2\ mg^3\ P}\left(\frac{dP}{dt}\right)^2 \tag{A8}$$

from which the CO_2 and N_2 content can be estimated. Hanel (ref. 80) estimates the probable rms error in the mean molecular weight determination as about ±7%. However, this can be reduced somewhat with the following assumptions.

1) The probable error in the temperature measurement is ±1%;
2) The probable error in the pressure measurement is 22%;
3) The factor $C_D A/m$ can be determined to within ±1% using a reproduced Venus atmosphere on Earth;
4) The gravitational constant for Venus is known to within ±0.5%;
5) The error in dP/dt is ±2%.

With these assumptions and suitable smoothing techniques, the probable errors are ±4.5% for the density and ±5% for the mean molecular weight. The accuracy of the altitude determination is rather poor because the altitude is given by integration of the hydrostatic equation (and the errors). However, by successive iteration of trajectories in model atmospheres to obtain self-consistent solutions, the error can be reduced significantly.

A similar method for determining density from the drag deceleration of the sonde is given in references 81 thru 83. This method is applicable for the first few kilometers of free-fall where the velocities and decelerations are high, but since the station will be investigating this region in detail, the information is of doubtful value. The method could, however, be used to advantage with high ballistic coefficient sondes.

Table 14 lists the experiments and their characteristics. All measurements are to be made at 10-sec intervals starting on release. In the mean density atmosphere, this gives 144 measurements in each of the four channels and a total of 4032 bits of scientific data; housekeeping data will amount to about 1008 bits for a total of 5040 bits. A transmission rate of 3.5 bit/sec will suffice to read the data out in real time. The total number of bits generated in the upper density atmosphere is about 12 600.

TABLE 14. - SMALL SONDE EXPERIMENT COMPLEMENT

Experiment	Range of measurement	Weight, lb	Power, W	Bits/ measurement	Data acquisition
Temperature sensing, A	200 to 500°K	.25	.2	7	One measurement every 10 sec
Temperature sensing, B	450 to 800°K	.25	.2	7	One measurement every 10 sec
Pressure-static, A	0 to 10^4 mb	.5	.1	7	One measurement every 10 sec (only one range reads out)
Pressure-static, B	0 to 10^3 mb	.5	.1	7	
Pressure-static, C	0 to 10^2 mb	.5	.1	7	
Pressure-static, D	0 to 10 mb	.5	.1	7	
Pressure-impact	0 to 20 mb (diff)	.5	.1	7	One measurement every 10 sec
Totals	--	3.0	.9	28	28 bits every 10 sec

APPENDIX A

Table 15 gives the weight breakdown for the various subsystems. A figure of 20 Wh/lb was used to size the batteries for 1 hr of operation. The average density of the telemetry, experiments, structure, and batteries is about 0.1 lb/cu in. or about 173 lb/cu ft.

TABLE 15. - WEIGHT BREAKDOWN FOR SMALL SONDE

	Weight, lb	Power, Wh	Volume, cu in.
Experiments	3.0	.9	25
Telemetry			
4-channel multiverter Programer Master oscillator Synchronous generator	1.5	.6	20
Transmitter	1.0	3.5	10
Antenna	.5	--	
Batteries	.25	--	5
Structure, wiring, etc.	1.0	--	10
Thermal insulation	1.7	--	100
Drag device	.5	--	--
Total	9.5	5	170

Packaging this sonde in a 3-in.-diam cylinder results in a length of about 10 in. A 0.67-in.-thick layer of Min-K-1301 thermal insulation (0.8 lb) backed with 0.9 lb of 100-Btu/lb phase-change heat sink material keeps the internal temperature below 38°C (100°F) for a 1-hr descent in the upper density atmosphere. A drag device (flared afterbody, propellers, or a parachute) to give a ballistic coefficient of 1 slug/ft^2 might weigh about 0.5 lb. This would bring the total weight to about 9.5 lb. The dimensions of such a cylindrical sonde would be about 4.5 in. in diameter by 13.5 in. long with a rounded nose. A schematic of the small sonde is shown in figure 21.

The sonde described above is heavier (by a factor of two) than the 5-lb sonde postulated for the 200-lb BVS. However, since the estimates given above are conservative, it is felt that a 5-lb sonde could be developed using miniaturization techniques, similar to those used in developing gun probe payloads (ref. 84).

APPENDIX A

LARGE SONDE

The experiment complement for the large sonde is shown in table 16. There are four temperature sensors for redundancy, and a combination Pitot static tube/impactometer for measurement of atmospheric pressure during descent and surface hardness at impact. At impact, the Pitot tube moves back into the body against the action of a spring. Pulses are generated on the carrier frequency when the tube is sheared from the body and as it moves given distances into the body. The sonde will be destroyed several microseconds after it has moved the length of the tube.

The other experiments are concerned with the composition of the atmosphere and clouds. Gas and cloud samples for the mass spectrometer will be taken through two holes near the front of the sonde. The photometers, with appropriate filters, will measure the intensity of solar radiation at wavelengths absorbed by CO_2 and H_2O and at several nonabsorbed wavelengths for reference and detection of cloud layers. When the sonde descends far enough into the cloud layer *so* that there is no visible solar radiation, a small pulsed light source could be used to give back scattered radiation from the cloud particles. An estimate of the particle density can be obtained from this.

Figure 22 shows the number of science data bits generated as a function of time. The mass spectrometer, operating in the stepped mode, generates 497 bits every 3 minutes starting 1 minute after release. The other experiments and engineering measurements generate 98 bits every 10 sec. A transmission rate of about 25 bit/sec is sufficient. The total number of bits transmitted to the BVS in the upper density atmosphere (~1-hr droptime) is about 90 000 bits.

The weight breakdown for the large sonde is shown in table 17.

The average payload density is 0.045 lb/cu in. (70 lb/cu ft). Packaging this in a 7-in.-diam cylinder gives a length of 19 in. For a 0.67-in.-thick layer of Min-K-1301, the weight of the insulation and heat sink material is 8.5 lb. This could be reduced by packaging the payload in a sphere. A parachute with an effective area of about 1.6 sq ft is needed to get a ballistic coefficient of 1 slug/ft^2. The chute would have a diameter of about 15 to 20 in. and would weigh about 1 lb.

TABLE 16. - LARGE SONDE EXPERIMENT COMPLEMENT

Experiment/instrument	Range of measurement	Weight, lb	Power, W	Bits/ measurement	Data acquisition
Temperature sensing, A_1	200 to 500°K	.25	.2	7	One measurement every 10 sec
Temperature sensing, A_2	200 to 500°K	.25	.2	7	One measurement every 10 sec
Temperature sensing, B_1	450 to 800°K	.25	.2	7	One measurement every 10 sec
Temperature sensing, B_2	450 to 800°K	.25	.2	7	One measurement every 10 sec
Pressure-static A	0 to 10 mb	.5	.1	7	One measurement every 10 sec (only two ranges read out)
Pressure-static B	0 to 10^2 mb	.5	.1	7	
Pressure-static, C	0 to 10^3 mb	.5	.1	7	
Pressure-static D	0 to 10^4 mb	.5	.1	7	
Pressure-impact	0 to 20 mb	.5	.1	7	One measurement every sec
Pitot tube		.5			
Impactometer		.5	5	2-microsec pulses on carrier frequency	At impact only
Photometers and filters looking up	CO_2, H_2O absorption bands	6.0	3.0	Six 7-bit words	One measurement every sec
Mass spectrometer (MS)	H_2O, N_2, O_2, A, CO_2 gases or scan 10 to 50 amu	.0	10.0	497	One measurement every 6 minutes. 1 minute/analysis. First measurement at 1 minute
Cloud sampler for MS	Heat cloud sample	2.0	2.0	497	Present vaporized cloud to MS. One analysis every 6 minutes. 1 minute/analysis. First measurement at 4 minutes
Totals		22.5	16.8		

APPENDIX A

TABLE 17 - WEIGHT BREAKDOWN FOR LARGE SONDE

	Weight, lb	Power, Wh	Volume, cu in.
Experiments	22.5	16.8	600
Telemetry, etc.	4.5	8	40
Batteries	1.25		22
Structure, wiring	3		30
Totals	31.25	24.8	~700
Thermal control	8.5		~500
Parachute	1.0		
Totals	40.75	24.8	1200

Miniaturization of components, development of the sonde as a unit, and careful packaging could significantly reduce the weight and volume of the large sonde. It is estimated that, to perform the measurements described above, a sonde could be developed that would weigh as little as 20 lb and certainly less than 30 lb. Figure 23 shows how such a sonde might look.

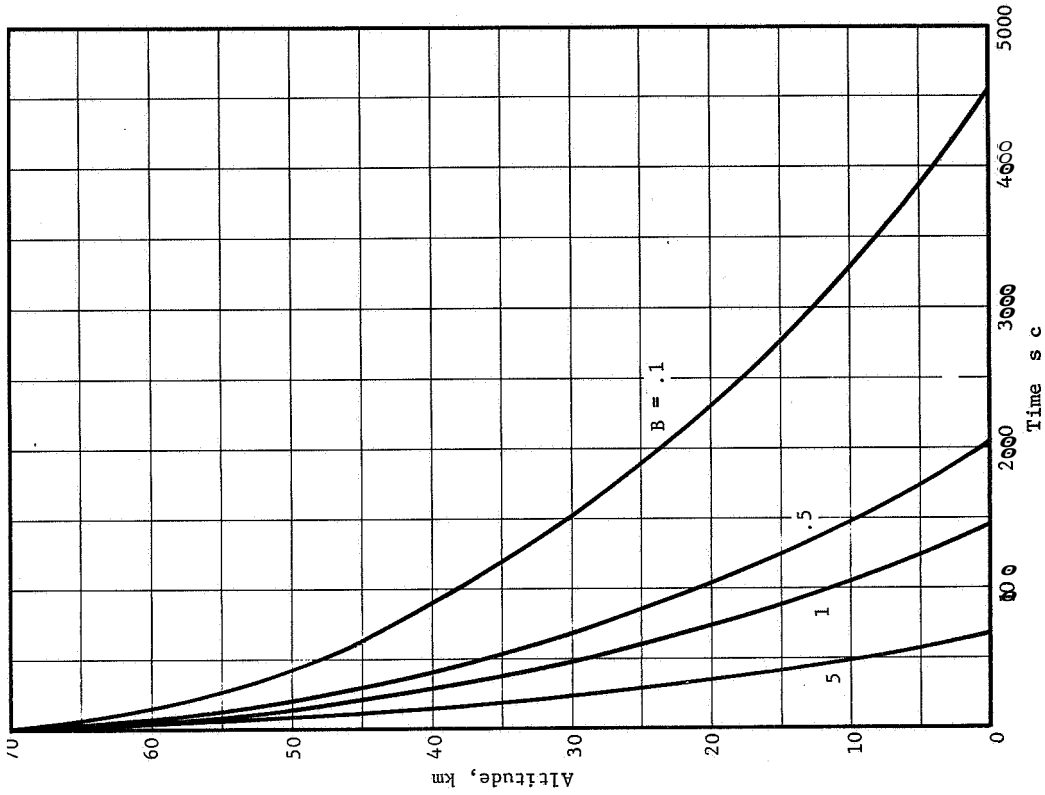

Figure 12. - Time vs Altitude for Upper Density Model

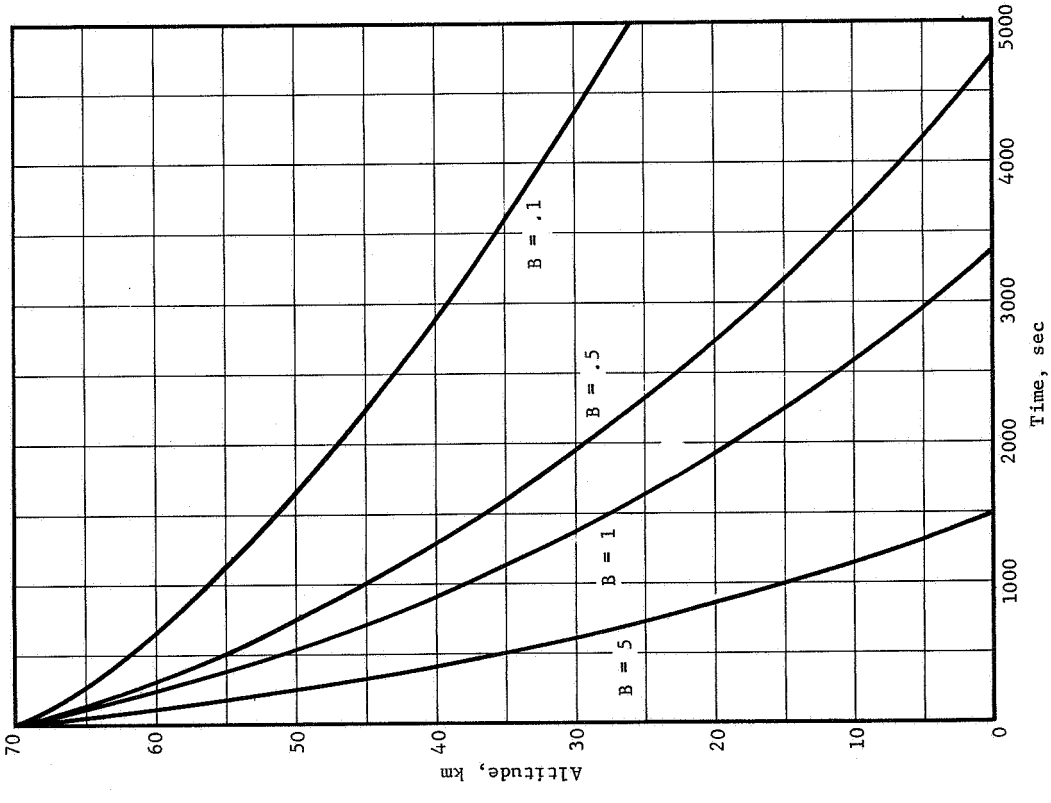

Figure 13. - Time vs Altitude for Mean Density Model

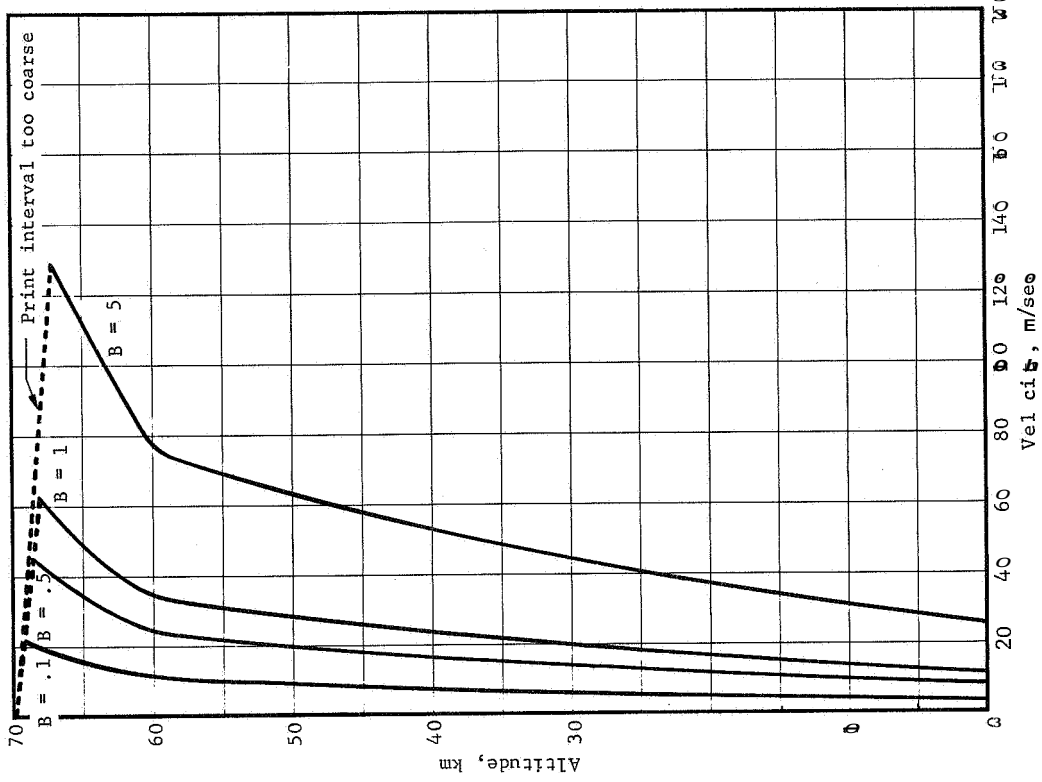

Figure 1 - Vel o fy vs A l fu p f r Wa p r a p s h Mo el

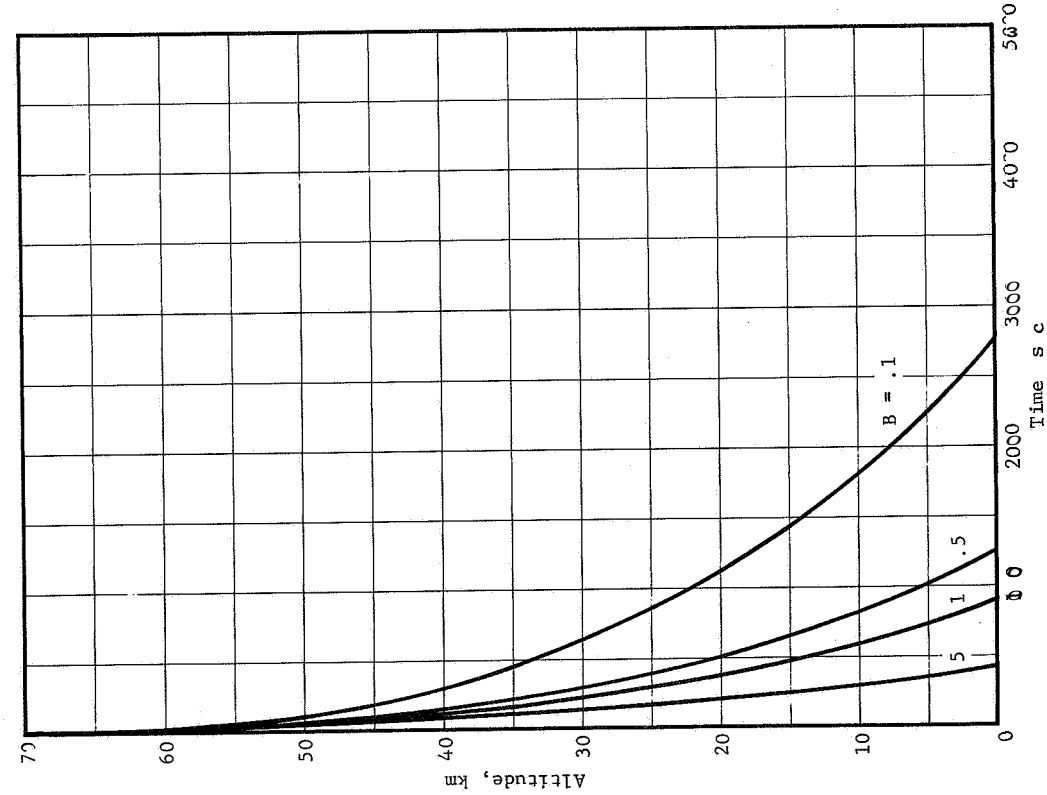

Figure 14. - Time vs Altitude for Lower Density Model

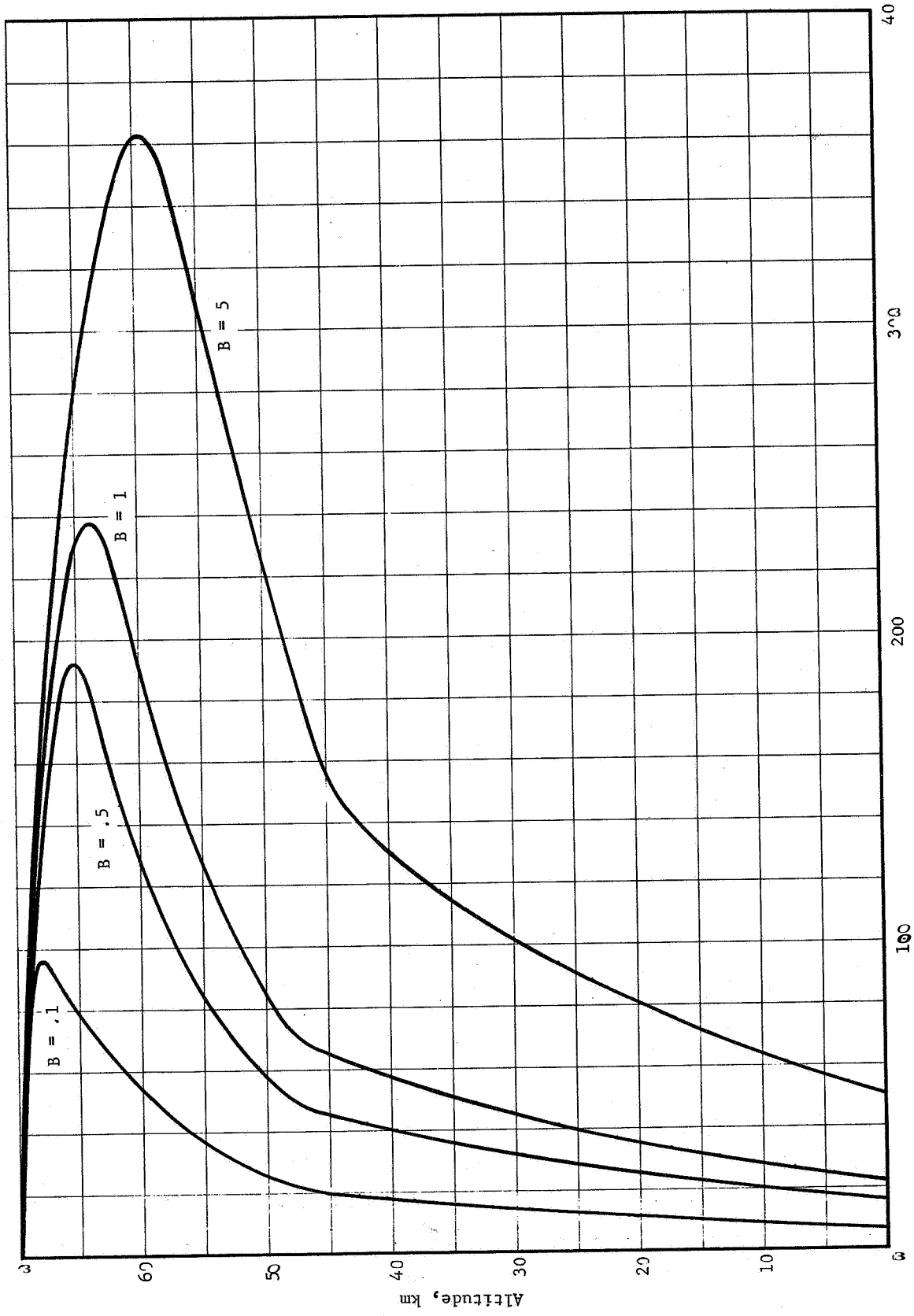

Figure 16. - Velocity vs Altitude for Mean Density Model

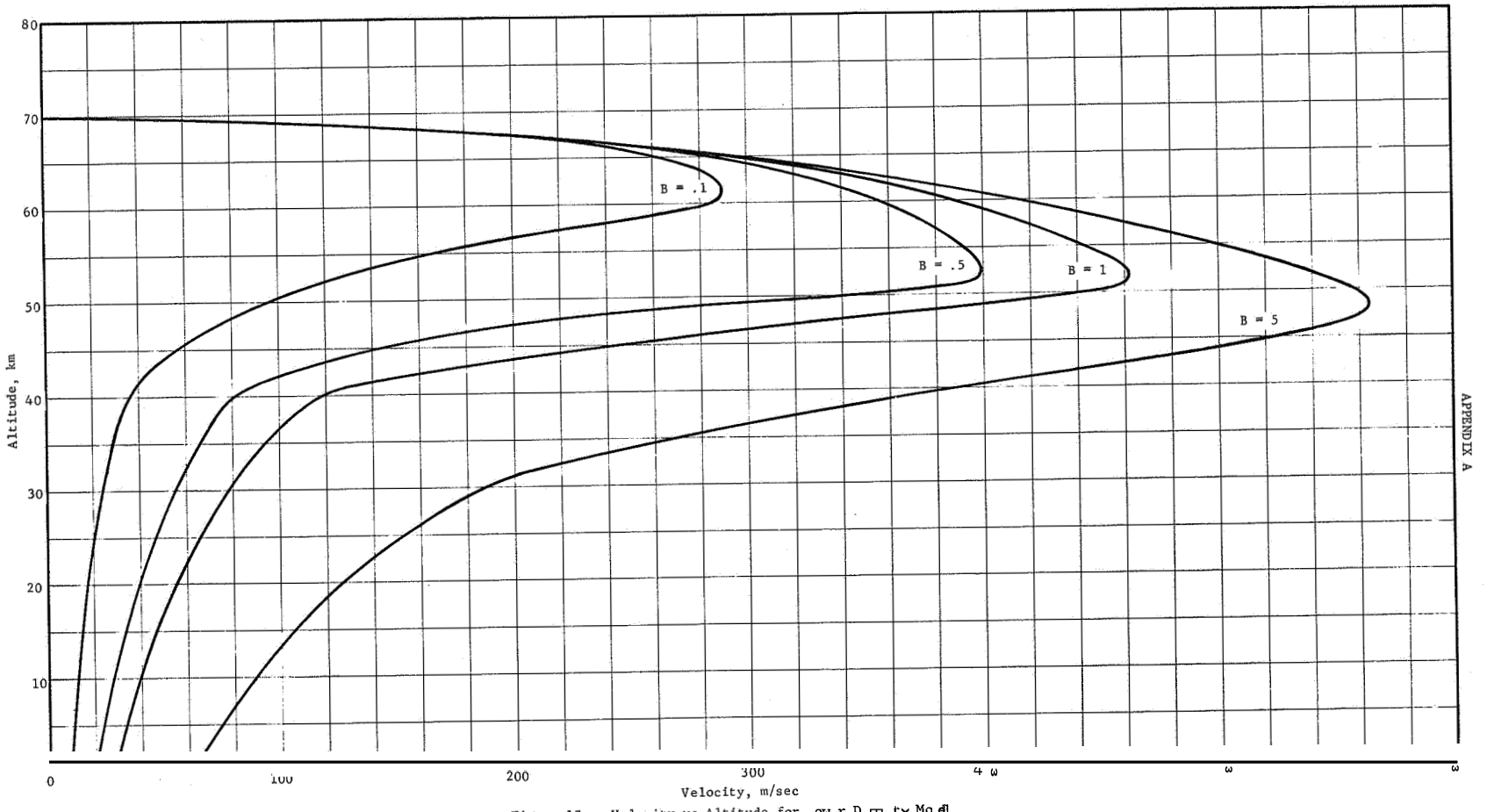

Figure 17. - Velocity vs Altitude for ow r D m t x Mo d l

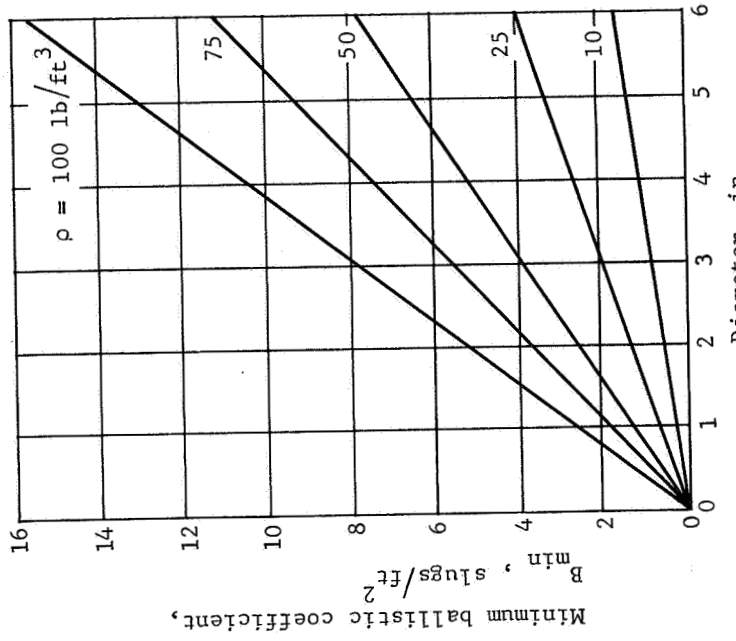

Figure 19. - Diameter vs Minimum Ballastic Coefficient

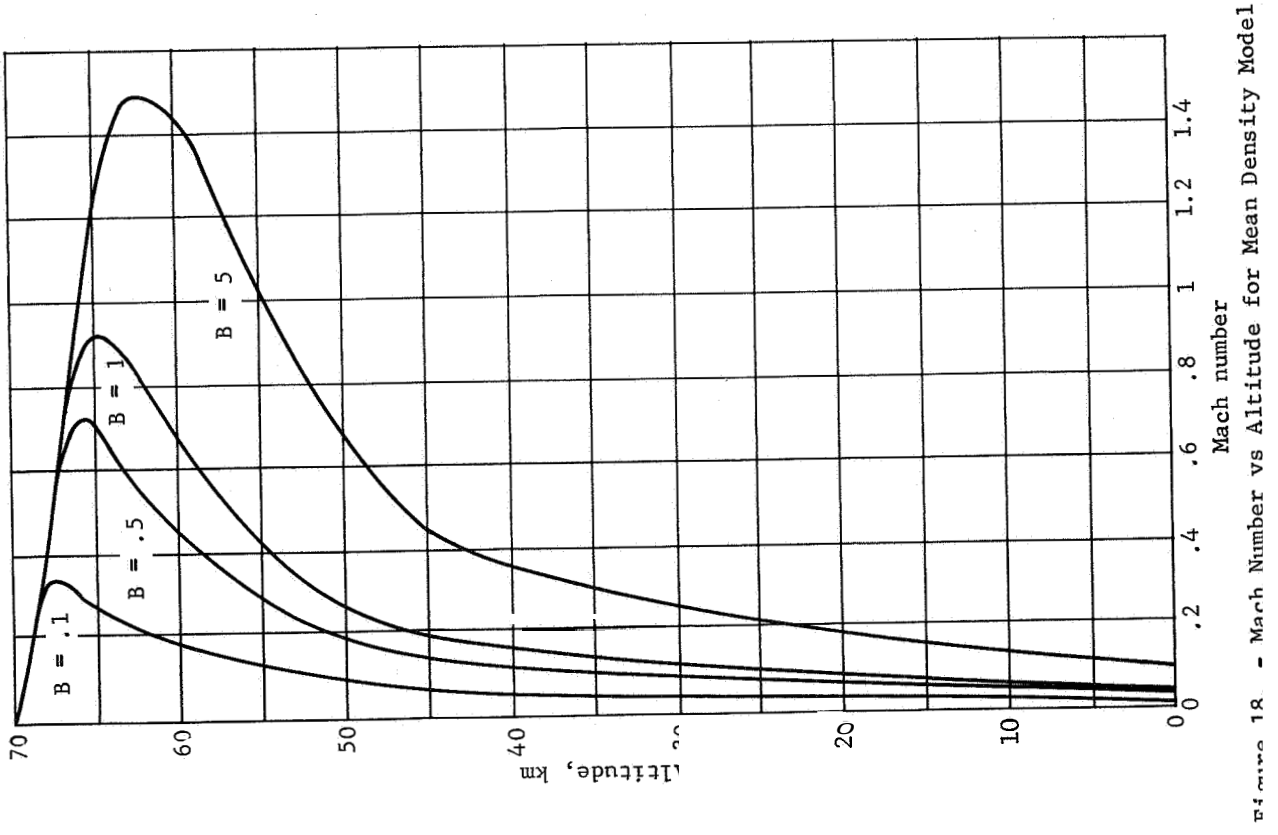

Figure 18 - Mach Number vs Altitude for Mean Density Model

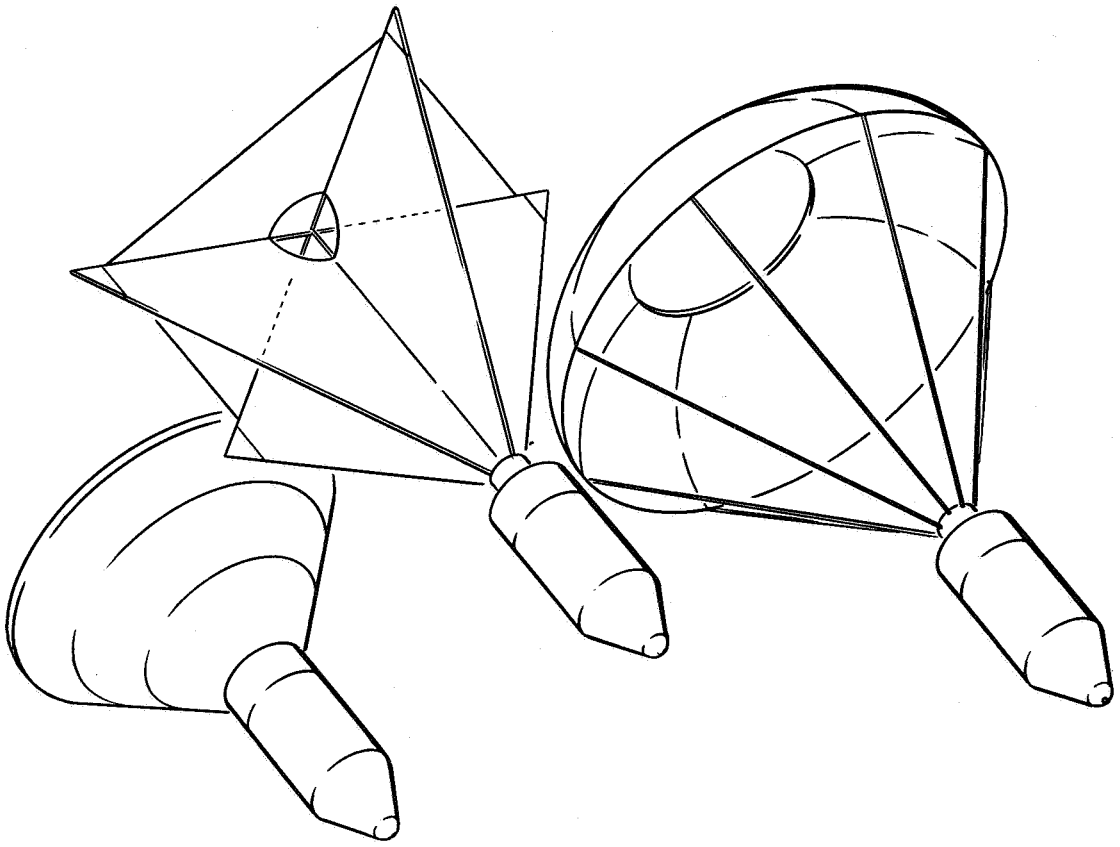

Figure 20. - Drop Sonde Decelerator Concepts

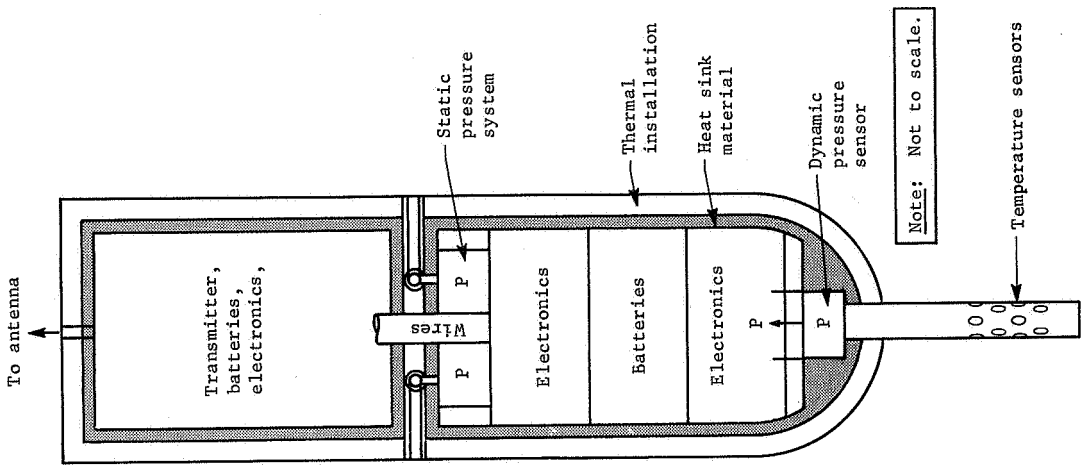

Figure 21. - Schematic of Small Sonde

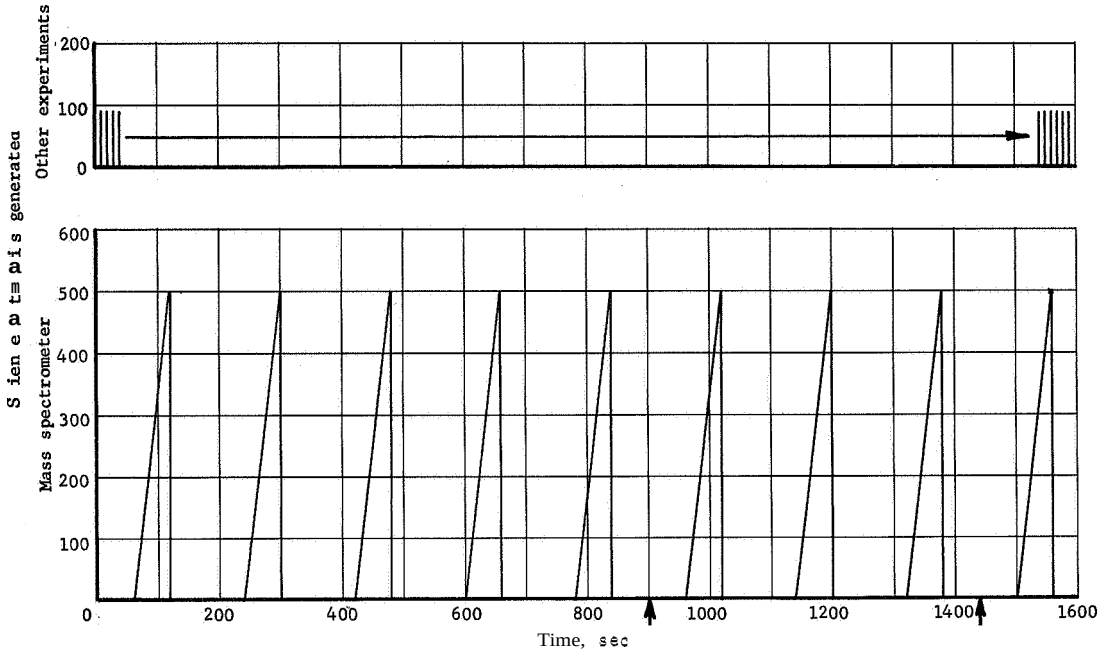

Figure 22. - Large Sonde Data Acquisition

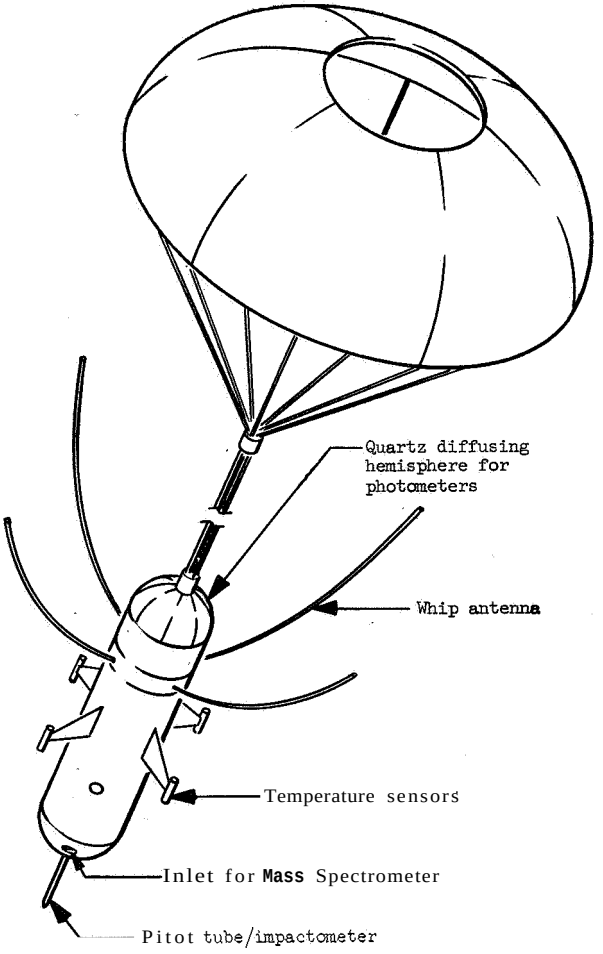

Figure 23. - Large Sonde Suspended from Parachute

APPENDIX B

DETAILED CHARACTERISTICS OF EXPERIMENTS

Experiments suitable for use on a BVS are examined to determine (1) physical characteristics, (2) operational requirements, (3) operational limitations, and (4) development status. The experiments are arranged according to the parameter measured. Some of the problem areas that might arise in the development of specific instruments are given.

The experiments discussed in this appendix represent a distillation of many candidate experiments considered for use on the BVS. While there are virtually no instruments being developed specifically for use in the Venus atmosphere, there are many conceptual designs for experiments to investigate the terrestrial planets. Most of these concepts (and all of the hardware) have been directed toward the exploration of Mars or the Moon and Earth. However, many of these experiments can be adapted, with suitable modification, for use on a BVS.

For this reason, many of the characteristics given are extrapolations based on existing instruments or estimations based on desired performance. Given several years of development, any of the instruments discussed can be built.

ATMOSPHERIC PRESSURE

OBJECTIVES

The objective of direct measurement of atmospheric pressure is to acquire data necessary to further define the Cytherean environment. Data from this experiment will also provide a cross check on data from atmospheric composition, temperature, and density measurements. Pressure sensors will be employed to take measurements at known altitudes, horizontal positions, and times. It is anticipated that the collection of pressure data will commence at station deployment and continue throughout the life of the station. Additional data will be obtained during station descent cycles to ~ 10 km if temperatures permit. The use of drop sondes can provide an alternative source of pressure data at altitudes below the buoyant station. Present atmospheric environmental data for Venus obtained from remote observations and theoretical arguments indicate that for 70 km to the surface, pressure extremes may vary from ~ 0.6 to 6 x 10^4 mb (~ 0.01 to 870 psia). Obviously, no

single range transducer will be suitable for the entire range and several types of transducers will be required. At least five sensors would be necessary having ranges of 0 to 0.1, 0 to 1, 0 to 10, 0 to 100, and 0 to 1000 psia. The transducers considered for the two lower ranges operate on the principles of (1) vibrating diaphragm, (2) thermal conductivity, or (3) variable capacitance. These lower range transducers would require overpressure protection. The higher pressure ranges could be covered by transducers operating on the principles of (1) variable capacitance, (2) variable reluctance, (3) semiconductor strain gages, or (4) potentiometric resistance change.

EXPERIMENTS/INSTRUMENTS

Variable Capacitance Diaphragm Transducer

In the variable capacitance diaphragm transducer, a diaphragm is located between fixed plates to form two capacitors. Pressure acting on the diaphragm causes it to deflect and change the capacitance of each of the capacitors. The solid-state circuitry for the sensor capacitors is contained within the transducer and provides a dc voltage output proportional to the difference of the two sensor capacitances. The Rosemount Engineering Company Model 830A pressure sensor could be used to cover the range of 0 to 100 psia.

Physical characteristics. - The Rosemount capacitive pressure gage is relatively heavy, weighing about 1.2 lb. Its dimensions are 3.5x2.5x2.7 in.

Operational characteristics. - The pressure sensor and associated electronics require 0.1 A, 28 Vdc ± 10%, 2.8 W power input. No warmup period is required.

The output of the device is 0 to 5 Vdc analog and could be externally converted to digital form. Seven-bit accuracy is sufficient.

No deployment is necessary other than providing the sensor direct access to the atmosphere and providing overpressure protection.

The sensor requires a thermal environment of 0 to +55°C during operation. Storage temperature range is from -55 to +120°C, but can probably be extended to meet sterilization requirements.

Operational limitations. - Atmospheric pressure measurements using the Rosemont pressure sensor and a 7-bit data word would have an accuracy of approximately 2% of full scale.

Development status. - Variable capacitance diaphragm pressure transducers for the ranges discussed above are available as off-the-shelf items from the Rosemount Engineering Company. Redesign to reduce the weight and volume and extend the operating temperature range is necessary.

Variable Reluctance Diaphragm Transducer

This type of pressure transducer operates on the variable reluctance principle. The sensor is a flat diaphragm of magnetic material mounted in a gap between two identical magnetic core and coil assemblies. Pressure acting on the diaphragm causes it to deflect and vary the reluctance in the magnetic circuit. Resultant variation in inductance of each of the coils occurs and is sensed by a bridge circuit in which the coils are connected. The ac voltage bridge output is converted internally to a corresponding dc voltage output if desired.

Physical description. - The Pace Engineering Company Models CP51 and CP52 are 1-3/4 in. in diameter and 4 in. long and weigh 1.0 and 1.2 lb respectively.

Operational characteristics. - Most standard models operate with 95 to 125 Vac, 60 *to 400* cps, 1 W, or 25 to *30* Vdc, 20 mA nominal.

The output is 0 to 5 Vdc analog, although standard models are available having ac voltage outputs. External conversion to digital form of 7-bit accuracy would probably be employed.

No deployment is necessary other than providing the sensor direct access to the atmosphere.

This type of sensor will operate accurately within the temperature range of -20 *to* +72°C with special compensation up *to* +120°C obtainable.

Operational limitations. - This type of pressure transducer covers a range of 0 to 0.1 psi to 0 to 10 000 psi. They are rugged, have no moving parts, but are relatively large and heavy.

Development status. - Pressure transducers of the variable reluctance type are readily available as off-the-shelf items from several vendors including Pace Engineering Company and Bourns, Inc. Some redesign will be required.

Potentiometer Diaphragm Transducers

This family of pressure transducers operates through the deflection of a diaphragm, pressurized capsule, or bourdon tube on the application of pressure. This deflection mechanically operates the wiper of a wire-wound or carbon film resistive element.

Physical characteristics. - Transducers using a bourdon tube sensing element such as the Bourns, Inc. Model 737 weigh about 4 oz and are 1 in. in diameter and 2.75 in. long. Transducers using a bellows or capsule sensing element are substantially larger, such as the Computer Instruments Corporation Model 4000 weighing 1.0 lb and having a dimensional envelope of 2x2x3.5 in.

Operational characterisitics. - No electrical power is required other than ac or dc excitation voltage and should not exceed 0.25 W.

The transducer will produce an analog voltage output depending on the potentiometer excitation employed. Voltage divider circuitry internal to the instrument can be obtained if required. Output voltage conversion to a 7-bit digital format would occur external to the instrument.

An operating thermal environment of -55 to 85°C is required for this type of transducer.

No deployment is necessary other than providing the sensor direct access to the atmosphere.

Operational limitations. - Potentiometric pressure transducers are available for ranges of 0 to 0.3 psi to 0 to 10 000 psi. The elimination or improvement in potentiometer wiper linkages has greatly increased the ruggedness and accuracy of these devices in flight vibration and acceleration environments. Also, development of carbon film resistive elements has provided increased sensitivity (resolution) over the older wire-wound potentiometers.

APPENDIX B

Development status. - This family of pressure transducers is highly developed with a long history of varied flight applications. Suppliers such as Computer Instruments Corporation and Bourns, Inc., can furnish a wide selection of these instruments from existing stock.

Semiconductor Strain Gage Transducers

Semiconductor strain gage pressure sensors use the piezoresistive effect (change in electrical resistivity with strain) of certain semiconductor materials such as silicon crystals. The deformation of a diaphragm under pressure is used to strain single or multiple semiconductor elements. The consequent change in resistance of these elements when arranged in a bridge circuit is sensed as a direct function of pressure. The semiconductor strain gages may be bonded directly to the diaphragm or mounted apart (unbonded) from the diaphragm. The Rosemount Engineering Company Model 810G is a transducer using a cylindrical silicon crystal structure having four resistive paths and bonded to a stainless steel membrane. Pressure acting on the membrane strains the semiconductor, and electrical bridge unbalance is monitored. The Servonics Instrument, Inc., Model 3508 transducer uses four semiconductor gages mounted on a spring remote from the sensing diaphragm. Deflection of the diaphragm under pressure is transferred to the spring by a push rod. The gages are arranged in a bridge, and their resistive changes are monitored as bridge unbalance.

Physical characteristics. - The Rosemount Engineering Company Model 810G transducer weighs 5 oz and is 1 in. in diameter and 3 in. long.

Operational characteristics. - Typical excitation voltages for strain gage transducers would be 5, 10, or 28 Vdc.

Analog output voltage depends on excitation voltage. Output up to 5 Vdc can be achieved with 25 Vdc excitation.

The operating temperature range for strain gage transducers is about -30 to +75°C.

No deployment is necessary other than providing the sensor direct access to the atmosphere.

Operational limitations. - Strain gage transducers cover pressure ranges from 0 to 5 psi to 0 to 10 000 psi.

Development status. - A large variety of flightworthy semiconductor strain gage pressure transducers are available from stock throughout the industry.

Vibrating Diaphragm Transducer

The vibrating diaphragm transducer measures pressure by sensing the damping effect of the gas on the vibration of a thin metal diaphragm. The diaphragm is mounted under radial tension between two closely spaced, insulated metal plates. One plate (the forcing plate) is energized by a dc potential and an ac voltage from an electronic oscillator set at the mechanical resonant frequency of the tensioned diaphragm. The diaphragm is thus driven to vibrate synchronously with the electrostatic forcing function. The diaphragm's vibration causes a corresponding periodic vibration in the capacity between the diaphragm and the other plate (the sensing plate). This capacitance can be detected and indicates the amplitude of vibration. Since the power required for a given amplitude of vibration is a function of the damping on the diaphragm, which in turn is a function of the gas pressure, the power can be monitored as an indication of the pressure.

Physical characteristics. - Vibrating diaphragm transducers as presently constructed at NASA, Ames Research Center, are about 0.8 in. in diameter and 0.6 in. long. These dimensions do not include the associated electronics.

Operational limitations. - This transducer is designed for pressure measurements in the range of 10^{-5} to 10^{3} mmHg with an accuracy of 1% over most of the range.

Development status. - At present, evaluation tests of the vibrating diaphragm transducer have been conducted at Nortronics Division of Northrop Corp. and at Ames. Approximately 50 units have been built at Ames for use in NASA wind tunnel applications. Although successful results have been obtained, many design and fabrication problems in the transducer and support electronics require further development. Development of this device for space application appears feasible where low pressures are to be measured over wide ranges.

APPENDIX B

Thermal Conductivity Transducers

This category of pressure sensing instruments uses the fact that heat conductivity of a gas at low pressures varies directly and linearly with the pressure. The Hasting-Raydist, Inc., Type D-7 probe is an example of a transducer employing this principle. Two Noble metal thermocouples are connected in series bucking and heated with an alternating current. The dc output of the couples is established at a given reference pressure of the gas in which they are exposed. As the gas pressure changes, the thermocouple circuit dc output varies. The system can be accurately calibrated and ambient temperature variation compensated by the addition of a third, unheated thermocouple into the circuit.

Physical description. - As in the case of the Hasting-Raydist, Inc., Type D-7 sensor, the thermocouple elements can be arranged in a tubular probe of 0.375 in. in diameter and about 6 in. long. The associated electronics (ac source and dc amplifier) can be mounted remotely.

Development status. - An extensive history exists of development and application of pressure sensors employing thermal conductivity principles. Pirani and thermocouple gages are used frequently in industrial and laboratory applications for pressure measurements in the range of 10^{-4} to 10^{3} mmHg. The problems and limitations of these devices are well understood. The development of a thermocouple gage for space pressure measurements in the range cited seems quite feasible.

Table 18 is a pressure sensor comparison matrix.

Typical Pressure Sensor

Since this study is one of feasibility, and since there is such a wide variety of pressure sensors that could be adapted for use on a BVS, a "typical" pressure sensor was defined:

Weight	.5 lb
Power	.1 W
Size	1 in. diam, 1 in. long (body) 2x1x1 in. (electronics) plus inlet tube and wires

This typical sensor is nonexistent; however, there should be no problems in developing it.

TABLE 18. - PRESSURE SENSOR COMPARISON MATRIX

Operating principle	Representative supplier	Optimum operating pressure ranges	Weight	Size	Power, W	Development required
Variable capacitance	Rosemount Engineering Co.	0 to .1 psi to 0 to 200 psi	1 2 lb	∃ 5x2.5x2 7 in.	2.8	Minimal
Variable reluctance	Pace Engineering Co.	0 to .1 psi to 0 to 1000 psi	1.2 lb	1.75 in. diam by 4 in. long	0 6	Minimal
Potentiometric	Bourns, Inc	0 to .3 psi to 0 to 1000 psi	1.0 lb	2x2x3.5 in.	0.25	Minimal
Semiconductor strain gage	Rosemount Engineering Co.	0 to 5 psi to 0 to 1000 psi	5 oz	1 in. diam by 3 in. long	0.5	Minimal
Thermal conductivity	Hasting-Raydist, Inc.	10^{-4} to 20 mmHg	[a]4 oz	[a].375 in. diam by 6 in. long	1 0	Develop flight-worthy electronics package
Vibrating diaphragm	None	10^{-5} to 10^{3} mmHg	[a]2 oz	[a].8 in. diam by .6 in. long	1 0	Develop flight-worthy transducer and electronics package (in progress at Ames)

[a]Indicates that figures do not include electronics.

APPENDIX B

ATMOSPHERE TEMPERATURE

OBJECTIVES

It is the objective of this experiment to measure the Cytherean atmospheric temperature as a function of altitude, location, and time in conjunction with simultaneous measurements of the pressure, density, and composition. Remote observation of microwave emissions from Venus has resulted in several temperature models for the surface. Infrared radiometry and thermal mapping of Venus from Earth and Mariner II has provided data from which atmospheric temperature profiles could be inferred. The overall temperature extremes in these models are 235 to 750°K from cloud top to surface. Direct temperature sensors carried on the buoyant station or in a drop sonde should cover a range of 200 to 800°K. Presently developed platinum resistance thermometer sensors are adequate to directly measure temperature over this range in an atmosphere sufficiently dense to support the buoyant station. Since all station or sonde velocities are anticipated to be subsonic during measurement, no special Pitot or other devices will be necessary.

EXPERIMENTS/INSTRUMENTS

Platinum Resistance Thermometers

Platinum resistance thermometers contain a coil of pure, annealed platinum wire wound and supported so it is not subjected to mechanical strain caused by differential thermal expansion. Platinum resistance devices have their optimum operating range over 100 to 800°K and are generally superior over this range to other temperature sensing devices. The Rosemount Engineering Company Model 177 sensor is typical of such an instrument designed for spaceflight use and connection to a telemeter. The four-element bridge, of which the platinum resistance sensor forms one leg, together with a regulated power supply are packaged with the sensor in a single unit. To obtain heat accuracy over the desired range, two instruments can be used with ranges of 100 to 450°K and 400 to 800°K.

APPENDIX B

Physical characteristics. - The Rosemount Model 177 as packaged would not be suitable for this application. Because of the temperature environment anticipated, the bridge and voltage regulation circuitry would require repackaging and installation in a thermally controlled environment separate from the deployed sensing element. The platinum sensor element is extremely small and light, about 1 oz, 0.1 in. diameter, and 0.1 in. long. The weight and size of the required housing and deployment device are not included in these numbers. The separately packaged circuitry would weigh about 0.15 lb and occupy a volume of 1x1x2 in. Housing for the sensor element might weigh about 0.1 lb.

Operational requirements. - The instrument requires 28 Vdc at 0.2 W of power. Some warmup time is required to allow the joule heating of the platinum element to come to equilibrium.

The output of the instrument is 0 to 5 Vdc analog. Conversion to digital form would occur external to the instrument with a 7-bit data word providing sufficient accuracy.

The circuitry electronics operate in a temperature range of -25 to +85°C.

The sensor element will require deployment away from the atmosphere heated or cooled by the station. Means must be taken to shield the sensing element from solar radiation.

Operational limitations. - The two sensors have overlapping ranges of 100 to 450°K and 400 to 800°K. Temperatures beyond these range limits will not harm the sensors. With proper bridge circuit design and voltage regulation, the platinum element gage factor over the ranges selected will result in an accuracy of ±1% of full scale where a 7-bit data word is used. This accuracy is sufficient to satisfy objectives. The efforts of solar radiation and thermal wash from the station are possible sources of error, and proper deployment and shielding must be considered. Effects of solar radiation are minimized by the low thermal mass and the high reflectivity of the sensor.

Development status. - The temperature sensing system discussed above is well within the state of the art. The only development effort anticipated would be in the realm of sensor radiation shielding and deployment.

APPENDIX B

A similar sensor was developed several years ago by REC for NASA-Goddard as a candidate for use in a Martian lander. The instrument was again proposed by Ainsworth and Reber at GSFC for use on a Martian entry vehicle in November 1965. Present status is unknown, but no major problems in redevelopment for use on Venus are foreseen.

Thermistors

Thermistor temperature sensing devices are best applied over a range of about *400* to 700°K, although their consideration for use over 100 to 800°K is certainly feasible. The inverse temperature resistance characteristics of thermistors and other semiconductor temperature sensors is such as to make use of these devices over large temperature ranges impractical. One section of the characteristic displays a large, linear gage factor dR/dt for a small temperature increment, whereas the knee of the characteristic has a nonlinear shape requiring many calibration points over a more extended temperature range. These devices are advantageous because of their small size, low time constant, and large gage factors over small temperature ranges. To cover the range of interest in measuring the Cytherean atmospheric temperature, probably as many as seven thermistors would be necessary.

Physical characteristics. - The size and weight of thermistor elements for this application would be negligible since they are presently available from industry (Victory Engineering, General Electric, etc.) in barely visible sizes. The remotely located circuitry for the sensors consisting of bridge circuit and excitation voltage regulation circuits would weigh 1 lb and occupy a volume of 1x2x2 in.

Operational characteristics. - Thermistor temperature measurement systems for this application should operate on 10 or 28 Vdc at about 0.2 W of power.

The output of each thermistor measurement is 0 to 5 Vdc analog with external analog to digital conversion. A 7-bit data word accuracy would be sufficient.

The sensors would require deployment beyond the thermal effect of the station. Some protection from solar radiation would probably be necessary.

APPENDIX B

The circuitry associated with the remotely located sensors requires thermal control within -25 to +85°C.

Operational limitations. - Because of their temperature resistance characteristic, the application of thermistors could be limited to the range of 275 to 325°K with other sensors such as platinum resistance thermometers and thermocouples being used for other portions of the overall atmospheric temperature range.

Development status. - No significant develop problems are foreseen. Some development effort would be required in sensor deployment and shielding techniques.

Thermocouples

The use of thermocouples for temperature measurement has certain advantages over other devices where the temperature-sensitive zone must be small, the temperatures are relatively high, and the installation requires flexibility. All of these requirements could be imposed by the Venusian atmospheric temperature measurement task. Thermocouples would be an optimum temperature sensing approach for the 800 to 1000°K temperatures that might be encountered by a sonde at the Venusian surface. Thermocouples, of course, require reference junction temperature compensation and amplification of output signal. Over the past several years, the development of RV compensation using thermistors in bridge circuits rather than the older fixed temperature oven approach has resulted in more reliable, smaller, and lighter thermocouple system circuitry for spaceflight applications.

Physical characteristics. - The size and weight of the thermocouple would be negligible. The remotely located circuit electronics for a thermocouple would weigh about 4 oz and occupy a volume of 1x2x2 in.

Operational characteristics. - The thermocouple measurement system would operate from a 28 Vdc supply and require 0.25 W of power.

The output of the thermocouple system will be 0 to 5 Vdc analog. Analog to digital conversion will occur external to the system, and 7-bit data words will provide sufficient accuracy.

The remotely located electronics will require a thermal environment of 0 to 50°C.

APPENDIX B

The thermocouple must be deployed a sufficient distance beyond the thermal wash of the station.

Operational limitations. - Thermocouples could be satisfactorily used over the entire range of 100 to 800°K. Two thermocouple systems would provide optimum coverage. One system would employ copper-constantan from 100 to 600°K. The other system would be chromel-alumel from 500 to 800°K.

Development status. - A deployment technique for the sensors would require development effort. No development problems are anticipated.

RFA TEMPER URE

OBJECTIVES

The present controversy and the importance of surface temperature to theoretical models of Venus and to the possibility of life makes its measurement a requirement for any Venus mission. Primary consideration should be given to measurements at the subsolar and antisolar points and a pole. Secondary objectives would be to measure the large- and small-scale horizontal variations and to search for cool spots (e.g., high mountain peaks).

EXPERIMENTS/ INSTRUMENTS

There are several methods of determining the surface temperature from a BVS. The most straightforward way would be to extrapolate the atmospheric temperature measured from a drop sonde, or perhaps measure the atmospheric temperature at the surface from a parachute-landed drop sonde. However, a large number of sondes would be required to determine the horizontal variations by this method.

Another method would use an IR radiometer on a drop sonde that has penetrated the base of the cloud layer, if the cloud layer does not extend to the surface. This method also gives only local temperatures unless many sondes are used.

APPENDIX B

A microwave radiometer ($2\ cm \lesssim \lambda \lesssim 10\ cm$) on the BVS could measure the brightness temperature and thus infer the surface temperature and the horizontal variations. However, the interpretation of the observations is subject to the same ambiguities as the Earth-based microwave measurements because of the uncertainty in the origin of the microwave emission.

Thus, to measure both the absolute surface temperature and the horizontal variations, several experiments are necessary. It is proposed that all three experiments mentioned above be used -- temperature sensors and IR radiometers on drop sondes and a microwave radiometer on the BVS. A simple microwave radiometer on a drop sonde would be a valuable experiment to differentiate between the microwave emission from the surface and that which may originate in the lower atmosphere or clouds.

Infrared Radiometer

An IR radiometer operating in an atmospheric window should provide a good indication of the surface temperature once the drop sonde has penetrated the cloud layer and of the cloud temperature while in the layer.

The radiometer would be similar to the Mariner II instrument (ref. 85). It is estimated that such a radiometer could be designed to weigh less than about 2 lb with a power requirement of less than 2 W. No development work on such an instrument has been done.

Weight	5 lb
Power	3 W at *2400* cps
Size	7x5.5x3 in.
Data	10-bit samples, 600 bit/measurement

APPENDIX B

Microwave Radiometer/Surface Imager

The Mariner II microwave radiometer (ref. 86) is representative of this type of instrument. The instrument used on the BVS would be electronically scanned to give a thermal map of the surface. The development status of this instrument is not known but estimated characteristics (refs. 87 and 88) are tabulated below.

Wavelength	3 cm
Weight	25 lb
Power	10 W average
Size	3 ft by 3 ft by 2 $in.^2$ antenna 1 ft by 1 ft by 9 in. electronics

The antenna size given above corresponds to a radiometer for use on a flyby vehicle. Since the BVS will be much closer to the surface, a much smaller antenna (e.g., 1 ft by 1 ft by 2 in.) can be used to get the same resolution.

ATMOSPHERIC DENSITY

OBJECTIVES

The determination of the atmospheric density profile is of importance to the optimization of entry vehicle design. If the mean molecular weight is known, the density can be obtained from measurements of pressure and temperature. However, independent measurement of the density is to be preferred.

Acoustic Transmission Line Densitometer

An acoustic transmission line densitometer has been developed for measurements on Mars (refs. 89 and 90). With minor modifications, such as reduction of the microphone spacing to accommodate a wider dynamic range, this acoustic transmission line densitometer can be used to determine the Cytherean atmospheric density ρ, molecular weight $\bar{M}$, and the specific heat ratio $\gamma = C_P/C_V$. The velocity of sound in a gas is given by,

APPENDIX B

$$C^2 = \frac{\gamma RT}{\bar{M}} \text{ or } \frac{\bar{M}}{\gamma} = \frac{RT}{C^2} \tag{B1}$$

where R is the gas constant and T is the absolute gas temperature. In the acoustic transmission line densitometer, the absolute temperature T is known and the velocity of sound is measured with two microphones which are a fixed distance apart. Therefore, $\bar{M}/\gamma$ can be determined. During the sound velocity measurement, the acoustical impedance $Z = \rho_1 C$ of the gas will also be measured in the test tube. This yields the density $\rho_1 = Z/C$ in the tube of the densitometer. If the absolute tube temperature T_1 and the absolute ambient temperature T_2 are known, then we can determine the ambient density,

$$\rho_2 = \rho_1 \frac{T_2}{T_1} \tag{B2}$$

Knowing density and temperature of the ambient gas, and applying the gas law, the mean molecular mass can be determined,

$$\bar{M} = \frac{\rho RT}{P} = \frac{ZT_2R}{CP} \tag{B3}$$

Because $\bar{M}/\gamma$ has been obtained from the sound velocity measurement, the mean specific heat ratio, $\gamma = C^2M/(RT_1)$, can now be determined.

The proposed technique is to measure the velocity of sound through the gas spiral tube about 2 m long and 1 cm in diameter. For ease in illustration, figure 24 shows a linear arrangement of this tube. At one end of the tube, a generator drives a small sonic transducer at a constant frequency of about 4 kc. Two identical condenser microphones are placed along the tube with a nominal 4 wavelength separation. Both microphones resonate above 10 kc and form part of the wall of the tube. The test tube is extended beyond the second microphone and is acoustically terminated by damping material and rough wall surfaces to avoid reflections and standing waves in the tube. Since the two microphones and their amplifiers are identical, their phase shifts cancel each other. The phase shift as measured by the phase comparator is determined only by the wavelength of sound in the medium and, since the generator frequency is constant, by the velocity of sound in the gas.

APPENDIX B

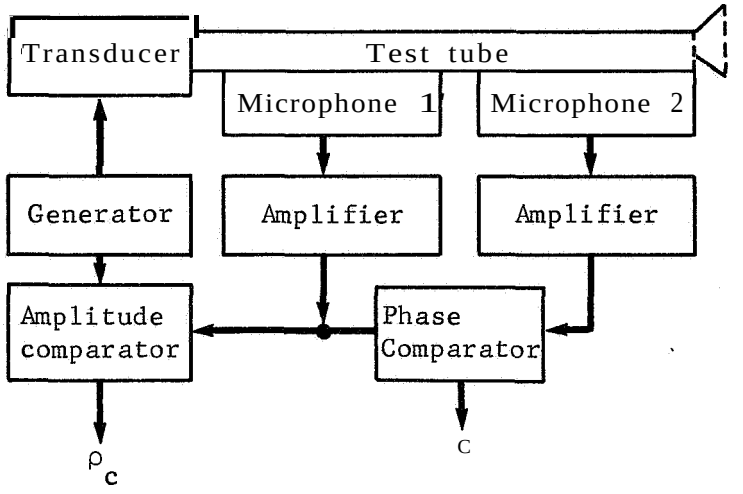

Figure 24. - Block Diagram of the Acoustic Experiment (ref. 90)

In addition to the determination of the speed of sound, the instrument is capable of measuring the density of the gas in the tube. The mechanical and electrical impedance of the sound generator are chosen so that the velocity of the diaphragm is essentially independent of the acoustic radiation impedance of the tube. Under these conditions the sound pressure developed in the air contained in the tube is proportional to the acoustical impedance. Since the microphone used responds to sound pressure, the electrical signal generated by the microphone is proportional to the acoustic impedance of the gaseous medium. This constant of proportionality, which also contains the transducer sensitivity, can easily be determined by calibration in an N_2 atmosphere over a nominal pressure range.

Physical characteristics. - The instrument is estimated to weigh 3 lb. In its present form, the dimensions are about 10 in. in diameter and 2.5 to 3 in. thick, including electronics.

Operational requirements and limitations. - Electrical power at 4 W is required for instrument operation. The gas temperature in the test tube must be measured or the test tube must be temperature controlled. The anticipated temperature range is -65 to +125°C. Good gas conduction between the sampling tube and the ambient atmosphere is required. The sampled gas should not be contaminated (ablation products, outgassing, etc.), and the sampling port must be arranged so that the effect of dynamic pressures on the test tube pressure is negligible.

APPENDIX B

Development status. - The instrument has been developed to the breadboard stage at NASA-Goddard under the direction of Dr. R. A. Hanel. Construction of a flight prototype should present no problem.

Other Densitometers

There are several other types of densitometers that rely on the absorption or scattering of radiation (beta, gamma, and X-ray) by the atmosphere. These types are advantageous for use on high-speed entry vehicles. The use of an RTG power source on the BVS would complicate the interpretation of data from these densitometers. Three typical instruments are summarized in table 19.

TABLE 19. - RADIATION SCATTER DENSITOMETERS

Type	Beta	Gamma	X-ray
Weight, lb	.8	5	10
Power, W	.2	5	25
Volume, cu in.	15	100	300

ATMOSPHERIC COMPOSITION

OBJECTIVES

A knowledge of the atmospheric composition is of prime importance to an understanding of the meteorology, the evolution, and the physical and chemical processes of the atmosphere; to the surface composition; to the possibility of life; and to the design of future entry vehicles. At present, CO_2, CO, HCR, HF, and H_2O have been identified spectroscopically as constituents of the atmosphere above the clouds. Nothing is known of the composition below the clouds although it is clear that CO_2 must be a major constituent. Spectroscopic searches for N_2O, CH_4, C_2H_4, C_2H_6, and NH_3 have been unsuccessful, and identification of O_2, NO_2, N_2O_4, and $(C_3O_2)_n$ is disputed. Estimates of the amounts of gases above the clouds are very uncertain, and the identity of the major

fraction of the atmosphere is unknown. Based on cosmic abundance arguments and terrestrial analogy, nitrogen is thought to be the major constituent with trace amounts of argon present.

The primary purpose of a composition experiment should be to search for and determine the partial pressures of major or important atmospheric constituents. Consideration should be given to CO_2, N_2, H_2O, O_2, A, He, Ne, and O_3. Secondary objectives should be to search for and identify trace constituents and volatile organic compounds; to obtain total pressure measurements; to obtain altitude profiles at different points in space and time; and to obtain indications of the composition of the clouds and surface. Supporting measurements of altitude, temperature, and pressure are required. Supplementary and complementary determinations of the composition by different experiments are desirable.

EXPERIMENTS/INSTRUMENTS

There are six classes of experiments that can be used to determine the composition of the atmosphere as shown in table 20. Within each class of instrument there are several different types. Several of these instrument types are described below.

Mass Spectrometers

Table 21 lists five types of mass spectrometers that have been used or proposed for use in space probes. A general description of the various types can be found in references 91 and 92. Detailed descriptions of the quadrupole and magnetic sector types are given below.

In general, the various types of mass spectrometers are similar in operating principle. Figure 25 shows a generalized mass spectrometer system and its major subsystems. A gas sampling subsystem is required to reduce the pressure of the ambient atmosphere ($\sim 10^4$ mb) to a value compatible with the inlet leak ($\lesssim$ 500 mb) and to prevent the mass spectrometer vacuum system ($\leq 10^{-5}$ mb) from becoming saturated. A small amount of atmospheric gas at the reduced pressure is allowed to flow through the inlet leak (−0.2 p diameter) into the ionization region. The use of such a molecular leak allows each gas to enter the instrument in proportion to its partial pressure. Ions are then formed by bombardment of the gas molecules with electrons from a hot filament.

TABLE 20. - ATMOSPHERIC COMPOSITION INSTRUMENTS

Instrument class	Principle	Parameter measured
Mass spectrometers	Magnetic and/or electric fields separate ionized atmospheric gases according to mass	Ion currents proportional to partial pressures of atmospheric gases
Gas chromatographs	Gases have composition dependent mobilities in sorbtive columns	Times of emergence from column gives composition, height of peaks gives amount
Single gas detectors	Specific property or reaction of gas used to determine its presence	Abundance of A, N_2, H_2O, CO_2, O_2, O_3 or other selected gases
Absorption spectrometers, spectrophotometers or radiometers	Solar radiation intensity measured as function of wavelength; atmospheric gases absorb at characteristic wavelengths	Presence of characteristic absorption line or band indicates presence of gas in atmosphere, intensity indicates amount
Emission spectrometers, spectrophotometers, or radiometers	Atmospheric gases emit radiation at characteristic wavelengths	Presence of characteristic emission line indicates presence of gas
Acoustic transmission line	Wavelength of sound and acoustic impedance in sample of gas in tube measured	Gas density, mean molecular weight, and specific heat ratio

TABLE 21. - MASS SPECTROMETER TYPES

Type	Principle of mass separation
Quadrupole	Superposed radio-frequency and static electric fields
Single focusing (magnetic sector)	Magnetic field perpendicular to ion paths
Double-focusing (magnetic and electric sectors)	Electrostatic energy separation followed by magnetic separation
Radio frequency	Resonant grids in ion paths
Time of flight	Time of flight of ions through grid structures

The resulting ions are focused into a beam and directed into the analyzer section where they are separated according to mass. The ions emerging from the analyzer section are collected and measured as an ion current proportional to the partial pressure of the gas to which the ion corresponds. The ion current is then processed and converted to a digital form.

Quadrupole Mass Spectrometer

Figure 26 shows a schematic of the quadrupole mass spectrometer. The analyzer section, in this case, consists of four parallel cylindrical electrodes (ideally hyperbolic in shape). Opposite electrodes are connected as shown in figure 27 and dc and rf voltages are simultaneously applied. The ions, which are injected parallel to the analyzer rods, are acted on by the superimposed electric fields and acquire complex oscillatory motions described by Mathieu's differential equations. The trajectories are stable or unstable depending on the rf, the rf and dc voltages, the dimensions of the quadrupole, and the charge-to-mass ratio of the ions. By a suitable choice of these parameters, all ions except those with a desired range of charge-to-mass ratios acquire unstable trajectories and are removed from the beam by collision with the electrodes while those with the selected m/q ratios proceed through to an ion collector giving a current proportional to their partial pressure. The mass spectrum is swept by varying the voltages or the radio frequency.

The ion collector is a solid-state semiconductor device with an input current range from 10^{-14} to 2×10^{-10} A covered by two automatically switched, overlapping ranges. The output is logarithmically compressed into a 0 to 5 V analog range.

The quadrupole mass spectrometer described below is capable of determining the partial pressures of gases with atomic masses between 11 and 45 amu. This range can be shifted to about 200 amu by redesigning the electronics if desired.

Two general methods for sampling the mass range are the continuous sweep mode, where all of the masses in any chosen mass range can be sampled, and the stepped mode, where several masses are chosen for investigation and sampled sequentially by stepping from one mass to the next. Both schemes will be used with the stepped mode being the primary. The gases to be investigated in the stepped mode are: H_2O (18), N_2 and CO (28), O_2 (32), A (40), CO_2 and N_2O (44), and their dissociation products C (12), N (14), and O (16). In-flight calibration can be performed by injecting a sample containing the five gases listed above.

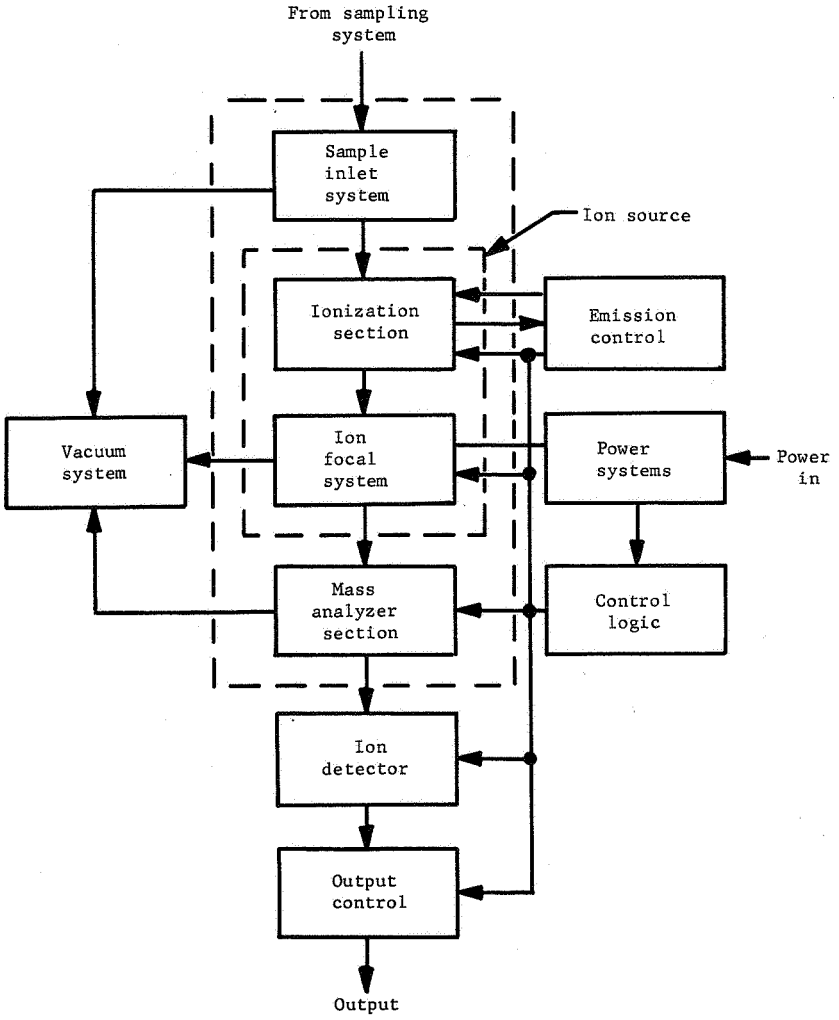

Figure 25. - Mass Spectrometer System

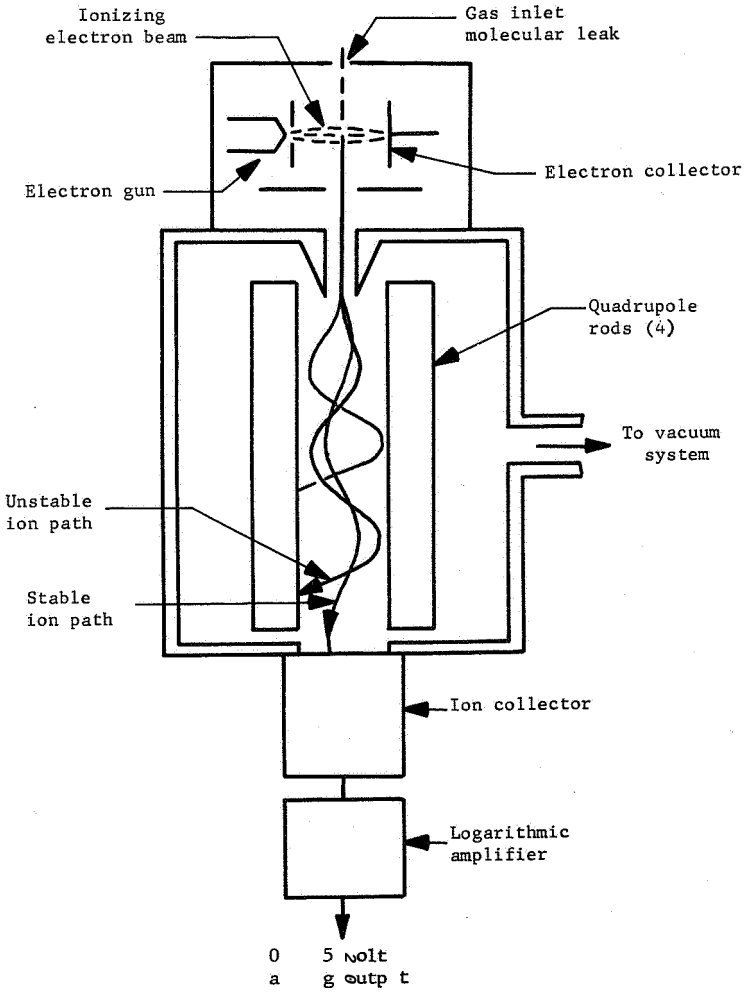

Figure 26. - Quadrupole Mass Spectrometer

APPENDIX B

Physical characteristics. - The instrument weighs about 8 lb plus the gas sampling system, which may weigh about 2 lb. The size is 8 1/8 by *14* by 2 13/16 in. excluding the gas sampling system but may be tailored for specific applications. All materials and components are heat sterilizable. Figure 28 shows the instrument that was developed for use on a Martian entry vehicle.

Operational requirements. - The mass spectrometer requires 28 V ± 10%, 10-W average, 15-W peak power input. The power in failure is 21 W. Some warmup time for the hot filament ion source is necessary. Power requirements for the sampling system are unknown at present.

The inputs from and outputs to the data system are as follows:

1) Inputs,
   a) Turn-on/turn-off command,
   b) Clock stop command to inhibit cycling for test purposes,
   c) Continuous mass scan control for test purposes,
   d) Stepped or swept mode control,
   e) Calibration command;
2) outputs,
   a) Detector (ion collector output),
   b) Detector range indicator,
   c) Stepped or swept mode indicator,
   d) Mass marker,
   e) Ion source temperature monitor,
   f) Log diode temperature monitor,
   g) Regulated B+ monitor,
   h) High-voltage monitor,
   i) Filament-on indicator.

All outputs are 0 to 5 V analog and will be converted to digital form.

APPENDIX B

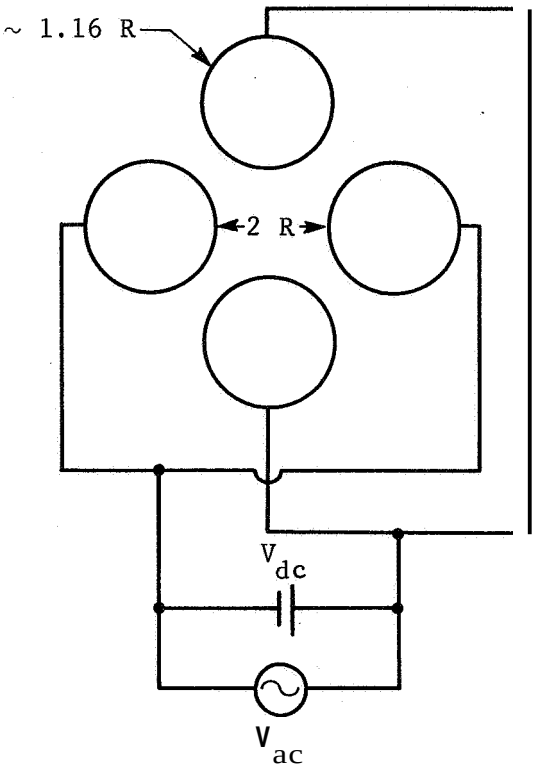

Figure 27. - End **View** of Quadrupole Electrodes

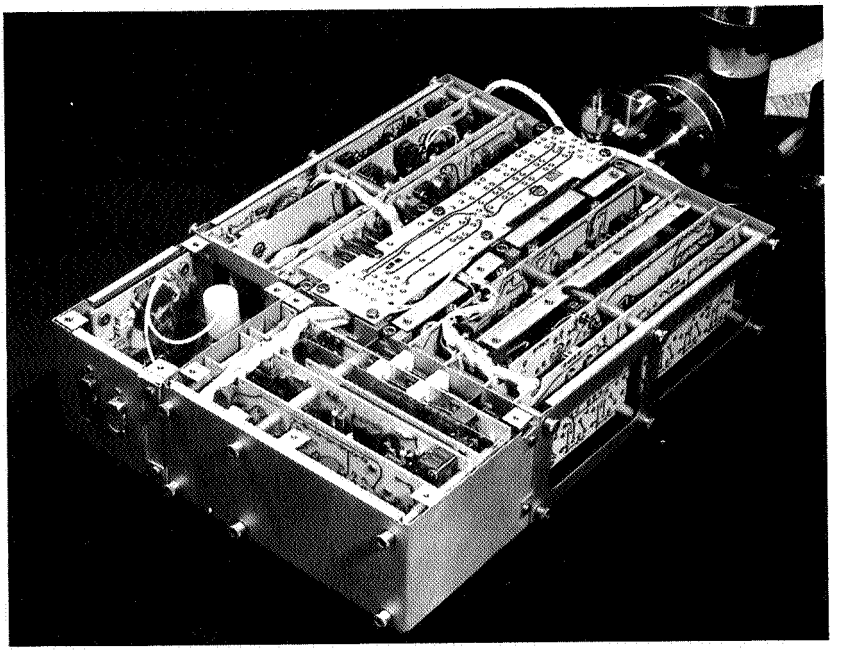

Figure 28. - Quadrupole Mass Spectrometer (Photo Courtesy of Scientific Data Systems)

APPENDIX B

Operating in the stepped mode, the instrument will measure the total ion current, the zero level, the ion currents for each of the eight masses, the zero level, and the total ion current during each measurement cycle. Since each data point requires 1 sec, this process takes 12 sec. Housekeeping data from outputs c) thru i) will be recorded before and after each measurement cycle. Measuring the detector output to 7-bit accuracy results in 84 bits/measurement; housekeeping data will contribute an estimated 28 bits for a total of 112 bits/measurement.

The mass spectrometer requires a sample of the ambient atmosphere. The gas sampling inlet should be placed so it avoids contamination by gases leaking from the buoyant device. (Nitrogen, ammonia, methane, hydrogen, or helium are possible contaminants.) This may necessitate the deployment of a long tube or hose unless a suitable technique for calibrating against the contaminants can be developed.

The electronics for the present instrument require a thermal environment between -10 and +65°C during operation. The gas sampling system should be kept at the temperature of the ambient atmosphere to prevent condensation of the gases.

Operational limitations. - The resolution is $\Delta m/m = 1/25$ for 1% crosstalk between adjacent peaks in the swept mode. Resolution in the stepped mode is $\Delta m/m = 1/20$ for a top-to-base width ratio of 0.5 and 1% crosstalk.

The lower limit of sensitivity of the quadrupole analyzer is about 10^{-9} mb. The sensitivity of the entire system is determined by the size of the inlet leak. The dynamic range of the detector is from 10^{-14} to 2×10^{-10} A or about 10^4.

The accuracy of the system for 7-bit data words is $\pm 4.5\%$ error in the knowledge of the ion currents. This allows the measurement of the ratios of any two partial pressures to $\pm 10\%$ accuracy, and the mean mass to be calculated to within 55%.

The mass spectrometer generates and is susceptible to high frequency (0.5 to 3 mHz) and stationary magnetic fields but shielding will minimize these effects.

As mentioned above, it is also susceptible to contamination by leakage gases. The presence of other gases in the atmosphere such as CH_4, C_2H_4, C_2H_6, and N_2O, which have the same m/q ratio

as the gases being investigated may cause false determinations. The use of other composition experiments will resolve these ambiguities.

The vacuum system is a 150 cc/sec sputter ion pump. The expected lifetime of the pump is not yet known.

Development status and problem areas. - The instrument was originally designed and developed by SDS Aerospace Systems (formerly CSC) for NASA's Goddard Space Flight Center and is currently available from SDS. The only major development necessary is in connection with a suitable gas sampling system.

The main advantages of the quadrupole type are its light weight and lack of magnetic fields. However, its requirement for stable radio frequencies and voltages make it slightly less reliable than the heavier magnetic sector type described below.

References 93 thru 95 describe quadrupole mass spectrometers used on rocket flights in the Earth's atmosphere.

Magnetic Sector Mass Spectrometer

This type uses a magnetic field to perform the mass separation. The ions entering the analyzer section with their velocity vectors perpendicular to a strong, uniform magnetic field are deflected into a circular arc. The radius of curvature of the arc depends on the magnetic field strength, the kinetic energy of the ions, and the mass of the ions. With the first two parameters held constant, ions with different masses will follow different circular paths as shown in figure 29. If the magnetic sector is preceded by an electric sector as shown in figure 30, the energy aberrations are reduced giving better mass resolution. The use of the electric sector allows a smaller magnet to be used.

Mass spectrometers of the double-focusing type have been used on Aerobee sounding rockets (ref. 96) and on the Explorer XVII satellite. The Explorer XVII instrument, which is described below, can be adapted for use on Venus by a suitable redesign of the inlet system and provision of a gas sampling system.

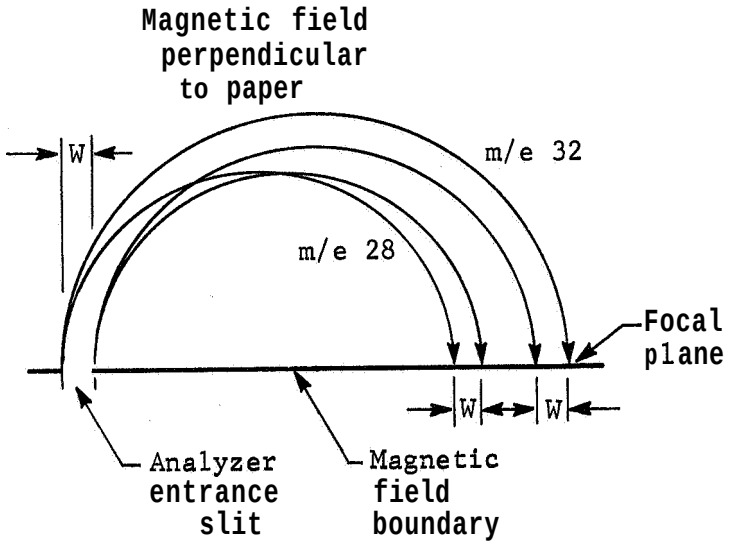

Figure 29. - Separation of Two Masses with Equal Energies and Entering Perpendicular to Focal Plane (Demonstration of Unity Magnification)

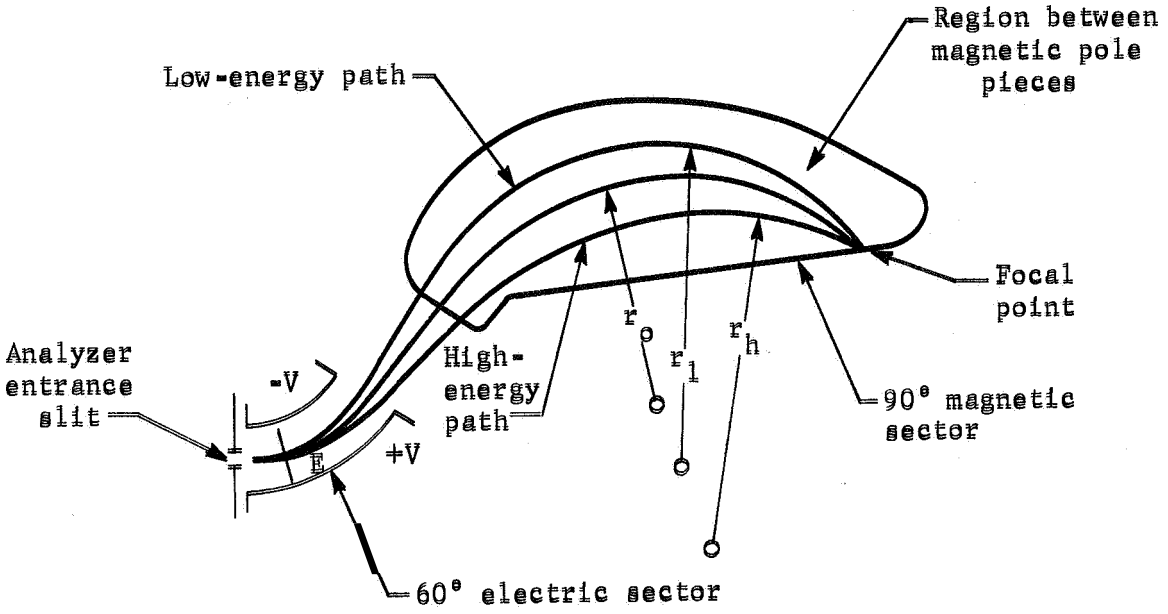

Figure 30. - Energy Focusing in a Double-Focusing Analyzer (ref, 92)

APPENDIX B

The Explorer XVII double-focusing mass spectrometer is fixed tuned to detect m/q ratios of 4, 14, 16, 18, 28, and 32 corresponding to He, N, O, H_2O, N_2, and O_2. However, for use on Venus, it should be tuned to 12(C), 14(N), 16(O), 18(H_2O), 28(N_2 and CO), 32(O_2), 40(A), and 44(CO_2 and N_2O). This would require eight detectors placed in a manner similar to that shown in figure 31. Swept tuning could be accomplished as in the Nier instrument (ref. 96) by sweeping the ion accelerator grid voltage. This reduces the resolution but increases the number of gases that can be investigated.

Physical characteristics. - The Explorer XVII instrument package weighed 22 lb, but the inclusion of a sputter ion pump to maintain internal vacuum and a gas sampling system for reducing the inlet pressure may increase the weight to about 26 lb. The approximate dimensions are shown in figure 32. Total volume of the spectrometer and associated electronics is less than 0.5 cu ft.

Operational requirements. - Power at 27 W, 28 Vdc is required for the mass spectrometer and its electronics. Power requirements for the sampling system are unknown.

The outputs of the eight detectors are compressed in a logarithmic amplifier to 0 to 5 Vdc outputs that are, in turn, converted to 7-bit digital words for telemetry. Housekeeping data bring the total number of bits per scan to about 150 bits.

Deployment and thermal control requirements are the same as for the quadrupole type.

Operational limitations. - The resolution is adjustable. Explorer XVII instrument gave $m/\Delta m = 11.7$ in the region of mass 30 for 2% crosstalk between adjacent peaks.

The minimum detectable partial pressure is about 10^{-11} mb in the ion source. The detectors are capable of detecting 5×10^{-16} A with two overlapping 4-decade ranges on a logarithmic amplifier giving a total dynamic range of about 10^7.

The instrument has a strong permanent magnetic field of about 1.0 to 2.5 kG near the magnet. Shielding can reduce this considerably.

The lifetime is one year (in satellite orbit) with minimum of 500 turn-ons.

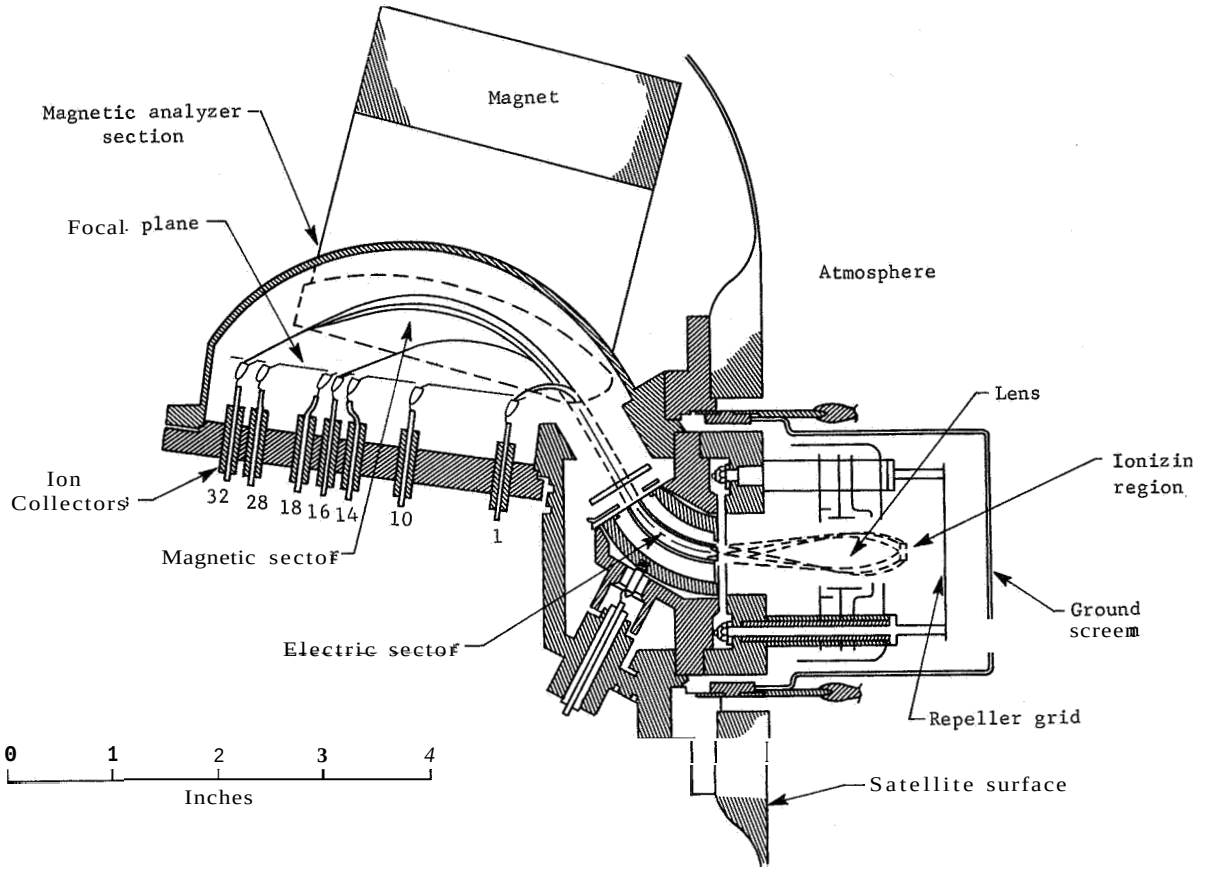

Figure 31. - Mass Spectrometer Configuration and Ion Path in X-Y Plane (ref. 97)

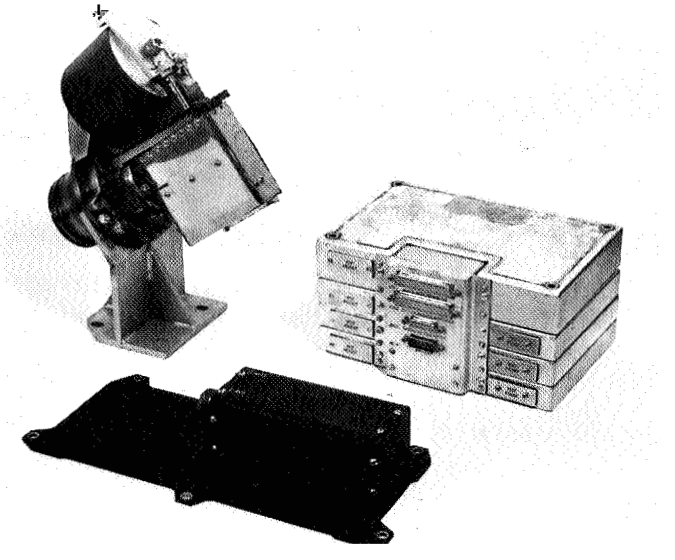

Figure 32. - Explorer XVII Instrument Package

Development status and problem areas. - The mass spectrometer described above was designed for use in a satellite. However, by adding a gas sampling system and a sputter ion pump, it could be adapted for use in the Cytherean atmosphere. SDS is working on an improved version that may weigh as little as 10 lb. This would be a very attractive choice for the buoyant station if there is no strong requirement for magnetic cleanliness. The inherently better reliability of the magnetic type over the quadrupole type may offset the additional weight of magnetic shielding. However, more information on the 10-lb magnetic type is needed before a tradeoff can be made.

Regardless of which type is the best choice, there are two major mass spectrometer subsystem developments that would be desirable. They are the development of a suitable gas sampling and inlet subsystem and the development of a field ionization ion source. The field ionization source eliminates the fragile, power consuming filament needed to generate the ionizing electron beam, also the breakup of complex molecules by electron bombardment ionization is greatly reduced with a field ion source.

Gas Chromatography

In a gas chromatograph, a sample of atmospheric gas is mixed with and transported by an inert carrier gas (e.g., helium) through a tube or column containing a material that allows the constituent gases to flow through at different rates. The material can be either activated adsorbing particles, liquid-coated inert particles, or a liquid coating on the walls of a capillary tube. The constituent gases have different affinities for the material in column. In the case of solid packing, the affinity is adsorptive; in the case of the liquid-coated packing, the affinity is related to vapor-liquid equilibrium. In either case, the constituent gases flow through the column at different rates so that the time it takes for each component to traverse the column is unique and reproducible. Therefore, each component emerges from the column at a given time after injection and is identified by its characteristic retention time. Detectors at the end of the column sense the presence of any gas other than the carrier gas and give an indication of the quantity. One major disadvantage is that a specific column packing may separate certain components but leave others unresolved. Therefore, several columns with different packing materials may be required to fully analyze the atmospheric composition. Another interesting possibility is to use a mass spectrometer in series with the chromatographic columns to separate components that neither instrument could resolve by itself.

APPENDIX B

There are two gas chromatographs being developed for use in planetary exploration. One is for the Surveyor program, the other is intended for analysis of the Martian atmosphere. Both can be adapted for use in the Cytherean atmosphere, although no work toward this specific end has been done.

Surveyor Gas Chromatograph

The Surveyor gas chromatograph was designed to be soft-landed on the moon to provide an analysis of the volatile constituents in a sample of the lunar surface material (refs. 97 thru 99). An oven is to be used to heat the surface sample and drive off any gases present. The use of such an oven for atmospheric analyses is not necessary but would be desirable for analysis of cloud or dust particles. For this reason, a modified Surveyor gas chromatograph is proposed as a candidate for determining atmospheric, cloud and dust composition, and the presence of organics.

Cloud and dust particles will be collected and placed in the oven that will then be sealed and heated in steps to ~500°C. The gases thus liberated at each step will be injected into a helium carrier gas stream as a short slug. The atmospheric gas sample will bypass the oven. The sample gas is then divided and transported through three parallel analytic columns by the helium carrier gas. The constituents of the sample gas are separated in the columns and the retention times for each component measured by glow discharge detectors at the end of each column.

The three columns allow 28 different components to be analyzed as follows:

Hydrogen	Butane	Hydrogen cyanide
Oxygen	Methanol	Benzene
Nitrogen	Ethanol	Toluene
Carbon monoxide	Propanol	Ammonia
Carbon dioxide	Acetone	Hydrogen sulfide
Water	Formaldehyde	Acetylene
Methane	Acetaldehyde	Acrolein
Ethane	Propionaldehyde	Formic acid
Propane	Acetonitrile	Acetic acid
		Butyric acid

The detector outputs, which have simultaneous high- and low-sensitivity readouts, are then processed for transmission. The transmitted data can be used to determine the identity and approximate

quantity of each volatile or gaseous constituent in the sample. One analysis requires 100 minutes to complete including the time required for oven heating and backflushing with the helium carrier gas.

Figure 33 shows a schematic of the gas chromatograph. A more detailed description of the operation can be found in references 97 and 99.

Physical characteristics. - The Surveyor instrument weighs 14 lb and is contained in a box 8x8x10 in. References 97 and 99 contain photographs of the instrument showing the construction. The instrument is heat sterilizable (125°C for 36 hr) and designed for immersion in ethylene oxide for 24 hr.

Operational requirements. - The instrument requires a maximum electrical energy supply of 24 Wh for each 100 minute analysis as follows:

1) Raw battery power,

   Voltage, 22 + 6/-4 Vdc,
   Maximum power, 72 W,
   Maximum current, 5 A,
   Energy drain, 22.1 W;

2) Regulated power,

   Voltage, 2 ± 1% Vdc,
   Maximum power, 0.44 W,
   Maximum current, 15 mA,
   Maximum energy, 0.75 Wh;

3) Special power (for detectors),

   Voltage, 1000 ± 10% Vdc,
   Maximum current, 100 mA.

A typical detector output signal is shown in figure 34. Because of the difficulty in automatic zeroing of the detector a derivative readout of the chromatographic peaks is used. A typical derivative chromatogram and its integral is shown in figure 35.

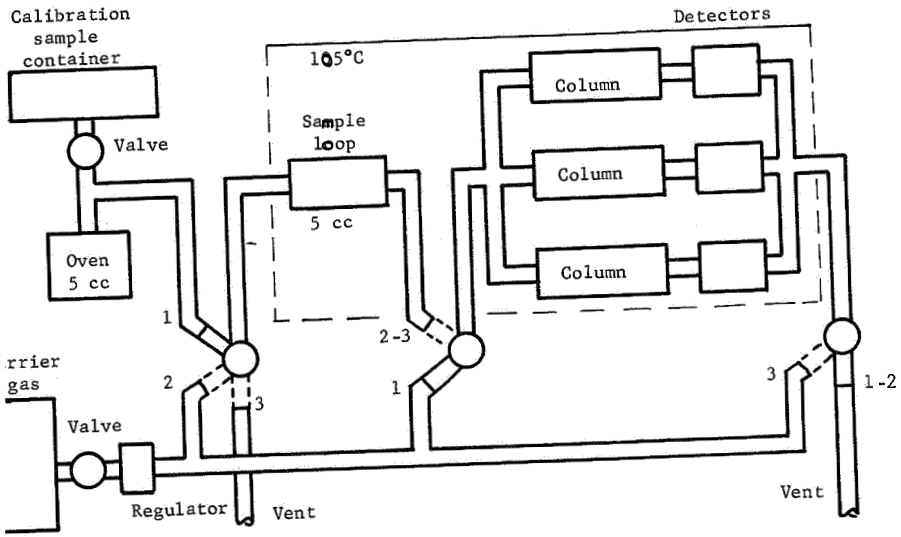

Figure 33. - Surveyor Gas Chromatograph Schematic

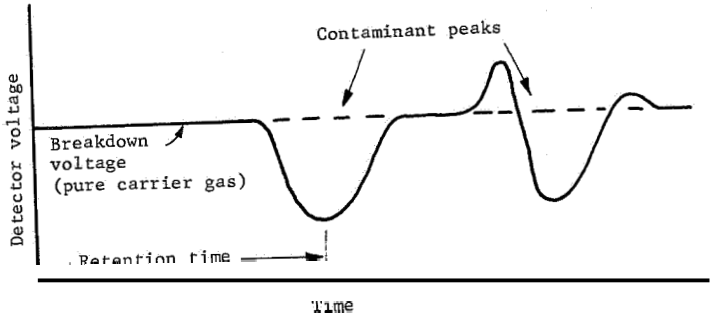

Figure 34 - Typical Detector Signal

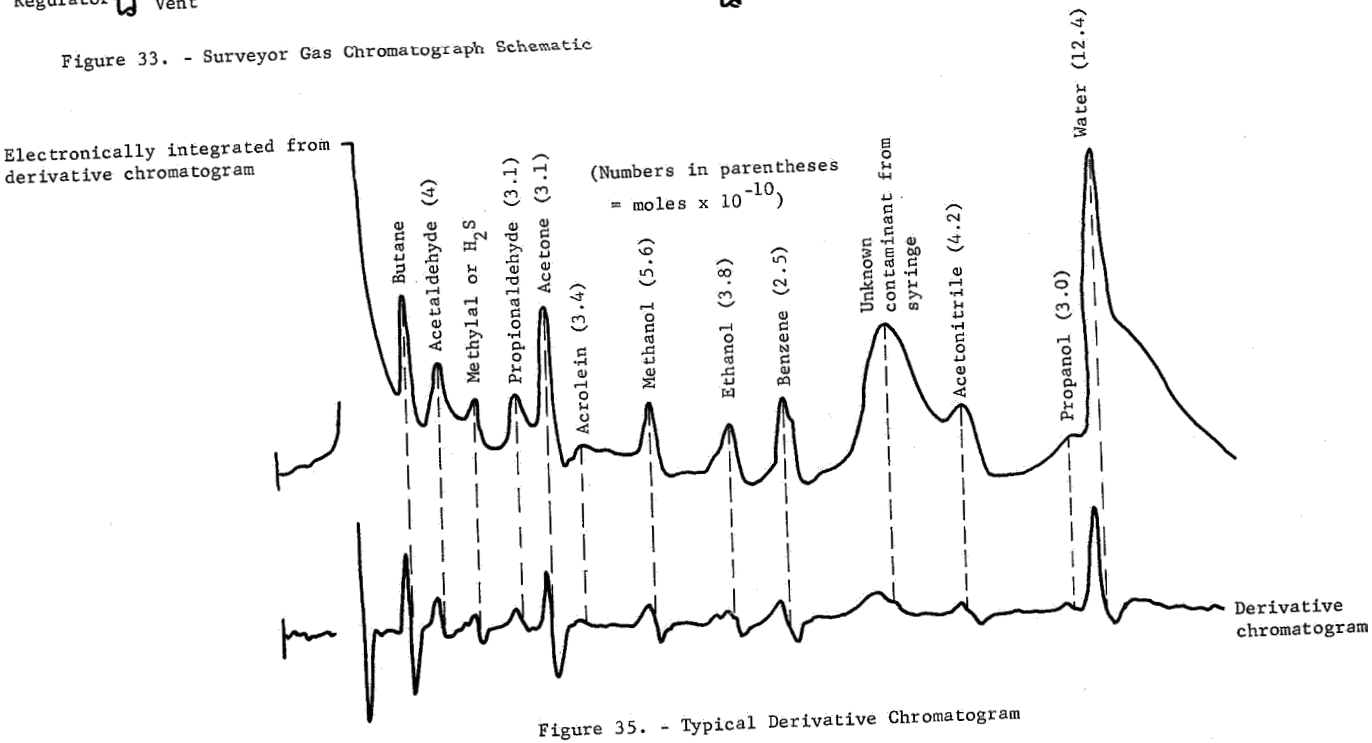

Figure 35. - Typical Derivative Chromatogram

Each column has a detector that is simultaneously read out at low and high sensitivity (100 times amplification of low). Therefore, six output channels are required. Seven bits per reading should suffice. Data on column temperatures, retention times, and carrier gas pressure are also required bringing the total number of bits per reading to 91.

If only the retention time (10 bits) and peak amplitude (7 bits) for each of the 28 gases is desired, the total number of bits per analysis is 632. Other housekeeping data may bring this to about 800 bits.

If a complete chromatogram such as is shown in figure 35 is desired, the total number of bits will be greatly increased (–10 000).

A sampling system to collect and deliver cloud and dust particles to the oven is required.

A thermal analysis of the gas chromatograph is given in reference 97. Briefly, the survival temperature range is -185 to +125°C and the operating temperature range is -50 to +125°C.

Operational limitations. - The instrument satisfactorily resolved all of the 28 components listed previously with the exception of formaldehyde, acetonitrile, hydrogen cyanide, carbon dioxide, hydrogen sulfide, and butyric acid. Further development work on the columns will allow these components to be resolved.

The minimum detectable quantity in the oven is 3×10^{-10} mole for each of the 28 components.

The minimum dynamic range of the combined high- and low-sensitivity detector channels is 10 000 times the minimum detectable quantity.

The Surveyor instrument is capable of twenty-one 100-minute analyses (limited by quantity of helium carrier gas and calibration sample gas).

Development status and problem areas. - Since the Surveyor instrument was designed to operate in the lunar environment, some redesign is necessary. The major redesign will be in the thermal control area to compensate for the difference in heat transfer properties in the lunar and Cytherean environments.

Redesign of the columns to separate gases other than the 28 previously listed (e.g., argon, $HC\ell$, N_2O, C_3O_2, etc.) will also be necessary.

Provisions for sampling the atmosphere and bypassing the oven will have to be made.

The Surveyor instrument was developed by Beckman Instruments, Inc., for JPL and a prototype delivered to JPL and tested in December 1962. The performance is described in reference 97. Present status is unknown; however, the instrument is not scheduled for use on any of the Surveyor flights (probably because of the high power requirements).

Micro Gas Chromatograph

This instrument is being developed by JPL for use during entry into the Martian atmosphere (refs. 100 thru 102). However, since it is designed to make a rapid analysis for only three gases (A, N_2, CO_2), its utility on a buoyant station is questionable. A brief description is given below (details can be obtained from refs. 100 thru 102).

Physical characteristics. - The instrument will weigh about 3 or 4 lb and be packaged in a box about 4x4x6 in. (including batteries and A/D signal conditioning).

Operational requirements. - Power requirements are unknown but 2 to 3 W should be sufficient. Data handling is discussed in reference 102.

Development status. - A breadboard model has been constructed and tested at JPL; a prototype is being assembled.

Melpar Gas Chromatograph

Melpar, Inc., has performed a study for JPL on the design and fabrication of breadboard and prototype models of a gas chromatograph for analysis of the Martian atmosphere (ref. 103). The instrument separates 12 components; the gases NH_3, CO_2, H_2O, H_2, N_2, O_2, A, CH_4, and CO can be quantitatively measured and N_2O, C_2H_6, and Kr can be detected. References 91 and 103 describe the performance and components in detail.

Physical characteristics. - It is estimated that the instrument will weigh about 5 lb and will be packaged in a box 5.5x5.5x 8 in.

Operational requirements. - Since column heating is to be supplied by a chemical heat source, the power required for the electronics is only 1.5 W. However, 4 W has been allocated for the operation, so that 2.5 W could be used for heating if desired.

Peak amplitudes and retention times for each of the 12 components are read to 7-bit accuracy as are column temperature and carrier gas pressure for a total of 336 bits/analysis. Allowing for housekeeping data gives approximately 350 to 400 bits/analysis.

The columns require an operating temperature of 333°C.

Operational limitations. - The detectors used are ionization cross-section types that are susceptible to ionizing radiation. Therefore, shielding from RTG radiation is necessary, unless another type of detector is used.

Development status. - Development by Melpar appears to have been discontinued on this particular instrument.

Gas Chromatograph Development at JPL

JPL appears to be the only NASA center actively engaged in developing gas chromatography for space exploration. The techniques of micro gas chromatography (ref. 100) are being used to develop impact hardened (–10 000 g) and sterilizable gas chromatograph components. Work is also aimed at developing a gas chromatograph for use in a pyrolysis/gas chromatograph/mass spectrometer system for detection of life-related compounds. The emphasis is on components rather than a complete system. However, these components could easily be assembled into a workable system once a specific application presents itself.

Without going into detail, it can be stated that development of gas chromatograph components is well underway (refs. 104 thru 106) and that these components could be assembled into a working system for use on a Cytherean buoyant station. The ideal system would be a combination pyrolysis/gas chromatograph/mass spectrometer for atmospheric, cloud, and dust composition and for detecting life-related compounds. Such a system might weigh about 15 lb and require 10 to 15 W of power.

APPENDIX B

Analysis by a-Particle Scattering

This instrument has been proposed by JPL to measure the three suspected major components (A, N_2, and CO_2) of the Martian atmosphere (refs. 91 and 107). N^{14} is detected by observing protons produced by a-particle bombardment:

$$ {}_7N^{14} + {}_2a^4 \longrightarrow {}_8O^{17} + {}_1p^1 \qquad (B4) $$

C^{12} $\left(\text{in } CO_2\right)$ and A^{40} can be measured by observing 180° Coulomb backscattering of the α- particles:

$$ E_S = E_o \left(\frac{A - 4}{A + 4}\right)^2 \qquad (B5) $$

where

E_S = energy of backscattered α

E_o = incidence energy of α

A = mass number of target nucleus $\left(C^{12} \text{ or } A^{40}\right)$

The experimental arrangement is shown in figure 36. Redundant N^{14} $\left(\text{in } N_2\right)$ and O^{16} $\left(\text{in } CO_2\right)$ measurements can also be made with the alpha-particle detector.

Physical characteristics. - Preliminary estimates of weight and power allocations are given in Table 22.

APPENDIX B

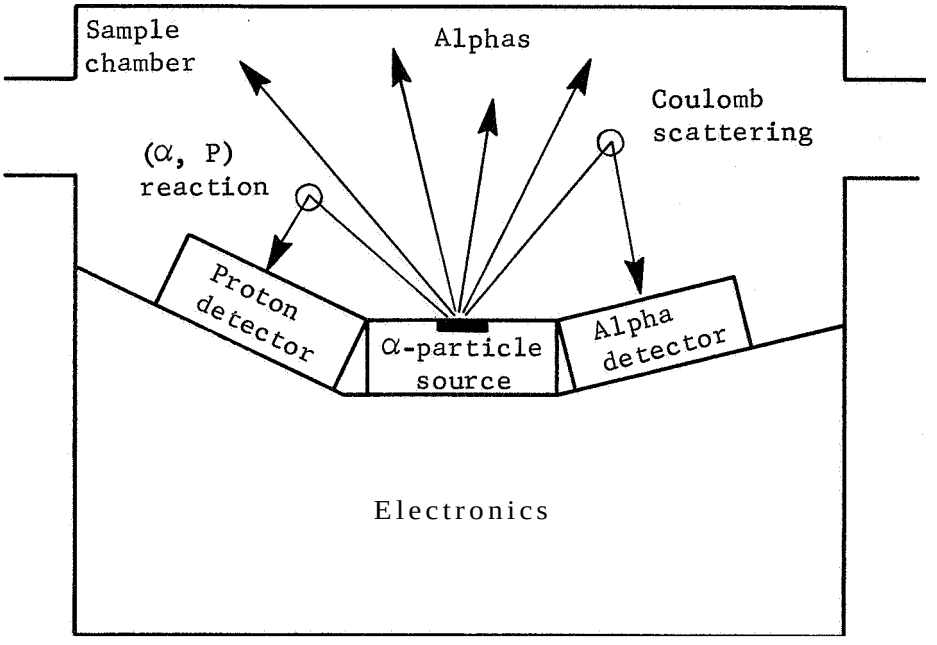

Figure 36. - Layout of Source, Sample, and Detectors

TABLE 22. - PRELIMINARY WEIGHT AND POWER ALLOCATION ESTIMATES

Unit	Power, MW	Weight, lb
Analog circuits	240	.5
Digital circuits and sequencing	235	1.0
Power supply	360	.5
Mounting for source and detectors		.5
Total	835	2.5

Operational requirements. - See Table 22 for power requirements. Six bit accuracy from each of 5 channels (C, A, N, O α detector and N proton detector). Reference 107 discusses the data handling in detail.

Operational limitations. - The instrument and sample must be protected from RTG radiation and cosmic ray and solar proton background.

APPENDIX B

Development status. - A breadboard model of the experiment was being assembled in *1964*, but present status is unknown.

Kryptonate Detectors

In this type of composition detector, radioactive krypton (Kr^{85}) is imbedded in a solid that reacts with the gas to be detected. The erosion of the surface of the solid by the reaction allows the previously bound Kr^{85} to escape. Thus, a measurement of the radiation level *(0.67* MeV betas) from the solid is a measure of the reaction rate of the gas with the solid. Gases such as ozone, sulfur dioxide, hydrogen sulfide, have been detected using this method. A kryptonate oxygen detector has been studied by Parametrics, Inc., for JPL (refs. 108 and 109). However, the characteristics of the instrument are presently unknown.

Single Gas Detectors

Many types of single gas detectors are being studied (see ref. 110) for use in the Martian atmosphere. These usually rely on some property or effect (not always unique) of the gas being sought for their operation. Such methods are not suitable for analysis of an unknown atmosphere of widely varying possible composition, at least not in the early stages of exploration. They are, however, very suitable for use as auxiliary experiments to confirm an analysis by mass spectrometry or gas chromatography. The characteristics of several (ref. 111) of these single gas detectors are given in table *23.*

TABLE 23. - SUMMARY OF COMPOSITION INSTRUMENTS

Instrument	Weight, lb	Power, W
Quadrupole mass spectrometer	10	15
Double focusing magnetic MS	10	15 to 20
Surveyor-type GC	*14*	*72* peak *(24* Wh)
Melpar-type GC	5	*4*
Pyrolysis/GC/MS (JPL)	15	10 to 15
α-particle scattering	*2.5*	1.0
H_2O	1.5	1.0
O_2	1.5	1.0
O_3	1.5	1.0
A	1.5	1.0
N_2	1.0	1.0
CO_2	1.0	1.0

APPENDIX B

The only information on A and N_2 detectors found in the literature (ref. 150) lists only the estimated weights and powers given in table 23. Nothing is known of the development status of these instruments.

Absorption Photometry

Solar pointing photometers with appropriate filters could be used to determine the atmospheric transmission as a function of altitude and, hence, the composition and cloud structure. The filters should be selected to pass radiation in the absorption bands of CO_2, H_2O, O_3, and O_2 and at one or two wavelengths outside the absorption bands. A study of the continuous absorption in the near ultraviolet ($A \leq 4000$ Å) would give information on scattering properties of the atmosphere. Silicon detectors could be used for the region 4000 Å $\lesssim A \lesssim 10\,000$ Å. The near: infrared to 3 μ could be covered by a PbS detector; PbSe (cooled) could be used to about 6 μ. Photomultipliers are necessary for the ultraviolet. Table 24 lists the estimated characteristics of photometers in the three spectral regions.

TABLE 24. - FILTER PHOTOMETERS

Spectral region	Visible	uv	Near IR
Weight, lb	.2 oz + .6 oz each	1.75	2
Power, W	.3	1.5	2

The light weight of the silicon detectors permits very good coverage of the visible region. Twenty detectors with integral filters and electronically switched sampling would weigh only 20 x 0.6 oz + 2 oz = 14 oz and require 0.3 W.

APPENDIX B

CLOUD COMPOSITION

OBJECTIVES

At present, there are strong indications that the clouds, or at least the upper layers, are composed of ice crystals. However, because of the high surface temperatures and pressures, it is possible that the lower clouds may be composed of exotic compounds. The analysis of such compounds would require a gas chromatograph or mass spectrometer. Other experiments such as an IR spectrometer or a water vapor sensor are also possibilities.

The primary objective is to determine the composition of the upper clouds. The composition of the lower clouds as a function of altitude, temperature, and pressure is a secondary objective.

EXPERIMENTS/ INSTRUMENTS

The instrumentation for determining composition has been discussed in the previous section. A cloud sampling and delivery system must be developed. Figure 37 shows one concept for collecting a cloud sample and presenting it in gaseous form to a gas chromatograph. The same system could be used for collecting dust particles, biota, or condensable gases. Such a system might weigh about 2 to 4 lbs and require less than 10 W.

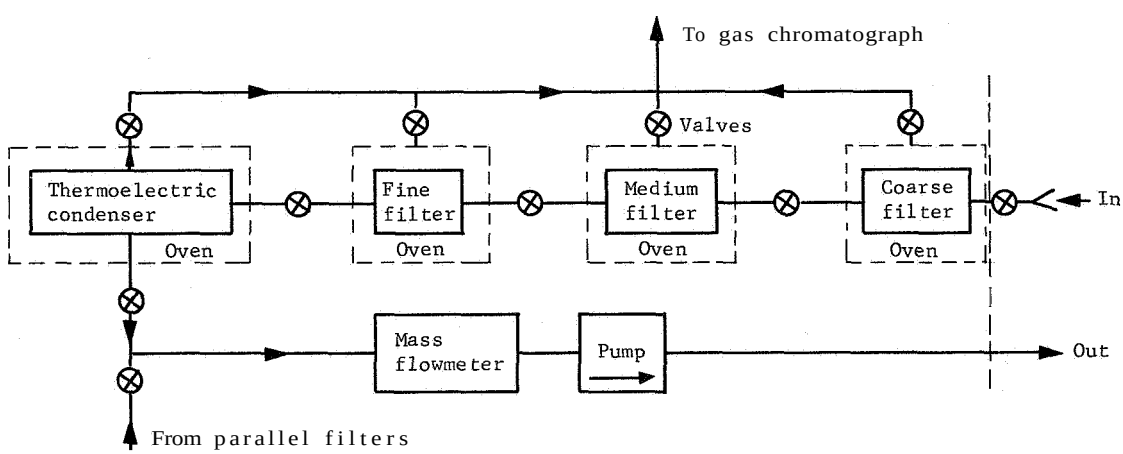

Figure 37. - Cloud Sampling System

APPENDIX B

There are two major problem areas in designing a system to present cloud samples to an analyzing instrument. The first is the separation of the sample in the form of particulates (e.g., solidified gases, dust) or liquid droplets from the atmosphere. The second is the concentration and conversion of the sample into a form suitable for analysis.

The collection of solid particulates can be accomplished with filters and blowers or electrostatic precipitators (ref. 112). The collection of liquid droplets is somewhat more difficult and will require a filter similar to a chromatograph column.

After the sample is collected it must be presented to the analyzing instrument in a suitable form and concentration. The solidified gas particles and liquid droplets can be vaporized easily and presented to a gas chromatograph or mass spectrometer for analysis. The dust particles (e.g., quartz) are not so easily vaporized and may require "wet" chemical analysis. Instruments similar to those proposed for lunar surface analysis (e.g., X-ray diffractometer, alpha scattering, or neutron activation) are also possibilities, Another method would be to examine the particulates with a petrographic vidicon microscope as discussed in the next section,

EXOBIOLOGY

OBJECTIVES

While the elucidation of the origin and evolution of life should be accorded the highest priority in the overall exploration of the solar system, a systematic investigation of life on Venus cannot be conducted intelligently until more is known of the environmental conditions existing below the Cytherean clouds. Indeed the determination of the physical and chemical conditions of the Cytherean atmosphere and surface as a potential environment for life should be the first step in a systematic biological investigation (ref. 113). Also, since the reluctance to assign high priority to the biological exploration of Venus is based mainly on the apparently high surface temperatures and the uncertainty in our knowledge of the environment below the cloud tops, an elucidation of these factors might completely alter the belief that Mars is a more likely abode for life than Venus.

APPENDIX B

Other goals of a biological exploration of Venus are (ref. 113):

1) Determination of whether life is or has been present on Venus;

2) Characterization of that life, if present;

3) Investigation of the pattern of chemical evolution, in the absence of life.

The realization of these goals is heavily dependent on a definition of the attributes of life and an understanding of the living state, as well as a knowledge of the Cytherean environment, The problem of describing life so that tests and experiments can be devised to search for extraterrestrial life is discussed in references 113 thru 115.

The dominant fact remains that no single life detection experiment or criterion can satisfactorily demonstrate the nonexistence or characterize the existence of extraterrestrial life. Unequivocal conclusions can only be formulated through the use of an automated biological laboratory -- the concept of which is not yet fully defined but is discussed in the references.

Thus, the systematic conduct of biological explorations and the intelligent design of experiments for such investigations requires some preknowledge of what is being sought and of the prevailing environmental conditions. Because of the uncertainties in the present knowledge of the Cytherean environment and of the possible life forms that might exist on Venus, it is proposed that the biological exploration of Venus be conducted (at least in the early stages) with the following specific goals:

1) Determination of the physical and chemical conditions of the Cytherean atmosphere and surface as a potential environment for life;

2) Determination of the organic composition of the atmosphere and of any dust present in the atmosphere and clouds;

3) Search for actual biota that may exist suspended in the atmosphere or attached to dust suspended in the atmosphere through the use of one or more experiments such as a vidicon microscope, a Gulliver growth experiment, or a Multivator experiment.

This last goal is accorded lowest priority for an early mission.

APPENDIX B

EXPERIMENTS/INSTRUMENTS

Determination of Environment

The experiments and instruments for determining the Cytherean environment are discussed in other sections of this report. Some environmental measurements that are relevant to the existence of life are:

1) Atmospheric and surface temperatures;

2) Pressure;

3) Major and minor atmospheric constituents, expecially organics;

4) Light levels as a function of altitude and wavelength, expecially in the uv;

5) Location of temperate zones on the surface.

Presence of Organic Compounds

Instrumentation for analyzing the organic content of the atmosphere and clouds has been described in the section on atmospheric composition. A discussion of gas chromatography and mass spectrometry as techniques for exobiology is given in references 116 and 117.

Life Detection Experiments

Many experiments have been proposed for the detection of extraterrestrial life or some manifestation of it. References 118 and 119 describe several of these experiments. Two typical life detection experiments that could be used on the BVS are described below.

Vidicon Microscope

The vidicon microscope, focused on dust and aerosols collected from the atmosphere, could provide details on the specific form, size, symmetry, optical properties, surface features, pigmentation, and internal structure of any micro-organisms present. In addition, the microscope could be extended to carry out microspectrophotometry and microfluorometry. This instrument would be a valuable tool for the analysis of the aerosols and dust particles themselves.

APPENDIX B

Figure 38 shows a simple, fixed focus, phase contrast microscope. The instrument, developed at Stanford and JPL, observes a 100-μ field of view with 0.5 μ resolution, which is imaged on the face of a vidicon tube. Such an instrument might weigh between 10 and 15 lbs and require 5 to 10 W.

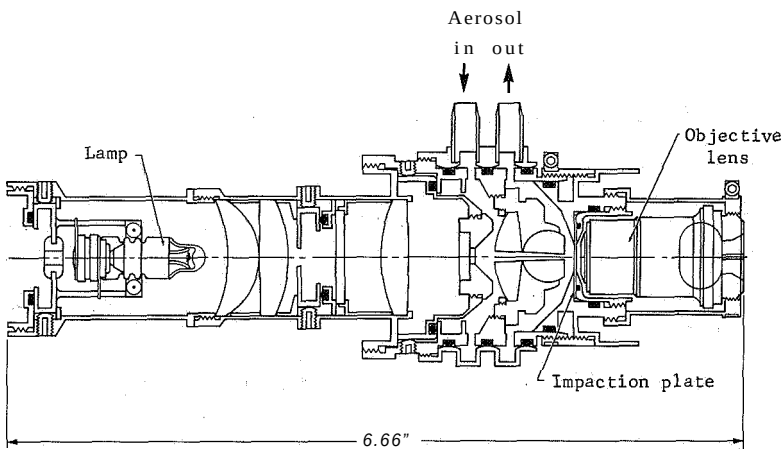

Note: An aerosol for carrying particles is injected into the instrument and is impacted onto the impaction plate through a nozzle implanted in the consenser lens. The objective lens and the lamp are fixed in relation to the plane of focus. The sample is collected through a gas-operated aerosol aspirator. The instrument has no mechanical moving parts (ref. 119)

Figure 38. - Abbreviated Microscope

More complex instruments could employ spatial and spectral scanning, automatic focusing, changes in magnification, moving-tape dust collectors, spectrophotometry, and fluorometry (ref. 120).

A more versatile instrument is described in references 121 and 122. This so-called petrographic microscope was developed at JPL for remote observation of crushed Lunar rock samples. The instrument could easily be adapted for observing particulate matter and any organisms collected from the Cytherean atmosphere. The estimated characteristics of such an instrument are given below.

APPENDIX B

Physical characteristics. - The microscope and sample handling subsystem would weigh between 5 to 8 lbs and could be packaged in an 8x8x3-in. box. The vidicon subsystem would weigh between 5 to 10 lbs and would be contained in a cylinder 3 in. in diameter by 8 in. long. The complete package would weigh about 10 to 18 lbs.

Operational requirements. - The sample handling subsystem would require about 40 W in 40-msec pulses for the stepping motors, 8 W for the encapsulation heaters, and 2 W for the light source. Total energy for encapsulating one sample and moving it into the field of view is about 2 Wh. Vidicon power is about 5 to 8 W.

For 200x200 element pictures with 6-bit picture elements (64 levels) the total data per picture is about 255,000 bits including synchronization, identification, and other diagnostic data. A total of about 20 pictures per sample is satisfactory (4 focus levels per field of view, 5 fields of view). This gives a total of 5.1 million bits per sample.

The vidicon faceplate must be kept below 40°C while taking and reading off pictures.

Operational limitations. - The tremendous amount of data generated is a major limitation on the feasibility of this instrument.

Development status, - The petrographic microscope is being developed at JPL (refs. 121 and 122). A vidicon microscope suitable for observing dust particles and organisms could be developed using the same techniques. The design of a sample collection and delivery system presents the main problem.

Minimum Biological Laboratory (MBL)

This instrument incorporates several different approaches to life detection, namely, metabolism and growth. The following experiments have been proposed (ref 123) for integration into a single package:

1) Metabolism of radioactive substrates and evolution of labeled gases;

2) Detection of photosynthesis, heterotropic-autotropic system;

3) Detection of photosynthesis, autotropic system;

4) Firefly bioluminescent assay for microbial ATP;

5) Metabolic uptake of phosphorus;

6) Metabolic uptake of sulfur.

A detailed description of each experiment is given in reference 123. The MBL requires a sizable sample of dust. This could be collected by filtering dust, aerosols, biota, etc., out of the atmosphere over a period of days or weeks, Figure 39 is a schematic of an MBL taken from reference 123. Since the experiment was proposed for use on a Mars lander, several experiments are shown deployed on the surface. However, these experiments could be performed as well on a sample of dust collected from the atmosphere. Tentative specifications for the instrument (exclusive of a sampling system) are given below.

Physical characteristics. - The instrument package volume would be in 1200 cu in. (11x11x10 in.) and would weigh 18 ± 3 lbs.

Operational requirements. - The instrument requires 10 W maximum power and 30 W-min total energy for operation. Thermal control power is necessary to maintain cultures between 5 and 15°C. Data is read out at 0, 3, 10, 20, 30, and 100 hr from 9 channels at 50 bits/channel per readout for a total of 2700 bits,

Development status. -*The MBL is merely a concept at present but the development of the biological techniques is well underway at Hazelton Laboratories, Inc., and several NASA research centers,

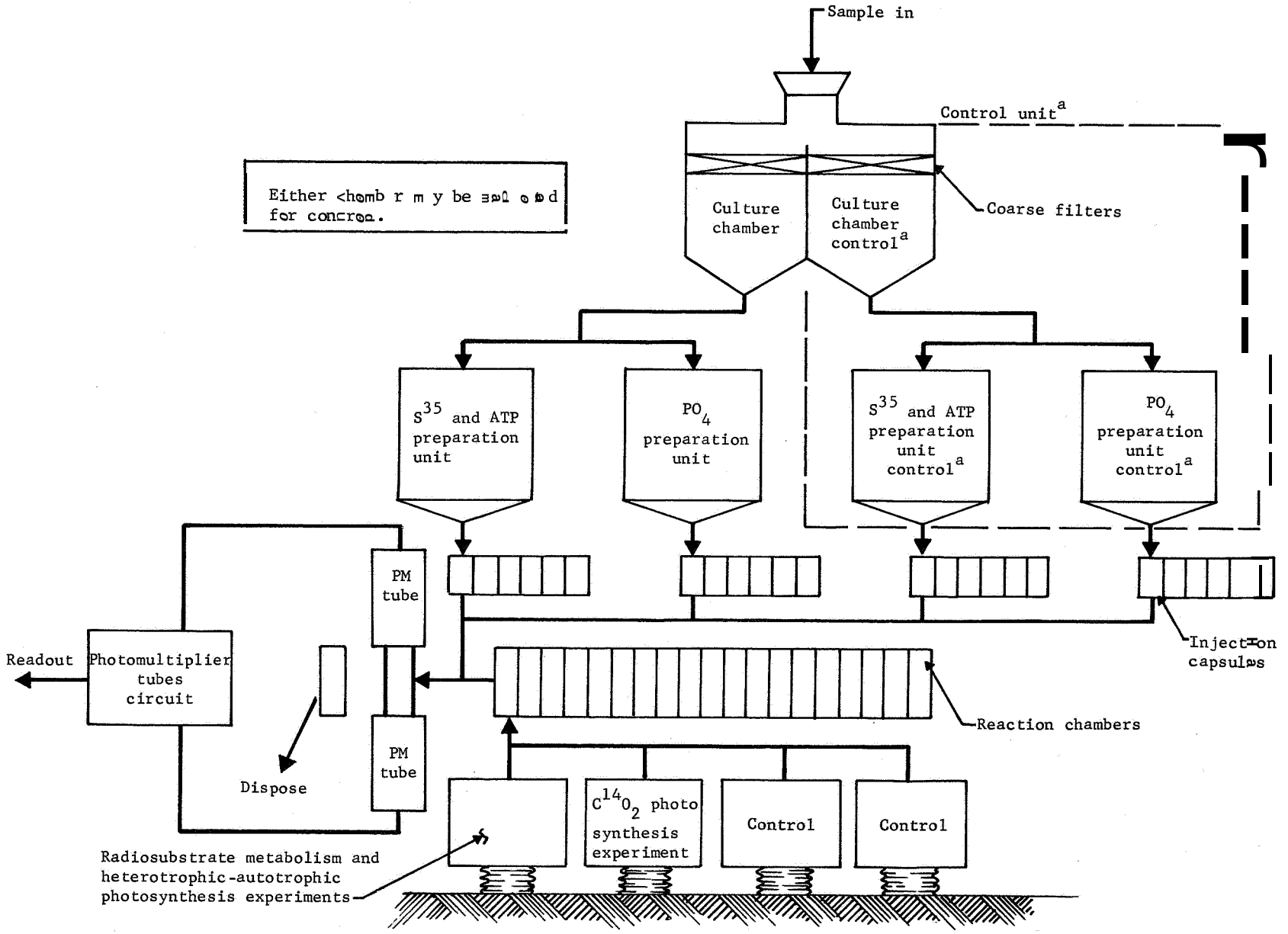

Figure 39 - MBL Schematic (ref. 123)

APPENDIX B

WINDS

OBJECTIVES

Virtually nothing is known about the atmospheric circulation of Venus. Wheel spoke markings observed in the visible emanating from the subsolar point have been interpreted to be caused by high altitude wind streams. Also, observations of time variable IR temperatures suggest that the cloud tops are in a state of turbulence. The development of large-scale theoretical circulation models has yielded mean wind velocities of from a fraction of 1 cm/sec to 8 m/sec. These studies reveal that the general circulation will be in the meridional direction from the subsolar point to the antisolar point.

The objective of the wind experiment is to measure the mean wind velocity and direction at altitudes from above the cloud tops to the surface. Such information, although limited in quantity by the gathering capability of only one station, will contribute toward understanding the Cytherean circulation and toward providing design data for future missions.

EXPERIMENT/INSTRUMENTS

Several experimental approaches exist for measuring wind parameters from the buoyant station aside from the tracking of the station from the orbiter. They are (1) use of a radar-altitude-Doppler-velocity-system (RADVS) on the buoyant station, (2) deployment of radar targets from the station, and (3) deployment of a special drop sonde from the station.

All of these methods assume positional knowledge of the buoyant station with respect to planetary coordinates.

Tracking and Position of the Station

Description. - Positional tracking of the buoyant station from the orbiter together with employment of RADVS equipment from the station will permit determination of mean wind velocity and prevailing direction at the station altitude. Orbiter position will

be tracked from Earth and become better defined for each orbit. The orbiter will interrogate a transponder on the station to obtain the ranging information necessary to determine the station position. Since motion of the station will caused by wind circulation at the 70 km altitude, tracking data will describe the general direction of the prevailing winds.

The RADVS equipment located in the station will determine the station altitude and velocity. The velocity components sensed are referenced to the three principal axes of the station. The resultant velocity vector may, therefore, be defined. However, its direction relative to planet coordinates must be obtained from the above-mentioned station tracking method.

Physical characteristics. - The RADVS will weigh 50 lb including antenna, It is anticipated that the electronics will require a 10x10x10-in. volume. The antenna (single, multifeed dish) will be about 3 ft in diameter.

Operational requirements. - The RADVS equipment will operate from the station 28 vdc bus and require 100 W when operating. Several operation periods per day of about 15 minutes duration each are anticipated. Several minutes warmup for the klystron will be required. If a system standby mode proved necessary, a 10-W power requirement would exist. Otherwise the equipment will be turned completely off when not operating.

No special deployment will be required for the RADVS equipment. The antenna, of course, must be mounted to have an unimpeded view of the surface.

Probably the most significant environmental consideration relates to the klystron. Pressurization for this tube may be necessary at the 70 km altitude to prevent corona. Also, a fixed operating thermal environment for the klystron of 145°C will be necessary. The required operating thermal environment for the other electronics will be 0 to 55°C.

The signal output of the RADVS will be 4 digital words of 7 bits each for every measurement. Three of the words will be the digitized frequency count of the three velocity components while the 14 word will reflect altitude. Fifteen measurements at 1-min intervals are expected for each duty cycle resulting in a total of 420 bits. Additional housekeeping data bits will be necessary to monitor status of the equipment.

Operational limitations. - The data gathered on Cytherean atmospheric circulation by this experiment would be limited by the use of a single, passive monitoring point (the buoyant station) at a fixed altitude. This limitation can be lessened by cycling the station to lower altitudes. Also, the system weight and power requirements are quite large for operation at a 70 km altitude, Such a system is relatively independent of variations in surface features although some bias error would be introduced.

Good time correlation between time of station track and time of experiment duty cycle will be necessary.

Development status. - The RADVS was developed for the Surveyor program by Ryan. It was employed successfully at ~ 12 km altitude. Considerable development is anticipated to enable its use at a 70 km altitude.

Special Drop Sondes

Description. - The deployment of one or more drop sondes from the BVS at several points along its path will be a direct, reliable method for conducting a wind velocity experiment. This experiment method will yield measurements of the horizontal acceleration components produced by wind forces acting on the probe. Also, corresponding altitude measurements will be taken at known times together with azimuthal orientation data.

The drop sonde will be configured as a cylindrical body having a spherical nose and either a flared afterbody or parachute. A sonde having ballistic coefficient of 1.0 will reach the surface from 70 km in about *24* min assuming the mean atmospheric density.

The sonde will include two accelerometers for measuring the horizontal wind-induced acceleration components along the two principal transverse axes. A three-axes altitude gyro will provide azimuthal orientation data and will be initialized with reference to the buoyant station coordinates. (It is assumed that station coordinates will be known with respect to planetary coordinates.) Altitude sensing via a radar altimeter for a small sonde such as this would be impractical from a weight, size, and power standpoint. Therefore, static pressure measurements will be taken under the assumption that other experimental data will identify the pressure-altitude profile for the Cytherean atmosphere.

APPENDIX B

The knowledge of horizontal acceleration and the vertical velocity component will permit calculation of wind shear vs altitude. To integrate wind velocity from the measured wind acceleration, the initial transverse velocity of the sonde must be known. It is assumed these data can be obtained from either orbiter-station tracking data or RADVS equipment on the buoyant station.

Physical characteristics. - Each drop sonde will be a cylindrical projectile having a spherical nose and either a flared afterbody or parachute. The nose diameter will be about 6.5 in. and the sonde, including flared drag surface, will be 18 in. long. The sonde will weigh approximately 7.5 lb.

Operational requirements. - The sonde will be powered from internal batteries and require about 8 W during a 25-min operating descent period.

The sondes will be deployed from the buoyant station at different, selected points along its path with a zero vertical velocity component. Ejection of the drag device or the parachute may be employed to shorten descent time (from 30 km to surface) if excessive heating is sensed.

The output of the sonde instruments will be converted to 7-bit data words. The total bit accumulation for each measurement will be:

(2)	accelerometers (2 axes)	14 bits
(1)	pressure sensor	7 bits
(1)	attitude gyro (3 axes)	21 bits
	Total	42 bits measurement

At a measurement rate of every 10 sec during descent, ~ 6000 bits will be accumulated from each sonde.

The sondes will require thermal control during descent so that high atmospheric temperatures near the surface will not cause excessive temperature levels for the instruments. An operating thermal environment for the instruments of 0 to 55°C will be required.

Operational limitations. - The accuracy to which the direction of wind-induced accelerations can be determined will rely on the accuracy to which buoyant station coordinates can be referenced to planetary coordinates. Also, an accurate integration of wind

velocity from acceleration measurements will require accurate determination of the initial transverse velocity of the sonde (i.e, the station transverse velocity), Further, the relatively high velocities experienced from 70 to 50 km (up to 235 m/sec) may prohibit sensing of the existing wind shear forces.

Development status. - Development effort is anticipated to evolve an adequate thermal control system for the sondes.

MAGNETIC FIELDS

OBJECTIVES

The objective of the magnetic field experiment is to establish whether a Cytherean magnetic field exists, and if so, determine magnitude, direction, multipolarity, and orientation of the magnetic field. Determining the existence and characteristics of a Cytherean magnetic field will be important for the study of the planet's interior structure and for various characteristics of the planet such as radiation zones. These measurements might also allow some conclusions about magnetic characteristics of the planet's surface.

Because the intensity of F of the magnetic dipole field decreases roughly with the third power of the ratio of planet radius a to the distance r between planet center and point of measurement [$F = K\,(a/r)^3$ or for $r = a + h$ and $h \ll a$, we obtain $F \simeq (1-3\,h/a)K$], a decrease in magnetic field intensity of approximately 0.05% per altitude increase of 1 km is expected. Therefore, the magnetic field intensity at 100 km altitude should be about 95% of the surface intensity. This shows that balloonborne measurements are representative of the surface magnetic field.

During the Venus flyby, Mariner II was as close as 35,000 km to the planet. But no magnetic field attributable to Venus was detected. This implies that the magnetic dipole moment of Venus is less than 1/10 to 1/20 of the Earth's. The intensity of the Earth's magnetic field varies between 0.7 and 0.25 G. Therefore, a magnetometer range of about 10 000 gamma ($1\ G = 10^5$ gamma) is suggested for the balloonborne Cytherean measurements.

APPENDIX B

EXPERIMENTS/INSTRUMENTS

The characteristics of several types of space-qualified magnetometers are given in table 25.

TABLE 25. - TYPICAL MAGNETOMETER CHARACTERISTICS

Instrument	Weight, lb	Average power, watts	Volume, cu in.	Operating range, gammas	Spacecraft carrying instrument type
Search coil magnetometer				> 0.5	Pioneer 5,
Flux gate magnetometer	3.4 to 5.8	.7 to 6.0	40	±64 to ±10 000	Mariner 2, IMP, Pioneer 6, Explorers 6 and 12
Proton precession magnetometer				> 7000 to 100 000	Vanguard 3
Rubidium-vapor magnetometer	3.1	1.2 to 3.5	150	.1 to 50 000	Ranger 1, IMP
Triaxial helium magnetometer	5.5	7.0	200	±360 (nulling)	Mariner 4

The history of space magnetometry is well documented (refs 124 thru 135), and no problems are forseen in developing a magnetometer for use on a BVS. However, the utility of magnetic measurements from a BVS, at least in the initial exploration of Venus, is somewhat doubtful. Magnetic measurements of Venus will be more useful if made from an orbiter.

APPENDIX B

ELECTRICAL DISCHARGES

OBJECTIVES

Within the Earth's atmosphere, lightning is a secondary phenomenon. That is, it is a manifestation of certain primary mechanisms within the Earth's meteorology, climatology, and geophysics. The same generality must be assumed valid for lightning in the Cytherean atmosphere. Experiments to detect and measure lightning from the BVS should be quite secondary to such direct atmospheric experiments as measurement of pressure, temperature, and composition. The mechanism of the Earth's atmospheric electricity is reasonably well understood and substantiated with empirical data, However, significant gaps in the understanding still exist, such as the manner in which the charge organization within cumulonimbus clouds is formed.

A large amount of data has been gathered in recent years pertaining to Earth lightning parameters such as stroke duration, rate, location, etc. These data have contributed to increased knowledge of the Earth's meteorology and to improved methods in weather forecasting and radio engineering. However, this information has been obtained through highly coordinated experiments using complex techniques. Further, the experiments have been conducted in the relatively well-known environments of the Earth's surface and atmosphere. Performance of lightning experiments in the Cytherean atmosphere more sophisticated than the basic detection of strokes or measurement of the electric field gradient is not considered feasible for this mission.

EXPERIMENTS/INSTRUMENTS

Experimental methods considered for detecting lightning stroke occurrence are: (1) detection of sferics and whistlers with radio receivers, (2) detection of thunder sound-pressure levels with microphones, (3) detection of visible light energy with uv sensors; and (4) measurement of the atmospheric electric field gradient using an electrometer. Obviously, although these techniques are feasible in the Earth's environment, they might fail completely in a Venus application. Solar and galactic noise might be of sufficient amplitude and at frequencies as to totally obscure sferics.

APPENDIX B

Thunder does not always occur with Earth lightning strokes and the same might well hold true for Venus. Sufficient uv light energy from the sun might penetrate the Cytherean atmosphere, making lightning uv light sensors useless. Most accurate use of an electrometer would require its deployment via radio sonde or cable to avoid distortions in the electric field caused by the buoyant station. To increase the probability of success, the lightning detection experiment should employ at least several of the four methods under consideration; and since the buoyant station will be in equilibrium at 70 km, a sonde to deploy the instruments to lower altitudes should be considered.

Very Low Frequency (vlf) Receiver

Description. - In the mechanics of an Earth lightning stroke, the principal source of radio disturbance (sferic) is the return stroke, It exceeds the sferic magnitude emanating from the leader by about a factor of 10, and is about 0.0001 sec in duration. Although a sferic is detectable over a broad band of frequencies, it is best monitored for the detection of lightning stroke occurrence in the 3 to 100 kc band. A very simple vlf receiver with a whip antenna could monitor sferics caused by lightning strokes.

In an experiment to monitor sferics, a further consideration would be the detection of so-called whistlers. The detection of whistlers in the Venusian atmosphere could suggest the presence of an ionosphere. The Earth whistler is caused by low-frequency sferic radiations being refracted by the Earth's ionosphere back into the atmosphere. The higher frequencies (~ 10 kc) arrive at the Earth ahead of the lower frequencies (~ 3 kc) and yield a characteristic sound, decreasing in pitch, at the monitoring radio receiver. Whistlers are detected in the hemisphere opposite to that in which the causative lightning stroke has occurred as they apparently follow a line of force of the Earth's magnetic field.

Physical characteristics. - A vlf receiver and associated electronics for monitoring sferics and conditioning data would weigh an estimated 3.5 lb and occupy a dimensional envelope of 2x4x6 in.

Operational characteristics. - The vlf receiver would operate on 28 vdc and require 2.0 W.

Deployment of a whip antenna would be required. The experiment should be performed at altitudes below that of the buoyant station.

Since the purpose of this experiment is only to detect the lightning stroke occurrence, bilevel (on/off) indication of occurrences within a preestablished time interval would be adequate. A receiver output signal above a preselected threshold level will operate a solid-state bilevel switch producing a single bit for each occurrence ("on" condition). The bits will be accumulated over the set interval and stored in a buffer register. A maximum of 20 bits for each performance of the experiment is anticipated.

The receiver requires an operating thermal environment of 0 to +55°C.

Operational limitations. - The receiver will be limited to the detection of signals within the frequency range of 3 to 100 kc and above a selected threshold level. The selected threshold will be well above the anticipated solar and galactic noise levels. Should these noise sources exceed their anticipated levels, discrimination of sferics could become impossible.

Development status, - Minimal development is foreseen to provide a sterilizable antenna and receiver package suitable for this application.

Ultraviolet/Visible Light Detector

Description. - Detection of lightning stroke occurrence by sensing the uv light radiated (mostly from the return stroke) will be feasible provided the Cytherean upper atmosphere provides sufficient backscattering of solar uv energy. This experiment approach will consist of a lens and filter assembly to focus uv light from a lightning stroke on a solid-state detector.

Physical characteristics. - The optics, photocell detector, and associated electronics would weigh 2.0 lb and have a dimensional envelope of 4x4x4 in.

Operational characteristics. - The uv light detection system will require 28 vdc and use 0.25 W of power. The system optics should have an unobstructed field of view below the station.

APPENDIX B

The amplified output of the photocell when above a preselected ambient level will operate a solid-state bilevel switch to indicate the occurrence of a lightning stroke. Single bits for each detected stroke will be accumulated over a set interval in a buffer register. Up to 20 bits maximum per experiment cycle is anticipated.

The optics could operate in a thermal environment of from -90 to +500°C. The photocell and electronics will require a thermal environment of 0 to 55°C.

Operational limitations. - The experiment detector system will discriminate light of 1000 to 4000°A wavelength. Its successful performance is premised on the assumption that lightning-produced uv light can be detected from the ambient uv light in the Cytherean atmosphere. Conditions that could cause temporary or permanent fogging of the lens system require investigation before use of this experiment technique.

Development status. - No special development is anticipated to provide a sterilizable uv light-detection system for this application.

Microphone

Description. - This experiment method is predicated on detecting lightning stroke occurrence by sensing the associated thunder sound pressure level with a microphone. Usually, the increase in pressure because of dissociation, heating, and ionization is sudden enough along the path of the lightning stroke to result in thunder. However, it is fairly common, expecially regarding cloud-to-cloud discharge, that the energy release is not sudden enough to produce a pressure transient sufficient to result in thunder.

To detect thunder, a microphone will be employed with the necessary signal conditioning electronics.

Physical characteristics. - The microphone will weigh 2.0 *oz* and be ½ in. in diameter and 3/4 in. long. The required electronics will weigh 1.0 lb and measure 1x4x5 in.

Operational characteristics. - The microphone system will operate from 28 vdc and require 2.0 W. The amplified output of the microphone when above a preselected ambient level will operate a solid-state bilevel switch to indicate the occurrence of thunder. Up to 20 bits, maximum, per experiment cycle is anticipated.

APPENDIX B

The microphone will be located to most advantageously sense the sound pressure level of the thunder.

The microphone and its electronics will require an operating thermal environment of 0 to +55°C.

Operational limitations. - The difficulties of monitoring lightning stroke occurrence by detecting its associated thunder are significant. Not all lightning produces thunder. Sound pressure levels will vary greatly, depending on magnitude of the stroke and distance from the monitoring point. This wide level variation makes selection of a switching threshold difficult.

Development status. - Some effort will probably be necessary to develop a microphone to withstand direct exposure in a 400°K Cytherean atmosphere.

Electrometer

Description. - The electric field potential gradient within the Earth's atmosphere varies with altitude but a representative figure for fair weather would be ~ 150 V/m. However, during thunderstorm activity potential gradients of 10 000 to 100 000 V/m are common between cumulonimbus clouds and the Earth's surface. The use of an electrometer to take potential gradient measurements in the Cytherean atmosphere could yield information on the planet's atmospheric electricity. In such an application the electrometer will be deployed from the buoyant station via a radio sonde that will descend at a low velocity. The electrometer will sense the potential gradient and establish a corresponding bias on the plate of the electrometer tube causing variation in grid current. These variations in grid current cause corresponding changes in the audio frequency of a modulator that in turn modulates a radio carrier. The modulated radio wave is fed to an antenna and transmitted back to the buoyant station.

Physical characteristics. - The electrometer, associated electronics and batteries will be packaged together to weigh 2.0 lb and have a dimensional envelope of 2x6x6 in. Required receiver and signal conditioning electronics in the buoyant station will weigh 1.0 lb and occupy 1x2x6 in.

Operational requirements. - The electrometer and its associated electronics will use self-contained batteries. The support electronics in the buoyant station will operate from 28 vdc and require 1.0 W of power.

The electrometer will be deployed on a slowly falling radio sonde to provide measurements at several altitudes and avoid distortions of the electric field caused by the buoyant station. Further deployment of the electrometer collector plates will be required and their proper orientation must be maintained.

The modulated carrier signal received at the buoyant station will be processed to separate the original, modulating analog signal from the electrometer. This signal will be sampled approximately 10 times during descent of the sonde. The 10 samples will be converted to 7-bit words for a total of 70 bits.

Thermal requirements of the electrometer package housed in the radiosonde will be 0 to 85°C. The support electronics on the buoyant station will require a 0 to 55°C environment,

Operational limitations, - Obviously this experiment will provide only a rough profile of electric field vs altitude. More data could be acquired by a higher sampling rate and the use of several electrometers could cover a wide range. However, more definite knowledge of the Cytherean atmospheric temperature, wind, and density would be required before an experiment approach could be designed having a satisfactory probability for success.

Development status, - Electrometer radio sondes have seen consistent application by meteorologists in measuring the Earth's electric field as well as other atmospheric parameters. Development effort would be minimal, primarily to harden the electrometer tube against shock and packaging to resist the high thermal levels anticipated at lower altitudes.

SURFACE HARDNESS

OBJECTIVES

The surface characteristics of Venus are almost completely unknown. Because of the complete cloud cover and apparently high thermal environments close to the surface, it does not seem feasible to attempt direct surface experiments from the buoyant station

or from a sonde during the first mission. However, an experiment to test the surface hardness could yield useful and definitive information. For this experiment, a freely falling penetrometer ejected from the buoyant station will impact on the surface. The objective is the transmission of data that will give indications of the nature of the surface material. Such information would be of importance in the future design of a Venus lander. A more extensive survey of the Cytherean surface could, of course, be achieved by the dispersal of a group of penetrometers over a known surface area. Measurements of altitude at release and drop time of the penetrometer would provide a cross reference for the atmospheric density experiment. Location of the penetrometer impact point on the Cytherean surface could be determined from a knowledge of the station position.

EXPERIMENTS/INSTRUMENTS

A penetrometer can be defined as a surface impacting device having an acceleration sensor and a capability to transmit acceleration data. The data can be transmitted via either a hardwire between the penetrometer and the station or an rf telemetry link. For obvious reasons, the latter approach is the only one considered for this application. Because the Cytherean atmosphere has sufficient density, the orientation of the penetrometer at impact can be predicted and a unidirectional accelerometer can be used. Development of omnidirectional accelerometers is presently in progress; however, their use in this application is not anticipated.

Impact Accelerometer

Description. - The penetrometer will be comprised of an impact housing, unidirectional accelerometer, signal conditioning electronics, power supply, transmitter, and antenna. All components must be impact hardened and packaged to operate through a 10 000 g transient having a 0.15-msec rise time and 0.15-msec decay. This approximates a worst condition shock transient such as would be experienced by a hard, spherical nose projectile impacting into concrete at 30 fps. The projectile would be 3 in. in diameter and have a mass of 0.03 slug.

APPENDIX B

Physical characteristics. - The penetrometer will have a 3-in, diameter and be 8 in. long. It will weigh approximately 4 lb.

Since a receiver for the other drop sondes is required, a separate receiver for the penetrometer data is not necessary.

Operational Requirements. - The power supply for the penetrometer will be self-contained batteries. Power consumption will not exceed 2.0 W for approximately 30 min, the support equipment in the buoyant station will operate from 28 vdc at 2.0 W for 30 min.

No special deployment requirements will exist other than ejection of the penetrometer.

The receiving station electronics will require an operating environment of 0 to 55°C. The penetrometer electronics will require the same thermal conditions. Design considerations for the penetrometer must include protection against the possiblity of a 700°K environment at the surface and impact hardening to 10 000 g.

The received acceleration data from the penetrometer after separation from the rf carrier will be converted to a digital format and stored for later transmittal to the orbiter. Because impact into some elastic materials could produce a complex deceleration signature of very short duration (0.3 msec), a high sampling rate resulting in a very large data bit load would be necessary to accurately encode the raw signal. To reduce the bit quantity, it is anticipated that a signal conditioning technique will be employed whereby the occurrence of known g-levels are indicated by logarithmically spaced gates and encoded together with corresponding time axis information.

Operational limitations. - The wide variety of possible surface materials presents a problem in designing a penetrometer system. This system must be capable of handling shock transients from less than 50 g to 10 000 g. Transient time durations can vary from 0.3 msec to 30 msec. The acceleration signatures must be faithfully reproduced if impacted material is to be identified. Therefore, data bit quantity will be high, and schemes for compression must be considered. It appears that the best means for identifying the nature of the surface from the deceleration data will be comparison with signatures obtained at impact with a wide variety of Earth materials. The close approximation of penetrometer data with the impact deceleration signature of a known Earth material will permit accurate prediction of the nature of the surface impacted, its hardness, and bearing strength.

APPENDIX B

Development status. - A considerable penetrometer test history has been compiled at NASA's Langley Research Center. Impaction of various penetrometer designs into a wide variety of materials (cement, lead, balsa, sod, dust, etc.) at different velocities has demonstrated the technical feasibility of this surface measuring method, Additional impact testing of the penetrometer developed for this application would be necessary to acquire a library of the deceleration signatures at impact with various materials. No development problems of any significance are ancticipated in achieving the necessary impact hardening or thermal protection for the penetrometer.

APPENDIX C

ATMOSPHERIC CIRCULATION ON VENUS

A'lthough there have been speculations on the large-scale atmospheric circulation of Venus, quantitative investigations were begun only recently.* Some important radar and radiometric measurements enable us to estimate meaningful magnitudes of some physical parameters, such as rotation rate and surface temperature of Venus, which are critical to the features of atmospheric circulation of Venus.

This appendix discusses several Venusian atmosphere circulation models used in the calculation of wind velocities and flow patterns, the results obtained with these models, and an intercomparison of the results obtained with the different models, The possible mean wind speed and the wind direction at the level just above the visible cloud top is also discussed.

IMPORTANT PHYSICAL PARAMETERS

Rotation Rate of Venus

The sidereal rotation rate of Venus (ref. 136) is 243.1 days, retrograde. Therefore, the Coriolis parameter is about 4×10^{-3} times of that on Earth. The geostrophic wind equation is thus no longer valid.

Surface Pressure

The surface pressure, based on an estimate by Kaplan (ref. 137), is about $(10 \pm 3) \times 10^3$ mb. Other investigators (see, for example, ref. 138) predict a surface pressure of about 30 atm. The uncertainty is considerable and surface pressures between 1 and 200 atm cannot be ruled out with any certainty. Computations for wind velocity based on surface pressures of 10 and 30 atm are performed.

---

*See, however, the recent article by R. M. Goody and A. R. Robinson: A Discussion of the Deep Circulation of the Atmosphere of Venus. Astrophys. J., vol 146, no. 2, November 1966, pp. 339-355.

Note that while these surface pressures lie within the bounds of the model atmospheres given in NASA SP-3016, they correspond only roughly with the models.

Surface Temperature

On the basis of the Mariner II microwave observations during the 1962 conjunction, Kaplan (ref. 137) estimated the average surface temperature to be about 700°K. Owen (ref. 138) suggests a bright-side surface temperature of about 750°K, a dark-side temperature of about 640°K, and a dark pole temperature of about 540°K.

Cloud-Top Temperature

The cloud-top temperature is about 234°K. Based on the values of determined surface temperatures and assumed lapse rate, the top of the cloud is about 50 to 70 km above the solid surface,

MODELS OF LARGE-SCALE CIRCULATION

Since there are large uncertainties about various meteorological parameters, we use different models to estimate the wind velocities in the atmosphere of Venus.

Model 1

This is a simple, general model of thermally driven circulation developed by Haurwitz (ref. 139). Venus is considered to be a synchronously rotating planet; the zonal component of the wind is thus zero and the circulation reduces to a meridional component (here we define the meridional direction in the direction of the lines joining the subsolar and antisolar points, while the zonal direction is in the direction normal to the lines joining subsolar and antisolar points).

The wind speed can be represented simply as follows:

$$V = \frac{1}{2}\left[\frac{\alpha R \ln p_o/p}{k}\right]^{\frac{1}{2}} \qquad (C1)$$

and temperature difference between subsolar and antisolar points can be written as

$$\tau = \frac{2 k a \pi}{R \ell n\left(p_o/p\right)} V, \qquad (C2)$$

where

α = the difference in the rate of temperature change between subsolar and antisolar points, °K/sec

$$= \left[\frac{S(1-A)}{c_p \frac{\Delta p}{g}} - w\right]_{\text{subsolar point}} - \left[- w\right]_{\text{antisolar point}},$$

S = incident solar radiation at subsolar point = 4.11 $cal/cm^2/min$,

A = albedo = 0.75,

w = outgoing longwave radiation,

c_p = specific heat at constant pressure,

a = radius of Venus = 6000 km,

Δp = pressure difference between surface and top of troposphere, $p_o - p$,

p_o = surface pressure = 10 atm; 30 atm,

p = pressure,

g = gravitational acceleration = 880 cm/sec^2,

R = gas constant for Venusian atmosphere = 2.5×10^6 $cm^2/sec^2/deg$,

k = coefficient of friction, sec^{-1}.

It is assumed that $(w_{subsolar} - w_{antisolar})$ is zero, and the pressure at the tropopause level is 0.01 of the surface pressure. The results for different surface pressures and coefficients of friction are shown in table 26. This computation is based on the assumption that the outgoing radiation is the same at both subsolar and antisolar points. Therefore, this computation gives a maximum value of wind and temperature differences for various cases.

APPENDIX C

TABLE 26. - COMPUTED RESULTS OF THE MEAN WIND AND THE MEAN TEMPERATURE DIFFERENCES BETWEEN SUBSOLAR AND ANTISOLAR POINTS

p, atm	k, sec^{-1}	V, m/sec	τ, °C
10	5×10^{-5}	8.1	9
	1	5.8	14
	1	1.8	42
	$1 \times$	.6	135
30	5	4.7	5
	10^{-4}	3.4	8
	10^{-3}	1.1	24
	10^{-2}	.3	78

Model 2

This model was developed by Mintz (ref. *140)* for the atmospheric circulation of a synchronously rotating planet. It is based on the condition that the energy radiated to space in the dark hemisphere must be replaced by an energy transport across the terminator from the sunlit side. The meridional wind velocity at a level where pressure is 1/4 of the pressure on the surface is

$$V = \frac{\left[\left(\frac{4\pi a^2}{2}\right)\sigma T_e^4\right]}{\left[\frac{\pi a R T_2 P_o}{g}\left(1 - \frac{\gamma}{\gamma_d}\right)\right]} \qquad \text{(C3)}$$

where

σ = Stefan-Boltzmann constant = 5.7×10^{-5} $erg/cm^2/sec/deg^4$,

T_e = infrared brightness temperature = 237°K,

T_2 = temperature at middle of the atmosphere ($p = \frac{1}{2} p_o$)

γ = vertical temperature gradient,

γ_d = adiabatic temperature gradient,

The wind velocities for $\gamma/\gamma_d = 9/10$, various T_2, and different surface pressures are shown in table 27.

TABLE 27. - COMPUTED WIND VELOCITIES BASED ON MINTZ'S MODEL FOR VARIOUS MEAN ATMOSPHERIC TEMPERATURES, T_2, AND DIFFERENT SURFACE PRESSURES, p_o

p_o, atm	T_2, °K	V, m/sec
10	440	.75
	580	1.00
30	440	.25
	580	.33

This model cannot be used to compute temperature differences between subsolar and antisolar points. Also, friction ha5 not been taken into account. For a deep atmosphere, the frictional effect may be very important.

Model 3

This model assumes that the circulation starts from relative rest and that there is no horizontal temperature gradient to begin with, A heating function due to a net gain of radiative energy at the subsolar point and loss of radiative energy at the antisolar point is specified as the driving force of a meridional circulation (ref. 141). The wind velocity is written as

$$V = \frac{2D\beta}{p_o} J_o \left[2\beta \left(\frac{p}{p_o}\right)^{\frac{1}{2}}\right] \frac{2}{\pi} \left[\frac{\gamma}{1+\mu} \frac{\pi}{4} \sin \varphi + \frac{2\gamma}{3(4+\mu)} \sin 2\varphi + \ldots\right] \qquad (C4)$$

where

D = amplitude of the heating function,

β = 1.916,

APPENDIX C

$$\gamma = \frac{p_o a}{B_o c_p} ,$$

B_o = temperature between surface and the top of the atmosphere, °C,

$$\mu = \frac{\alpha^2 c^2 a^2}{RB_o} ,$$

c = coefficient of eddy viscosity.

The temperature difference between the subsolar and antisolar points can be written as

$$\tau = \int_0^{\pi} \frac{cp}{R} \frac{\partial V}{\partial p} dy = \frac{2cD\alpha^2 p^{\frac{1}{2}} \gamma}{Rp_o^{3/2}(1+\mu)} J_1 \left[2\alpha \left(\frac{p}{p_o} \right)^{\frac{1}{2}} \right] a \qquad (C5)$$

The computed wind velocities and temperature differences at level $P = p_o/2$ for $p_o = 10$ atmosphere and different coefficients of friction are shown in table 28.

TABLE 28. - COMPUTED WIND VELOCITIES AT TERMINATOR AND TEMPERATURE DIFFERENCES BETWEEN SUBSOLAR AND ANTISOLAR POINTS AT A LEVEL $p = 0.01\ p_o$ FOR DIFFERENT COEFFICIENTS OF FRICTION

p, atm	c, sec^{-1}	V, cm/sec	τ, °C
10	10^{-5}	6.6	.16
	10^{-4}	.5	.02
	10^{-3}	.1	0
	10^{-2}	0	0

This model yields a smaller wind velocity and temperature difference than that of previous models with the same surface pressure and coefficient of friction.

APPENDIX C

Model 4

This model is a linearized free convection model based on a given surface temperature distribution (ref. 141). The approach is similar to the one used in treating sea breeze circulations. Using the Boussinesq approximation and assuming the motion starts from rest, the solutions for horizontal and vertical velocities and the temperature disturbance from the mean are obtained, respectively, as follows:

$$V = \frac{K\lambda^3 k^2 D}{2\gamma}\left[e^{-\lambda kz} - \left(\cos\frac{\sqrt{3}}{2}Akz + \frac{\sqrt{3}}{3}\sin\frac{\sqrt{3}}{2}Akz\right) e^{-(\lambda kz)/2}\right]\sin kx$$

$$W = \frac{KD(\lambda k)^2}{2\gamma}\left[e^{-\lambda kz} - \left(\cos\frac{\sqrt{3}}{2}\lambda kz\,\frac{\sqrt{3}}{3}\sin\frac{\sqrt{3}}{2}\lambda kz\right) e^{-(\lambda kz)/2}\right]\cos kx \qquad (C6)$$

$$T = \frac{D}{2}\left[e^{-\lambda kz} + \cos\left(\frac{\sqrt{3}}{2}\lambda kz\right) e^{-(\lambda kz)/2}\right]\cos kx$$

where

D = one half of the surface temperature difference between subsolar and antisolar points,

γ = (mean lapse rate - dry adiabatic lapse rate) = 2°/km,

K = v = eddy conductivity or viscosity = 10^3 m^2/sec,

$k = 1/r_o = 1.64 \times 10^{-4}$ km^{-1},

r_o = radius of Venus = 6000 km,

$$\lambda = \left(\frac{g\alpha\gamma}{\nu K}\,\frac{1}{k^4}\right)^{1/6} = 605.$$

For a surface temperature difference between the subsolar and antisolar points of about 150°C, the computed profile of V, W, and T are shown in figure 40. The maximum wind velocity for this model is much greater than for any of the other models,

APPENDIX C

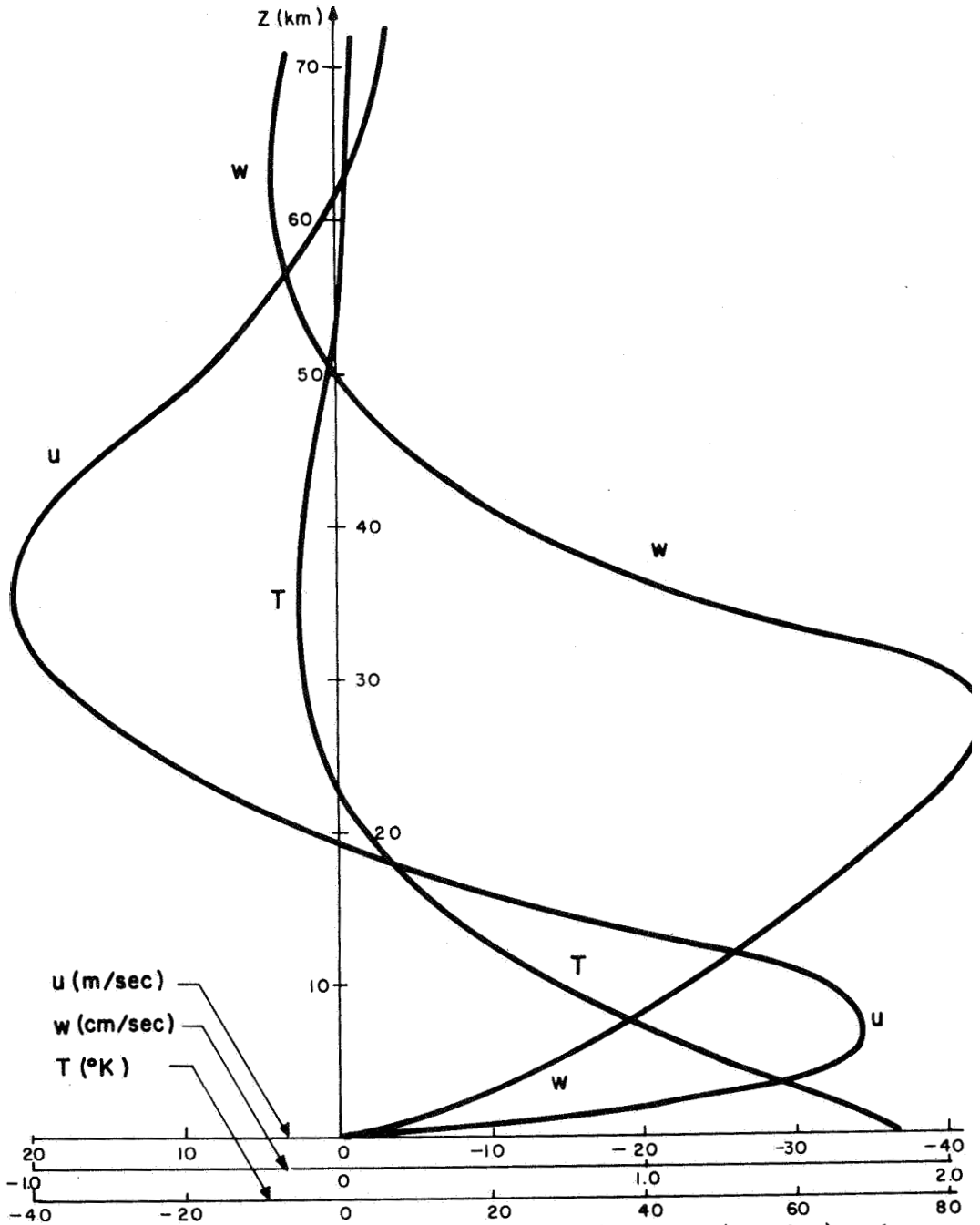

Computed horizontal and vertical wind velocities (u and w) and perturbatior temperature (T) for Venus atmosphere ($K = \nu = 10^3 m^2/sec$, $g = 8.8\ m/sec^2$; D = 70°K; r = 6100 km; $k = 1.64^{-4}/km$; $\alpha = 0.002$; $y = 2°/km$; $\lambda = 605$; $\varphi = \pi/2$ for u, and $\varphi = 0$ for w and T).

Figure 40, - Computed Profile for V, W, and T

APPENDIX C

Since the Boussinesq approximation is not adequate for a deep atmosphere and could lead to large errors, a similar convective model without the Boussinesq approximation has been developed (ref, 141). However, numerical results have not yet been obtained.

DISCUSSION

Wind Velocities on Venus

In view of the results of various atmospheric circulation models for Venus, the wind velocities are generally small except for Model 4. Models 1, 2, and 3 yield mean wind velocities from a fraction of 1 cm/sec to 8 m/sec for various conditions. The direct energy source driving the atmospheric circulation for these three models is the net gain of radiation energy as a result of the difference between the absorption of shortwave radiation from the sun and the emission of longwave radiation of the atmosphere. It seems that such an amount of net energy cannot produce a high wind velocity for a deep atmosphere with surface pressures of 10 to 30 atm. Model 4 yields a meridional velocity of about 33 m/sec, which is higher than that of other models. The energy source is from the surface over which a constant large temperature gradient is assumed. Since there may be relatively large errors involved in Model 4, the magnitude of wind will not be taken for intercomparison.

In Model 1, the friction is considered to be an important factor. For a small coefficient of friction such as 5×10^{-5} sec^{-1}, the wind velocity is about 8 m/sec for the case of a surface pressure of 10 atm. In comparison to Model 2, where friction is not included at all, the wind velocity computed from Model 1 is one order of magnitude larger than that of Model 2. This may be caused by the fact that the outgoing radiation is assumed constant along the meridional direction. Therefore, this wind velocity of 8 m/sec for Model 1 will be the maximum velocity. Model 3 yields very small wind velocities. Thus, based on Models 1, 2, and 3, we conclude that the mean wind velocity may not be more than 8 m/sec and that the uncertainty of the wind would not be too large for the range of the surface pressure varying from 10 to 30 atm.

APPENDIX C

We have also computed temperature differences between subsolar and antisolar points for different cases based on Model 1. However, the computed temperature differences hardly agree with the results estimated based on Mariner II data. The temperature difference near the surface based on Mariner II data, after allowance for the limb darkening effect, is about 200°K. Similarly, the temperature differences between two columns is estimated as 100°K. These values are higher than most of the theoretical values except for the case in which the friction coefficient for the Venusian atmosphere $\left(10^{-2} \text{ sec}^{-1}\right)$ is 1000 times as large as that for the Earth's. This large difference in temperature may be caused by the approximate nature of the model, Except for the improved Model *4*, which is accurately solved, theoretical estimates of temperature differences between subsolar and antisolar points cannot be very certain, and, in turn, the exact wind velocity cannot be obtained unless all the physical parameters are accurately determined.

Wind Direction on Top of Visible Cloud Layer and Formation of Diverging Cloud Bands

Since Venus is a nearly synchronous rotating planet, the circulation will be the form of the Hadley cell. Thus the air would rise at the subsolar point and sink at the antisolar point to form one complete cell. The visible cloud top of Venus has a temperature of about *230°K* in contrast to the surface temperature of 700°K. The height of the visible cloud top is about 50 to 70 km above the surface level, estimated on the basis of a lapse rate of 8°C/km, and at a pressure level of 1% of that on the surface. Presumably, the cloud top is then at the upper level of the Hadley cell. Therefore, the direction of circulation will be in the direction of the meridional direction from the subsolar point toward the antisolar point. Since the surface temperature is very high and clouds generally cover the whole planet, it is generally believed that the sunlit side of the Venusian atmosphere is thermally unstable and that convection will result. According to the study of vortex cloud patterns in hurricane (ref. 142) and related work (ref. 143), cloud bands tend to be oriented along the direction of the flow. For Venus, this would mean radial spoke cloud bands emanating from the subsolar point. Such a cloud system has been observed by Dollfus (ref. 36). The meteorological conditions accompanying the phenomena require that the atmosphere be unstably stratified and ,that the vertical wind shear be oriented along the direction of the flow, Therefore, we conclude that the wind direction above the cloud top is in the meridional direction and , from the subsolar point to the antisolar point, This is based on both theory and observation.

APPENDIX C

CONCLUSION

Based upon the four models discussed, the wind velocity on the top of the visible cloud layer is small and less than 8 m/sec. These theoretical evaluations are based on present knowledge of physical or meteorological parameters on Venus. If the assumed values of parameters have serious errors, e.g., surface pressure, the mean wind will also have a large error. However, the range is still quite small. The model of atmospheric circulation of a deep atmosphere is, of course, important. Results of a realistic nonlinear circulation model should be available in the near future.

The direction of the wind on the top of the visible cloud layer is believed to be from subsolar point toward the antisolar point along the meridional direction. The theoretical inference of the flow pattern agrees with diverging cloud patterns on Venus observed from the Earth's surface.

APPENDIX D

SCIENTIFIC MISSION PROFILE AND ESTIMATED TRAJECTORIES FOR A BUOYANT VENUS STATION

The following questions concerning the scientific mission of a buoyant Venus station are discussed in this appendix:

1) What points on and over the planet do we wish to sample?

2) What should be the spacing of observations in the horizontal and in the vertical?

3) At what points should drop sondes be released?

4) What is the probable trajectory of a buoyant Venus station? Where should the buoyant station be released initially to accomplish the desired sampling of the planet?

5) What is the length of time required to accomplish the desired sampling of the planet?

6) What are the advantages of two or three buoyant stations vs a single station?

DESIRED COVERAGE AND SAMPLING RESOLUTION

For a relatively rapidly rotating planet with moderate inclination, such as the Earth, the major variations of atmospheric and some surface parameters are the latitudinal (equator to pole) and seasonal variations. For a slowly rotating planet with small inclination such as Venus, which have a day that is 117 Earth-days long and an inclination $< 10°$, the major atmospheric and surface variations are probably from subsolar point to antisolar point and from subsolar (or antisolar) point to pole. To sample these expected variations, one would like to obtain observations over a path that includes subsolar, pole, and antisolar points.

Given such a path, or any horizontal trajectory, for the buoyant station, how frequently should observations be made? For sampling the large-scale variations of atmospheric parameters, measurements about every 100 km would be sufficient. To obtain some information on mesoscale variability, it is suggested that for one or two 100-km legs measurements should be made about 1 to 5 km spacing.

In view of the above discussion, it would be desirable to obtain vertical soundings using drop sondes at least at the following three points -- subsolar, pole, and antisolar points. If additional drop sondes are available, they should be released at the terminator and at evenly distributed points during the lifetime of the buoyant station. For the large-scale vertical variations of atmospheric parameters, measurements every kilometer would yield sufficient resolution. For detecting smaller scale features in the vertical profiles, measurements every 100 m for one or two 1-km legs are suggested.

Successful accomplishment of the coverage and sampling described above should provide a first estimate of the climatology of the Venus environment. It should be emphasized that with our present knowledge of the Venus atmosphere a single vertical profile or even a single direct observation of atmospheric parameters at one point would considerably enhance our knowledge.

ESTIMATE OF TRAJECTORY OF A BUOYANT STATION

To obtain observations from the subsolar point, pole, and antisolar point with the use of a single buoyant station requires the trajectory of the BVS to pass over these three points. The trajectory of the buoyant station with respect to the planet will be determined by the prevailing wind pattern. In this section, we attempt to determine whether it is indeed possible to pass over these three points with a single trajectory. If it is possible, where should the initial release of the buoyant station take place and how much time would it take? The analysis is based on a theoretical model of the wind pattern, since no observational indications of winds on Venus are currently available. As such wind information becomes available, it can be used to revise the present analysis.

For a synchronously rotating planet, the solar heating at the subsolar point and radiative cooling at the antisolar point would lead to the development of a direct atmospheric circulation from subsolar point to antisolar point at upper levels of the atmosphere. This is the type of circulation model we adopt for the winds on Venus, since the planet's actual rotation rate is so small that Coriolis effects on winds can be assumed negligible.

APPENDIX D

If Venus were in true synchronous rotation, the subsolar point would always be located at the same point on the planet. The trajectory of a balloon in such a case would follow the streamlines of the circulation pattern. The slight departure of Venus from true synchronous rotation leads to a rotation of the subsolar point with a period of about 117 Earth days. The trajectory of a balloon with respect to the subsolar point, pole, and antisolar points is now determined both by the circulation pattern and the tangential velocity of the planet with respect to the subsolar point. For example, a particle released at the subsolar point where the horizontal wind velocity is zero would have a component of motion with respect to the subsolar point that depends on the rate of rotation of the subsolar point, It is the combination of these two factors - circulation pattern with respect to planet and rate of rotation of subsolar point (or length of day on Venus) -- that will determine the trajectory of a balloon with respect to a frame of reference fixed by the sun, subsolar point, and antisolar point. We shall now indicate how such trajectories can be computed.

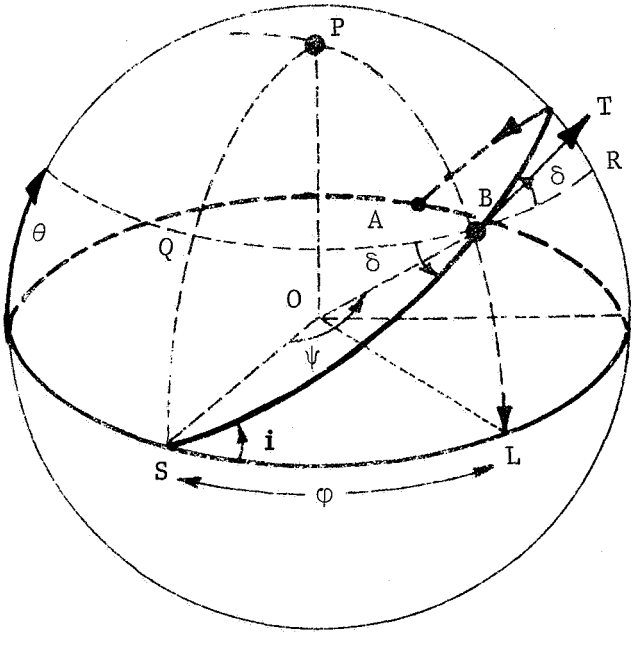

Figure 41. - Spherical Geometry for Determining Trajectory of a Buoyant Station on Venus

Figure *41* indicates the essential features of the spherical geometry required for the derivation. Assume S is the subsolar point and P is the pole. Venus is rotating with a small angular velocity, w, with respect to the subsolar point. The position of the balloon is assumed at point B, at latitude θ, and longitude φ. Both longitude and latitude are taken as zero at the subsolar point S. If the planet were in true synchronous rotation, the path of the balloon would be a great circle and would follow curve SB toward the antisolar point A. The angle i is the angle between the arc SBA of the great circle and the equator in the right spherical triangle SBL. The angle δ is the angle between the arc SBA and the latitude circle at B. It is worthwhile to mention here that these two

angles, i and 6, are different. The angle ψ is the angle between radii OS and OB.

The wind velocity at B is along the BT direction (tangential to point B in the SBA plane). However, when the planet does not have synchronized rotation, the rotation velocity of the planet-atmosphere system should be considered. The velocity components of the planet-atmosphere system due to rotation with respect to the subsolar point is

$$v_{\varphi} = a\ \omega \cos \theta$$
$$v_{3} = 0 \qquad \text{(D1)}$$

where a is the radius of Venus.

The velocity components of the circulation pattern are

$$w_{\varphi} = V_{o} \cos \delta$$
$$w_{\theta} = V_{o} \sin 6 \qquad \text{(D2)}$$

where V_o is assumed equal to $V_m \sin \psi$, where V_m is the wind velocity at the terminator. This form for the wind velocities is consistent with a circulation pattern in which the winds increase from zero at the subsolar to a maximum at the terminator and then drop off to zero at the antisolar point. The combination of these two velocity systems yields

$$V_{\varphi} = V_{o} \cos \delta + a\ \omega \cos \theta = a \cos \theta\ \varphi \qquad \text{(D3)}$$

$$V_{\theta} = V_{o} \sin \delta = a\ \theta \qquad \text{(D4)}$$

From the spherical geometry shown in figure 41, we can obtain the following relations.

$$\sin \varphi = \cos 6 \sin \psi \qquad \text{(D5)}$$

$$\sin \theta = \tan \varphi \tan \delta \qquad \text{(D6)}$$

substituting V_o and equations (D5) and (D6) into (D3) and (D4) and then dividing (D3) by (D4) leads to:

$$\cos\theta \frac{d\varphi}{d\theta} = \frac{\sin\varphi}{\cos\varphi \sin\theta} + \frac{a\omega}{V_m} \frac{\cos\theta}{\cos\varphi \sin\theta} \tag{D7}$$

Let $Y = \sin\varphi$ and $\alpha = a\omega / V_m$. Then, equation (D7) becomes

$$\frac{dY}{d\theta} = \frac{Y}{\sin\theta \cos\theta} + \frac{\alpha}{\sin\theta} \tag{D8}$$

Equation (D8) has the solution*:

$$\sin\varphi = k \tan\theta - \alpha \sec\theta = \frac{k \sin\theta - \alpha}{\cos\theta} \tag{D9}$$

where k is an integration constant.

Equation (D9) is the equation for the BVS trajectories with respect to the subsolar point. Each trajectory is determined by a specific constant **k**. The value of **k** for a given initial position and maximum wind velocity V_m at the terminator can be calculated from:

$$k = \frac{\alpha + \sin\varphi_o \cos\theta_o}{\sin\theta_o} \tag{DlOa}$$

where θ_o and φ_o are the initial latitude and longitude, respectively, of the BVS with respect to the subsolar point, Alternatively, given the desired latitude θ_T and longitude φ_T at which the BVS is to cross the terminator, the value of **k** can be computed from:

$$k = \frac{\alpha + \sin\varphi_T \cos\theta_T}{\sin\theta_T}, \tag{DlOb}$$

and substituted into equation (D9) to get the trajectory and, hence, the locus of initial positions that will give the desired terminator crossing.

---

*Use an integrating factor $\cot\theta$.

APPENDIX D

For Venus, the sidereal period of rotation is -*243.1* days and the sidereal period of revolution about the sun is *224.7* days. The angular velocity of a point on the Venus equator with respect to a fixed direction in space is -*0.0258* rad/day (see fig. *42);* the angular velocity of the sun with respect to this same fixed direction is *0.0278* rad/day. Therefore, the angular velocity of the sun as seen from a point on Venus' equator is *0.0538* rad/day and the length of one day on Venus is *116.8* Earth days. The corresponding angular velocity of Venus with respect to the subsolar point is then -6.23×10^{-7} rad/sec and the linear velocity of the atmosphere near the cloud tops (~ *6100* km) is $a w = -3.80$ m/sec. If we assume that the maximum wind velocity at the terminator is $V_m = 6.33$ m/sec, then $\alpha = a\omega / V_m = -0.60$. Several trajectories that result with this value of the terminator wind velocity are plotted in figure *43.* The points *S* and A are the subsolar and antisolar points, respectively. The points D and C are the source and sink of the trajectory field and are displaced from the subsolar and antisolar points. Trajectories diverge from D and converge at C. The pattern of trajectories shown in figure *43* indicates that there is no single trajectory that passes directly over subsolar, pole, and antisolar points. The most favorable trajectory for a buoyant balloon attempting to sample subsolar, pole, and antisolar points passes directly over the pole. The only trajectory that passes over both the subsolar and antisolar points is the equatorial trajectory **DSAC.**

The location of positions D and C depends on the value of $a\omega / V_m$ and is given by

$$\varphi_1 = \sin^{-1}\left(-\frac{a\omega}{V_m}\right) \qquad \text{(D11)}$$

For completely synchronized rotation, w = 0, then $\varphi = 0$). This means that the location of points D and C would coincide with S and A, respectively. That is, the pattern of the trajectories becomes symmetrical with respect to SPA and is exactly the same as the wind pattern. Then, if we release a balloon at the subsolar point, the balloon will pass over the pole toward the antisolar point. Since $w \neq 0$ in the actual case, a trajectory of a freely floating balloon cannot pass subsolar point, pole, and antisolar point in one pass.

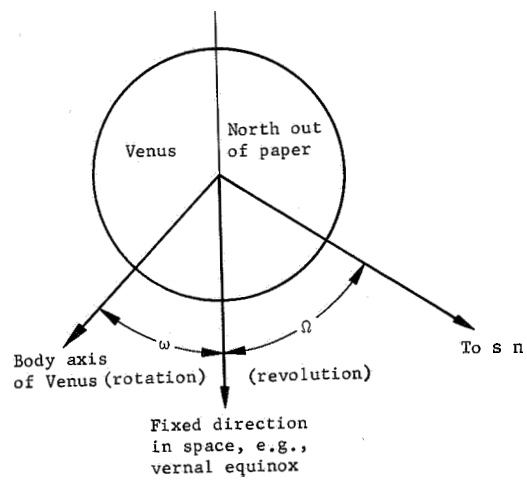

Figure 42. - Geometry for Determining Approximate Length of Day on Venus and Velocity of Point on Surface

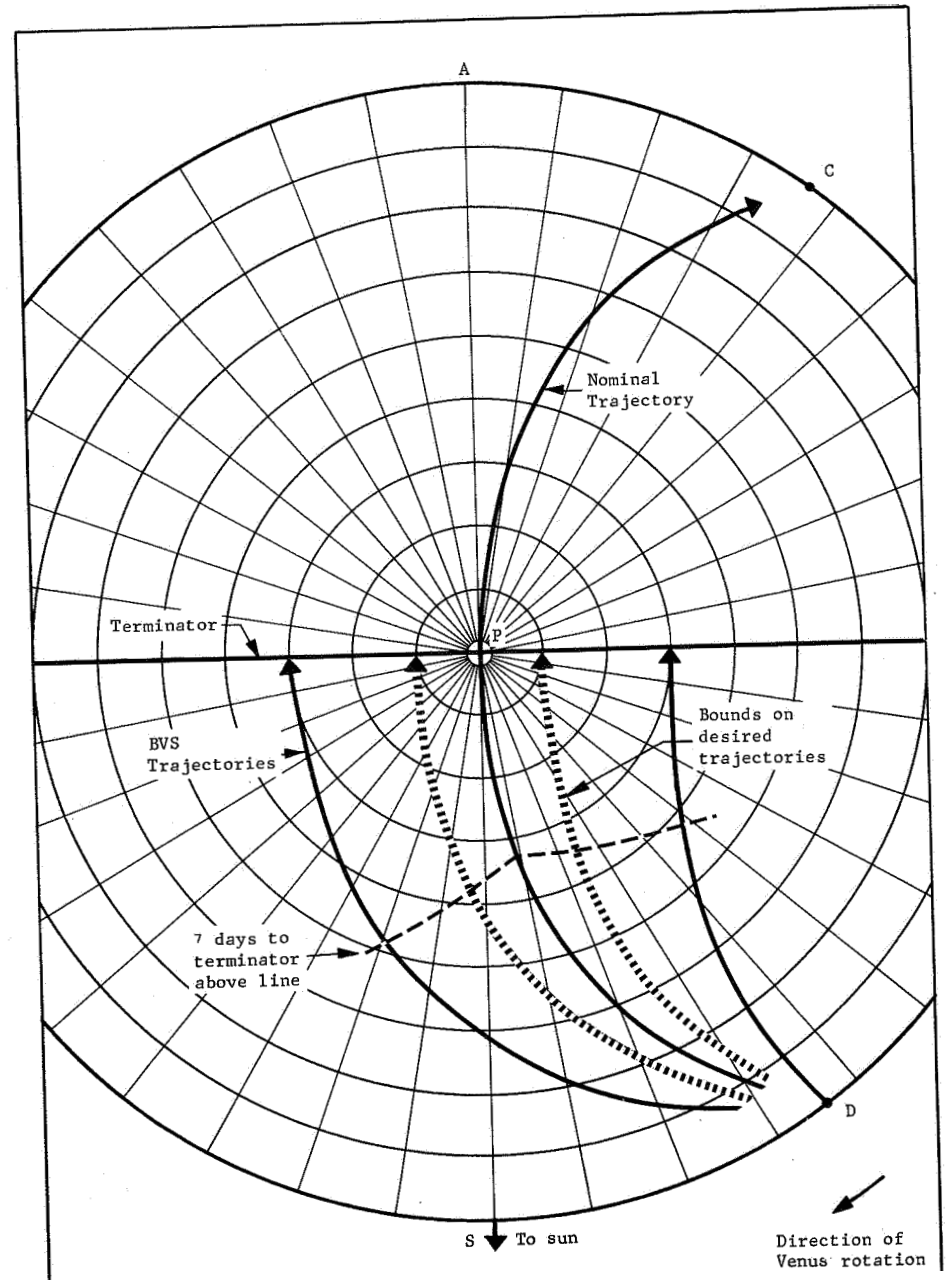

Figure 43. - BVS Trajectories Showing Desired Entry Locations

APPENDIX D

The time required for a BVS deployed at a given θ_o, φ_o to reach the terminator can be calculated from the above equations. The only velocity component needed is that in the meridional direction, V_θ, because rotation acts perpendicular to %. Therefore, we integrate:

$$\int_{o}^{t} dt' = \int_{\theta_o}^{\theta_T} V_\theta \qquad \text{(D12)}$$

to find the time it takes a BVS deployed at latitude θ_o to cross the terminator at latitude θ_T. Substituting for V_o and $\sin\delta$ in equation (D4) gives:

$$t = \frac{a}{V_m} \int_{\theta_o}^{\theta_T} \frac{d\theta}{\sin\theta \cos\varphi} \qquad \text{(D13)}$$

where φ is given by equation (D9) with the value of k given by equation (DlOa); θ_T is found from equation (DlOb). The integral in (D13) has no obvious analytic solution so numerical integration must be used.

For the trajectory that passes over the pole, φ changes slowly with θ and we can approximate (D13) by:

$$t \simeq \frac{a}{V_m} \sum_{n=N_o}^{N_T} \left[\frac{1}{\langle \cos\varphi_n \rangle} \ln \frac{\tan\left(\frac{n+1}{2}\Delta\theta\right)}{\tan\left(\frac{n}{2}\Delta\theta\right)} \right] \qquad \text{(D14)}$$

where

$$\langle \cos\varphi_n \rangle = \sqrt{1 - \sin^2\varphi_n}$$

$$\sin\varphi_n = \frac{k \sin\theta_n - \alpha}{\cos\theta_n}$$

APPENDIX D

$$\theta_n = \left(n + \frac{1}{2}\right) \Delta\theta$$

$$\Delta\theta = \frac{\theta_T - \theta_o}{N_T - N_o} \quad \left(N_T,\ N_o \text{ integers}\right)$$

If the BVS is deployed exactly at D, where $\theta_o = 0$, it will, in principle, never move away from D. That is, the time required to reach the pole is infinity. Therefore, the BVS should not be deployed at D, but some distance away. As an example, assume the BVS is deployed at a latitude of 5". If the BVS is to pass over the pole $\left(\theta_T = 90°,\ \varphi_T = 0°\right)$, the value of k given by equation (D10b) is $k = \alpha = -0.6$. For $\Delta\theta = 5°$, table 29 gives the times when the BVS reaches the given latitudes. If the BVS is deployed at 5" latitude and 30.25" longitude, it will pass over the pole in 38.2 days; if deployed at 45" latitude and 14.4" longitude, it takes only 10 days to reach the pole. The time is significantly reduced since the wind velocities are higher at the higher latitudes. The last column in table 29 gives the time required to reach the pole if deployed at the corresponding latitude.

For trajectories not passing near the pole, the approximation (D14) breaks down since φ changes more rapidly than θ and other integration techniques give more accurate results, (e.g., Simpson's Rule).

If the BVS were deployed at the subsolar point, it would travel along the equator to the evening terminator in a time:

$$\left.\begin{aligned} t &= \int_0^{-\frac{\pi}{2}} \frac{a \cos\theta}{V_\varphi}\, d\varphi = \frac{a}{V_m} \int_0^{-\frac{\pi}{2}} \frac{d\varphi}{\sin\varphi + \alpha} \\ t &= \frac{a}{V_m \sqrt{1-\alpha^2}} \log\left[\frac{\left(1 - \alpha - \sqrt{1-\alpha^2}\right)\left(1 + \sqrt{1-\alpha^2}\right)}{\left(1 - \alpha + \sqrt{1-\alpha^2}\right)\left(1 - \sqrt{1-\alpha^2}\right)}\right] \\ t &\simeq 6.66 \text{ days} \end{aligned}\right\} \text{(D15)}$$

Therefore, a BVS deployed at the subsolar point would pass over the antisolar point in about 13.3 days.

APPENDIX D

TABLE 29. - BVS FLIGHT TIMES VS LATITUDE FOR POLAR TRAJECTORY ($k = -0.6$)

n	Latitude, θ, deg	Longitude, φ, deg	Time, days	ΔT, days
1	5		0	38.19
	7.5	31.75		
2	10		9.15	29.04
	12.5	28.78		
3	15		14.37	23.82
	17.5	26.10		
4	20		18.02	20.17
	22.5	23.63		
5	25		20.82	17.37
	27.5	21.35		
6	30		23.10	15.09
	32.5	19.22		
7	35		25.03	13.16
	37.5	17.21		
8	40		26.71	11.48
	42.5	15.31		
9	45		28.21	9.98
	47.5	13.49		
10	50		29.58	8.61
	52.5	11.75		
11	55		30.83	7.36
	57.5	10.07		
12	60		32.01	6.18
	62.5	8.44		
13	65		33.13	5.06
	67.5	6.85		
14	70		34.19	4.00
	72.5	5.30		
15	75		35.22	2.97
	77.5	3.77		
16	80		36.23	1.96
	82.5	2.25		
17	85		37.21	0.98
	87.5	.75		
---	90	0	38.19	0

APPENDIX D

It should be understood that these results are based on theoretical estimates of the wind pattern. The general pattern of the BVS trajectories is very plausible; however, the exact locations of the points D and C or, equivalently, the value of the wind velocity at the terminator is extremely uncertain. If the wind speeds are greater than assumed, then the departure of the points D and C from the subsolar and antisolar points would be reduced. In this case, the trajectory that passes over the pole would pass closer to the subsolar and antisolar points than shown in figure *43*.

ADVANTAGES OF MORE THAN ONE BUOYANT STATION

The above discussion indicates that although it does not seem possible to pass exactly over subsolar, pole, and antisolar points with a single balloon trajectory, it does appear possible to come reasonably close to these points with a single buoyant station. The amount of time necessary to complete the required trajectory is estimated to be about 50 to 100 days. If more information on the wind field becomes available before the BVS mission, and if the new wind information agrees with the wind model used in our calculations of trajectories, then a single buoyant station mission to obtain the desired coverage of Venus would be practicable. If not, two or three separate buoyant stations would be desirable to assure successful sampling. Rather than relying on the wind field to position the balloon over the desired sampling points, the two or three buoyant stations could be injected initially over these points. For two stations, the recommended injection points are the subsolar and antisolar points. For three stations, the recommended injection points are the subsolar, antisolar, and pole points.

The realization of these desired injection points is critically dependent on the year, and hence on the possible orbits or approach trajectories that can be obtained. Indeed, even if the desired injection points could be attained, it is not at all obvious that the communication link between the orbiter or flyby and the BVS could be maintained for any length of time. Such considerations were beyond the scope of the present study; however, they are critical and should be investigated in any future study.

APPENDIX E

TRACKING INSTRUMENTATION

J. D. Pettus, M. L. Salis, and E. P. Friend
Martin Marietta Corporation

This appendix is the result of a study to investigate means of determining the position of the buoyant station in relation to a planet centered coordinate system, to recommend a reference coordinate system, and to investigate the measurements and errors involved.

A technique for locating the station has been suggested in .which the station is located in relation to the orbiter's orbit that is, in turn, referenced to an inertial coordinate frame.

The technique requires ranging measurements from the orbiter to the station and resolution of the ambiguity of two locations by an inertial navigation system on the station or a direction finding system on the orbiter.

Errors of as much as 1000 km under certain conditions can occur because of the lack of knowledge of the radius of the planet (±140 km), however, these errors can be retroactively reduced at any time that a more accurate knowledge of planet radius is determined,

Errors in ranging and in determining the radius to the orbiter at the point of ranging are expected to contribute less to position error than the planet radius uncertainty,

The greatest errors occur when the station is located within a few degrees of the orbital plane near the subapoapsis point because this is where sensitivity to errors have their greatest effect and where it is most difficult to resolve the ambiguity in position.

This analysis has been conducted assuming that the orbital parameters are known exactly. Two computer programs were written and used in the analysis to determine errors and sensitivities to errors in range measurement, planet radius and radius from the planet center of mass to the orbiter.

APPENDIX E

REQUIREMENT

The requirement to know the position of the BVS is based on the desire to identify the coordinates (referenced to Venus) of any interesting phenomena observed on the planet's surface or in the atmosphere and to map the predominant wind pattern.

The position accuracy desired can be arrived at by considering accuracy in locating phenomena by other means such as:

1) IR and optical measurements from Earth, *400* km;

2) Radar measurements from Earth, 100 km;

3) Radar measurements from the orbiter (bus), 10 to 50 km.

If the station can be located at the time of any given measurement to an accuracy relative to the surface of the same order of magnitude as the above, the data could be coordinated with other measurements from Earth and the bus. On this basis an accuracy of ±300 km horizontally and ±1 km above the local surface is taken as a tentative goal.

STATEMENT OF PROBLEM

The problem is to provide the desired station position data using readily obtainable information.

The dimensions that are or will be better known in this problem are:

1) The orbital parameters of the bus in relation to both the planet center of mass and the inertial reference frame;

2) The position of the bus in its orbit as a function of Earth time;

3) The diameter of the visible planet including cloud cover -- ±150 km;

4) Surface diameter -- ±280 km.

APPENDIX E

The orbital parameters will be defined more accurately with each orbit tracked. from Earth up to a data saturation point; however, without further literature search or analysis, it is not possible at this time to predict to what accuracy they will be known. Therefore, for purposes of this report it is assumed that the orbital parameters will be exactly known.

Values that are not known well enough to be of any use initially to this problem are:

1) Axis of rotation -- within 10" of orbit axis;

2) Sidereal period of rotation -- 250^{+4}_{-7} earth days (see Appendix F);

3) Magnetic fields -- unknown;

4) Surface landmarks.

The study ground rule requiring day/night operation as well as a desire to operate in and under the clouds precludes the continuous use of one more piece of datum -- the direction to the sun.

APPROACH TO THE PROBLEM

The approach to the problem is to make use of the most accurate piece of datum -- the orbit of the bus -- as the basic reference and to develop a concept that will permit refinement of the accuracy of location at such time as other parameters, such as surface radius and axis of rotation, become better defined.

The station can be located ambiguously and with some error in reference to the orbit by measuring the range from the orbiter at time t_1 and again at time t_2 as shown in figure *44* and by assuming that the station is located on a reference sphere with radius equal to the radius of the planet plus the altitude of the buoyant station above the surface. The points A and B give the ambiguous location. Methods of resolving the ambiguity require use of a direction finding technique in the orbiter or an inertial system in the station. These methods are discussed later. Since θ_1 and θ_2 are known if the orbital parameters are known and the ranges G_1 and G_2 are measured, the only unknown is the reference sphere radius. Once this is assumed using the best known data on surface diameter and by measuring the altitude of the station one can calculate the latitudes and longitudes of A and B on the reference sphere by using the following equations.

APPENDIX E

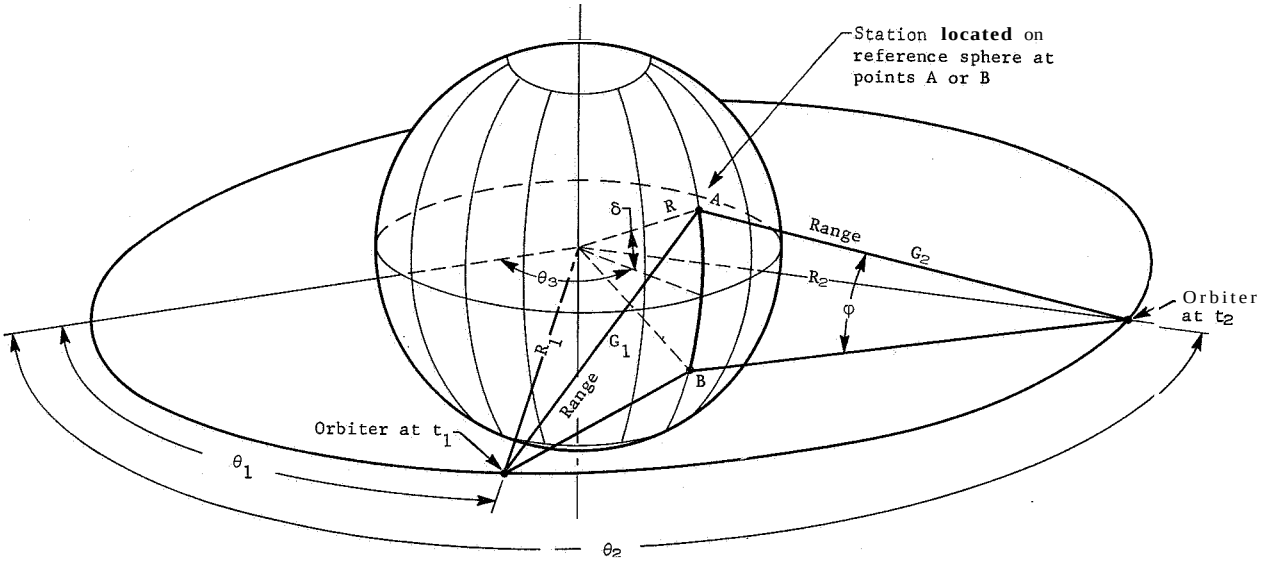

Figure 44. - Geometry for Determining Station Position in Reference to Periapsis and Orbital Plane

$$\text{Latitude (north or south)} = \delta = \arctan\left(\frac{R^2 \sin^2 (82 - e,)}{(P_1)^2 + (P_2)^2 - 2P_1 P_2 \cos(\theta_2 - \theta_1)}\right) \quad \text{(El)}$$

where

$$P_1 - \frac{R_1^2 + R^2 - G_1^2}{2R_1}$$

$$P_2 - \frac{R_2^2 + R^2 - G_2^2}{2R_2}$$

δ = latitude measured from orbital plane on reference sphere (north or south to be resolved)

R = radius of reference sphere

R_1 = distance from center of planet mass to orbiter at θ_1

R_2 = distance from center of planet mass to orbiter at θ_2

θ_1 = true anomaly at first point of ranging from the orbiter

θ_2 = true anomaly at second point of ranging from the orbiter

G_1 = range from orbiter to station (measured) at 8_1

G_2 = range from orbiter to station (measured) at θ_2

$$\text{Longitude} = 8_3 = \arctan \frac{P_2 \cos e_1 - P_1 \cos e_2}{P_1 \sin \theta_2 - P_2 \sin \theta_1} \qquad \text{(E2)}$$

where

θ_3 = longitude of the station measured on the reference sphere from the periapsis of the orbit and perpendicular to the orbital plane (see fig. *44)*

These parameters may be readily converted to the recommended coordinate system in which an inertial reference frame is used. However, for initial calculations and evaluation of the error sensitivities of the variables, the above equations were used.

ERRORS IN DETERMINING THE POSITION OF THE STATION

Various parameters contribute to the uncertainty in the location of points A and B. In reference to figure *44* these parameters are:

1) Errors in the range measurements G_1 and G_2;

2) The position accuracy of the bus at points P_1 and P_2;

3) Movement of the station between the first and second ranging measurement (equivalent to an error in range);

4) Errors in the altimeter measurement of the distance from the buoyant station to the surface of the planet;

5) Errors in the assumed distance from the center of mass of the planet to the surface below the buoyant station (error in the reference sphere radius).

An analysis of the sensitivity of the calculated station position for various station locations around the orbit (longitude) and for various latitudes was conducted by determining variations in latitude and longitude by successively incrementing R (the radius of the reference sphere), R_2 (the radial distance of the orbiter from the planet center of mass), and G_2 (the second range measurement from the orbiter) to determine actual position errors vs errors in the above variables. The following increments were used:

1) t20 km in R;

2) ±1 km in G_2;

3) ±5 km in R_2.

The results are shown in figures 45 thru 47. Obviously, the uncertainty in position is much greater when the station is located near the orbital plane ($\delta \simeq 0°$) and sensitivity to errors in R, R_2, and G_2 are extremely high under these conditions.

RESOLUTION OF AMBIGUITY BY INERTIAL NAVIGATION

Using the rf triangulation ranging scheme (defined in the final section of this appendix), which locates the BVS to two specific points on the reference sphere, it becomes necessary to resolve this ambiguity and provide means to subsequently have knowledge of the BVS position time history.

Since planet observables are not defined on Venus and celestial bodies cannot be reliably depended upon as visible due to the Cytherean cloud layer, the only type of system which would provide a known orientation and, therefore, be capable of yielding continuous positional information is a gyro referenced inertial platform. In the most optimistic use of this type of system, the BVS would be initialized in some known orientation, deorbited from the orbiting vehicle, enter the Cytherean atmosphere accurately retaining this original attitude frame and with an orthogonal triad of linear accelerometers monitor the BVS position throughout the mission.

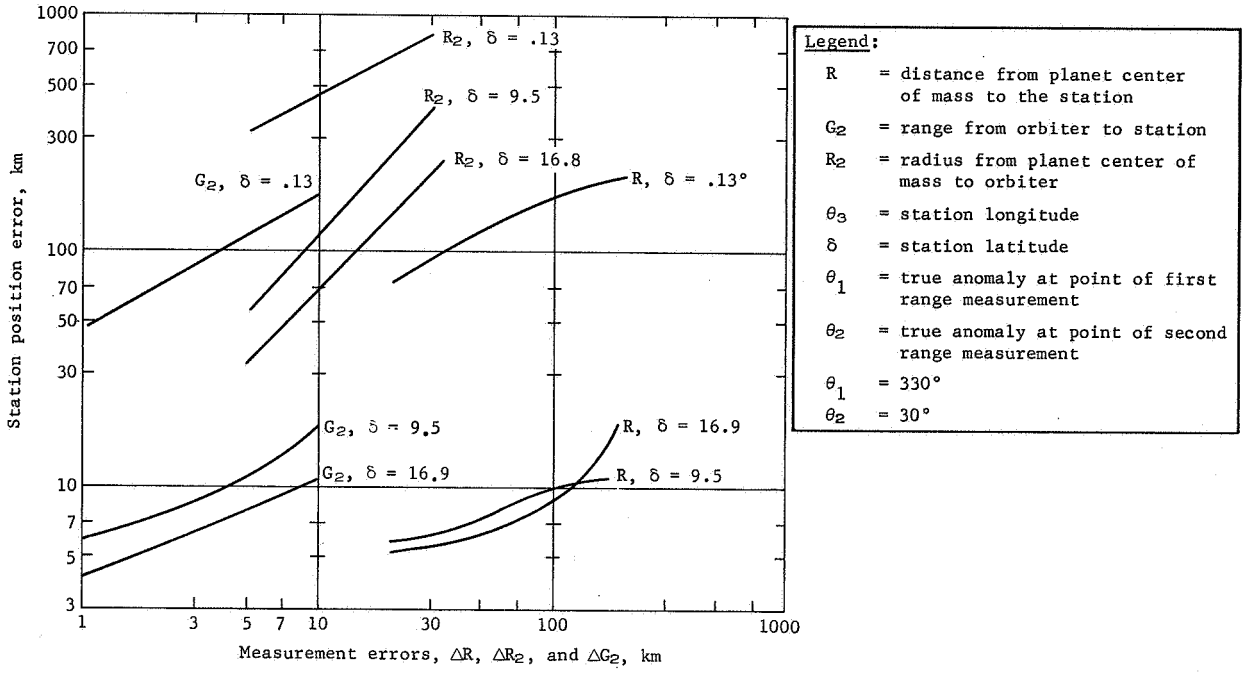

Figure 45. - Station Position Uncertainty vs Measurement Errors for $\theta_3 = 0°$

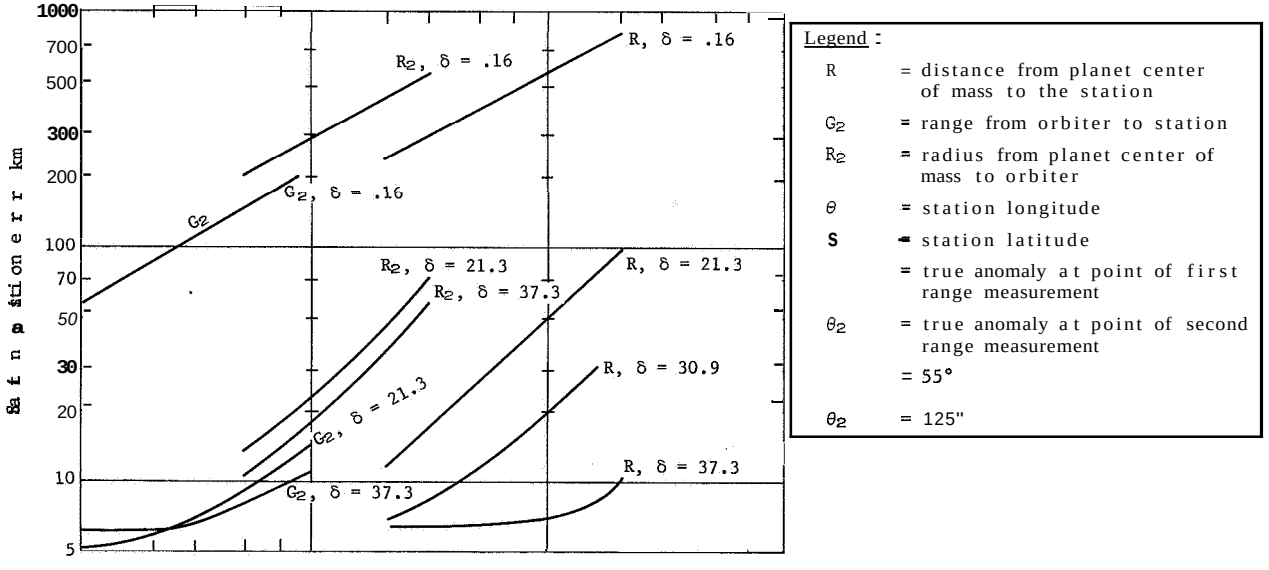

Figure 46. - Station Position Uncertainty vs Measurement Errors for θ = 90"

APPENDIX E

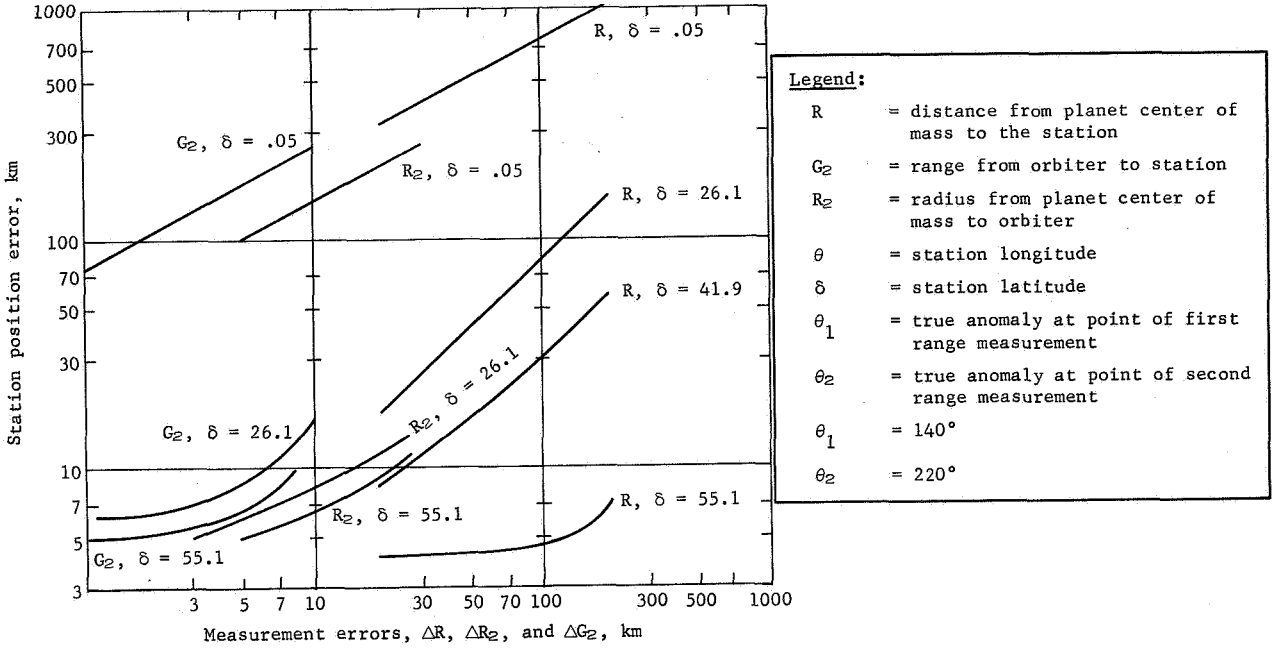

Figure 47. - Station Position Uncertainty vs Measurement Errors for $\theta_3 = 180°$

For missions involving the severe environment that the BVS will be subjected to during atmospheric entry, a system of this kind could not be expected to retain its original frame of reference and some method of checking the degree to which this occurs, and subsequent adjustments in the data evaluation would have to be effected post entry. In addition, the duration of the mission (4 weeks or greater) indicates substantial drift errors due mainly to gyro mass unbalance and means will have to be provided to account for errors of this sort.

The major problem associated with the severe entry environment is the possible damage to the inertial components and subsequent loss of mission navigation. If this problem can be resolved, the loss of original reference frame can be handled by a combination of the orbiter ranging information and accelerometer outputs over a long enough period to properly choose the correct position of the BVS.

The Nortronics NIT 130 Floated Sphere Navigation System has been tested to 75 g applied continuously without appreciable accuracy error and should therefore be expected to sustain a slightly higher environment for a relatively short time without permanent damage to the system. This system uses an outer sphere

mounted to the case with an inner sphere floated inside. The inner sphere contains the inertial components and the gyro pick-off signals as well as the accelerometer outputs are telemetered in and out limiting the physical connections between the inner and outer spheres to power leads.

The Kearfott MINS Inertially Gimbaled Platform and the Honeywell SIGN III Strapdown System are two other navigational systems that could sustain the environment of entry and accurately be initialized afterwards.

The size, weight and power requirements of the three systems mentioned are compared in table 30.

TABLE 30. - SIZE, WEIGHT, AND POWER COMPARISON OF THE CONCEPTUAL NAVIGATION SYSTEMS

	Size, cu ft	Weight, lb	Power, W
Nortronics NIT 130	.5	43	300
Kearfott MINS	.53	35	198
Honeywell SIGN III	.61	42	176

In any of these suggested systems the inaccuracy or misalinement from the attitude at deorbit should be substantial, but not completely misoriented. The errors will be on the order of several degrees in each direction. This in itself would be enough to resolve the ambiguity as shown in figure 48.

Assuming that the original orientation would be $Z_{B_{OR}}$ along the local vertical, $X_{B_{OR}}$ along the orbital path, and $Y_{B_{OR}}$ normal to X_B, and Z_B in a right-hand manner. AB represents the projection of the orbital path on the reference sphere. If A1 and B1 are the two points in question and the orientation post entry would be several degrees offset from the original (as shown in fig. 48) the accelerometer output of the $Y_{B_{OFF}}$ axis (assumed

positive) would at least be enough to denote a general movement to the right rather than to the left (on fig. *48)* and would be sufficient to choose B1 over **A1** as the actual first point.

The following discussion will be the general theory of operation of the navigation system assuming that we could not use our previous orientation knowledge (i.e., complete misalinement due to entry environment).

Upon deployment of the balloon, the platform will use the accelerometers in a loop that is an analog of the Schuler pendulum. This loop includes a gyro precession axis torquer, and a vertical accelerometer as the vertical reference. Since the Schuler pendulum maintains an accurate vertical reference, it can be used *to* generate correction signals to tilt the gyro spin axis to a vertically referenced plane rather than its inertial space reference. If the acceleration signal is integrated with respect to time, it represents the instantaneous velocity of the BVS. Dividing this velocity by the planet's radius gives the angular velocity at which the platform must rotate to remain tangent to the planet's surface. The Schuler tuned signal is applied to the gyro precession torquer, properly scaled to indicate the required angular velocity.

Upon commanding the platform normal to local vertical (Z_B axis down) the X_B and Y_B accelerometers are monitored from then on to correlate with the ambiguous ranging data to resolve the problem of position location. This will involve the orbiter making several ranging efforts yielding a result as shown in figure *49.*

Line AB represents the projection of the orbit on the reference sphere and A_N, B_N represent sets of double points, one of which is correct. It can be seen that for the outputs of the accelerometers as a function of time, there can be only one right-handed frame of orientation of X_B and Y_B ($i.e.$, $X_B \times Y_B = Z_B$) that will properly be matched to the acceleration curve data and so the correct pattern will be determined. As an example, suppose the accelerometer outputs are as shown in figure 50. Then the only possible system that would satisfy this data would be Frame A as shown in figure *49* as Frame B would have yielded a negative acceleration on the Y axis from position **3** to *4.*

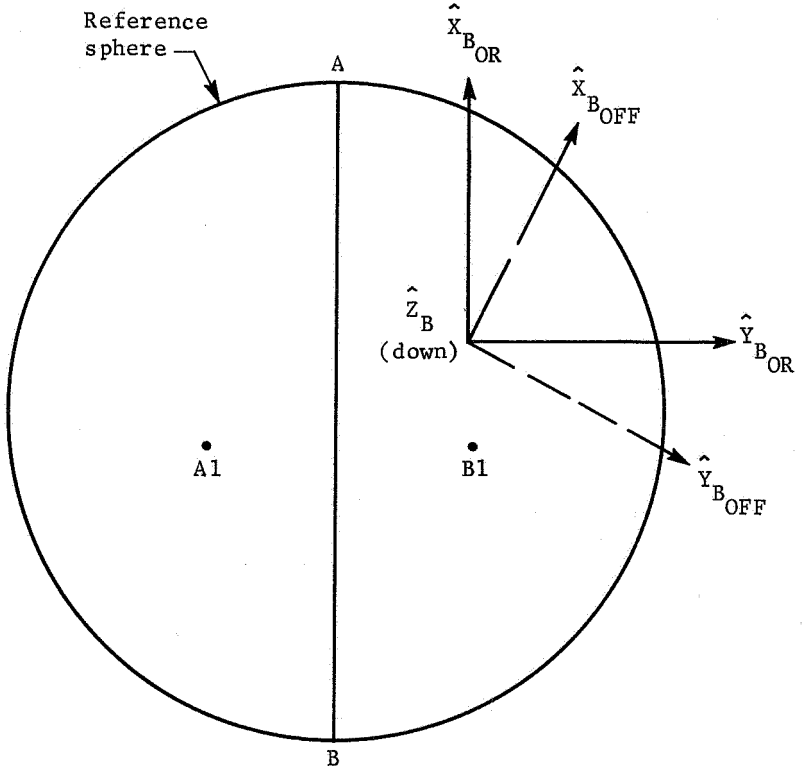

Figure 48. - Resolution of BVS Ambiguity Assuming Small Misalinement due to Entry

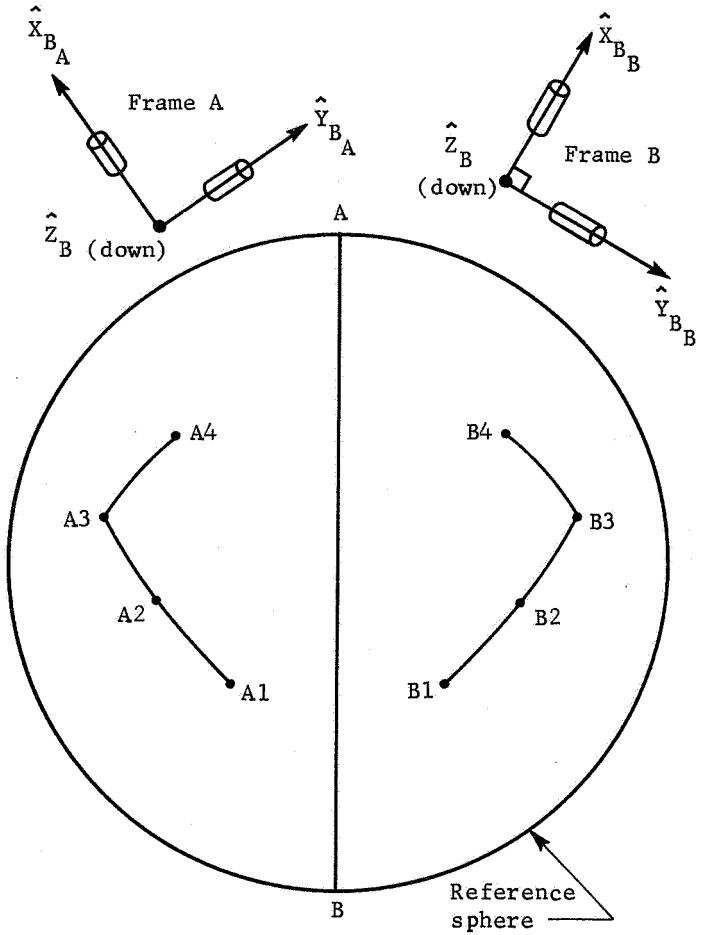

Figure 49. - Resolution of BVS Ambiguity Assuming Loss of Alinement due to Entry

APPENDIX E

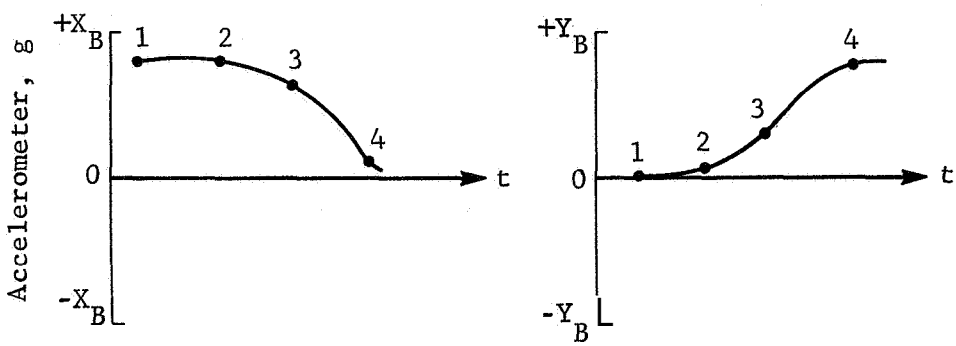

Figure 50. - X and Y Body ***Accelerometer Outputs***

Note that for the case in which the BVS moves in a straight line, the resolution of the correct point cannot be done. Only if the BVS has a curved path can this method be used. The probability of such a straight line path is very small.

A sun sensor package mounted on the local vertical reference plane could with two successive fixes (in azimuth of the sun to local vertical) resolve this problem if need be, but it is felt here that this would only add more complexity, weight, and cost to the system and then could only be used when the sun was visible (i.e., cloud layer could be occulting the sun from the BVS).

Once the orientation of the X and Y accelerometers are known, they will only be altered by the drift characteristics in the yaw gyro. These will be small, on the order of $\frac{1}{2}$°/hr/g. They can be constantly updated by the fix positions as given by the ranging information.

NAVIGATION WHEN OUT OF COMMUNICATIONS RANGE WITH THE ORBITER

The reference orbit specified in the statement of work for this study (10 000 by 1000 km altitude at periapsis and apoapsis) has a period of 1.37×10^4 sec or about 3.8 hr. Should the station stay within a few kilometers of the orbital plane the orbiting bus will lose contact with the station for from 2 to 3.7 hr depending on where the station is located in relation to the

apoapsis of the bus' orbit. However, should the station be blown away from the orbital trace, which is almost a certainty, much greater periods in which no contact will be encountered will occur.

For example, with the bus at apoapsis the station cannot be viewed after it has moved approximately 5000 km away from the orbital plane. At periapsis the station cannot be viewed after a drift of only 1500 km from the orbital plane.

If one assumes a maximum wind velocity of 28 km/hr in a direction perpendicular to the orbital plane, a period of approximately 54 hr is required for the station to drift out of range starting at the subperiapsis point. For an initial position at the subapoapsis point, a period of approximately 7.6 days is required, Should the station continue to drift at the same rate and in the same direction, it would take 18 days from the time communication was lost near the subapoapsis point until it would be reestablished near the subperiapsis point.

Figure 51 depicts the boundaries that represent those areas (shaded) in which the BVS would not be within communications range of the orbiter at any time on a given orbit.

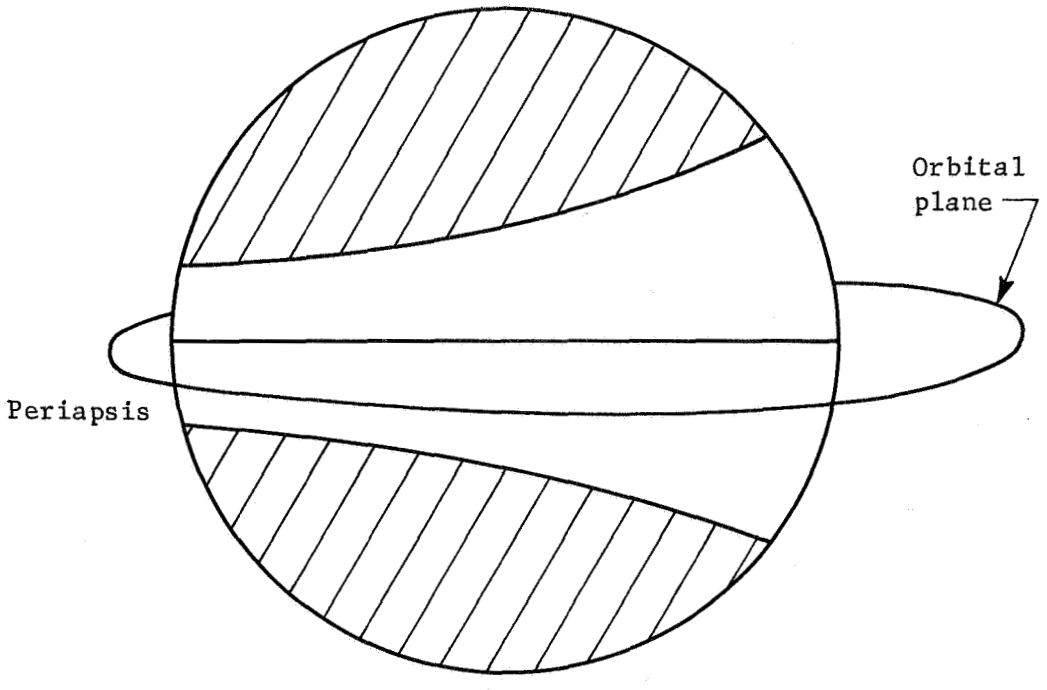

Figure 51, - Areas of Communication on Reference Sphere

APPENDIX E

It is very unlikely that communications would be lost for 18 days, but after the establishment of the BVS orientation, positional information could be obtained from the accelerometers whose major error would be in the drift due to gyro mass unbalance. Fortunately there is a direction associated with errors of this type, and with enough points initially before losing communications contact to obtain a pattern of drift, the data on the ground could be adjusted to compensate for the expected errors due to the measured drift early in the mission.

RECOMMENDED INERTIAL COORDINATE SYSTEM

Since planet rotation is not known, BVS location will be expressed in planet centered inertial coordinates with a celestial reference. A convenient choice would be the Earth equatorial inertial frame with the $\hat{X}_{EQ}$ axis of the system referenced to the first point of Aries, the Z_{EQ} axis parallel to the Earth's polar axis and the Y_{EQ} axis normal to the other two as shown in figure 52.

From Earth tracking data the path of the orbiter can be determined with respect to the Earth's reference system and can, therefore, be expressed in the $\hat{X}_{EQ}$, $\hat{Y}_{EQ}$, $\hat{Z}_{EQ}$ frame centered at Venus by the following orbital parameters:

- Ω - longitude of the ascending node from the $\hat{X}_{EQ}$ refer-
- i - the inclination of the orbital plane to the reference plane (equatorial Earth)
- ω - argument of periapsis
- θ - true anomaly of the crbiter

The coordinate frame defined by $\hat{X}_{OP}$, $\hat{Y}_{OP}$, and $\hat{Z}_{OP}$ as shown in figure 51 defines the frame where $\hat{X}_{OP}$ passes through periapsis. It is expressed in inertial equatorial coordinates via the transformation as described in detail later.

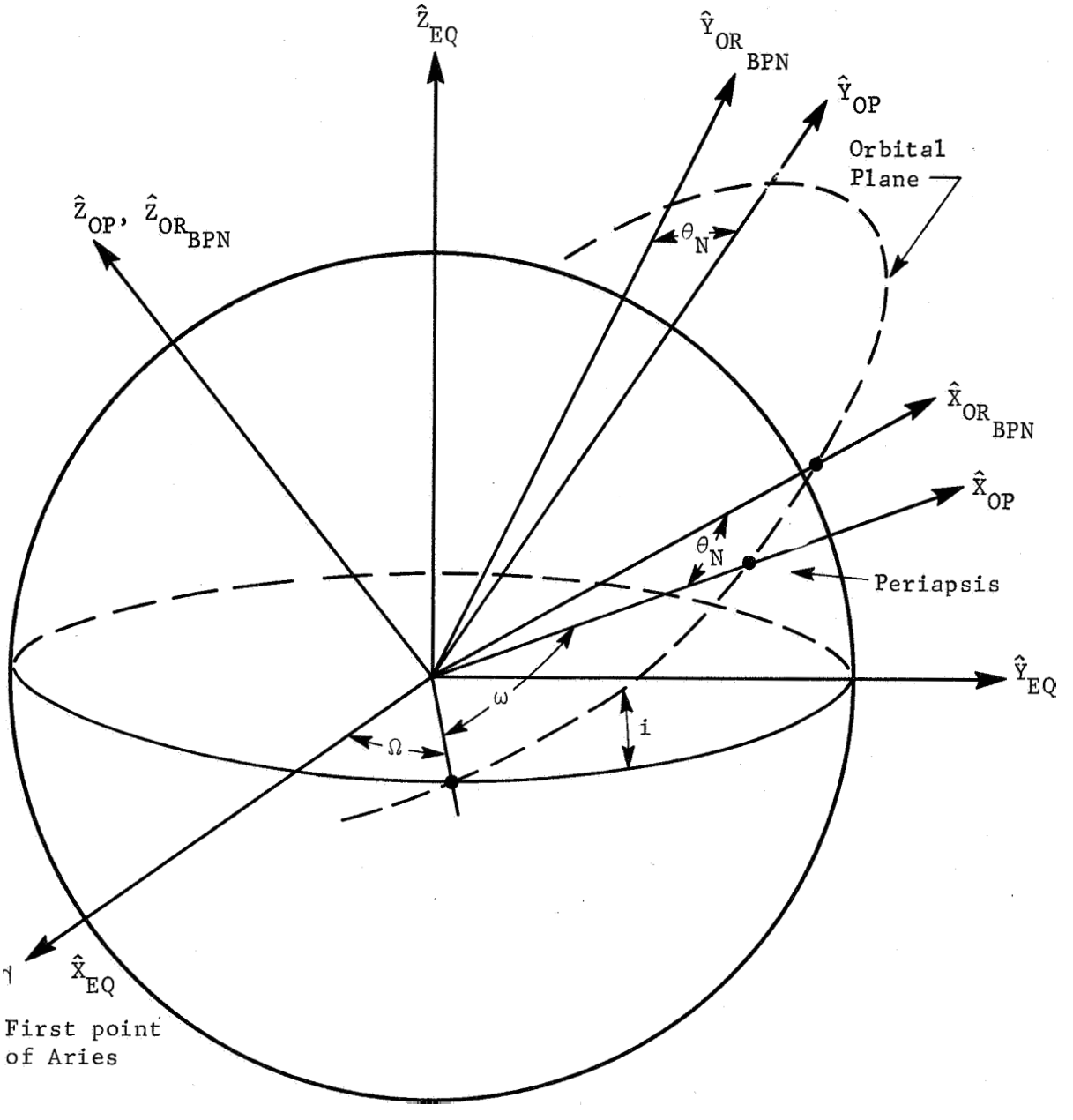

Figure 52. - Inertial Coordinate Frame

$$
\left.
\begin{aligned}
\hat{X}_{OP} &= (\cos w \cos \Omega - \sin w \cos i \sin \Omega)\, \hat{X}_{EQ} \\
&\quad + (\cos w \sin \Omega + \sin w \cos i \cos \Omega)\, \hat{Y}_{EQ} + \sin w \sin i\, \hat{Z}_{EQ} \\
\hat{Y}_{OP} &= (-\sin w \cos \Omega - \cos w \cos i \sin \Omega)\, \hat{X}_{EQ} \\
&\quad + (-\sin \omega \sin \Omega + \cos w \cos i \cos \Omega)\, \hat{Y}_{EQ} + \cos w \sin i\, \hat{Z}_{EQ} \\
\hat{Z}_{OP} &= \sin i \sin \Omega\, \hat{X}_{EQ} - \sin i \cos \Omega\, \hat{Y}_{EQ} + \cos i\, \hat{Z}_{EQ}
\end{aligned}
\right\} \quad (E3)
$$

The coordinate frame $\hat{X}_{OR_{BPN}}$, $\hat{Y}_{OR_{BPN}}$, and $\hat{Z}_{OR_{BPN}}$ is the one defining the orbiters position at any time where θ varies from 0" at periapsis to 360" when it is again at periapsis.

At a particular angle θ_N the X, Y, $Z_{OR_{BPN}}$ axis can be written in terms of the inertial equatorial frame as follows.

$$
\begin{bmatrix} \hat{X}_{OR_{BPN}} \\ \hat{Y}_{OR_{BPN}} \\ \hat{Z}_{OR_{BPN}} \end{bmatrix} = \begin{bmatrix} -\cos \ell \sin w \cos i \sin \Omega & \cos \theta \cos w \sin \Omega & \cos \theta \sin \omega \sin i \\ -\sin \theta \sin \omega \cos \Omega & +\cos \ell \sin w \cos i \cos \Omega & +\sin \theta \cos \omega \sin i \\ -\sin \theta \cos w \sin \Omega \cos i & -\sin \ell \sin w \sin \Omega & \\ +\cos \ell \cos w \cos \Omega & +\sin \theta \cos w \cos i \cos \Omega & \\ -\sin \theta \cos \omega \cos \Omega & -\sin \theta \cos w \sin \Omega & -\sin \theta \sin w \sin i \\ -\cos \theta \sin w \cos \Omega & -\sin \theta \sin \omega \cos i \cos \Omega & +\cos \theta \cos w \sin i \\ +\sin \theta \sin w \cos i \sin \Omega & -\cos \theta \sin \omega \sin \Omega & \\ -\cos \theta \cos \omega \cos i \sin \Omega & +\cos \theta \cos \omega \cos i \cos \Omega & \\ \sin i \sin \Omega & -\sin i \cos \Omega & \cos i \end{bmatrix} \begin{bmatrix} \hat{X}_{EQ} \\ \hat{Y}_{EQ} \\ \hat{Z}_{EQ} \end{bmatrix} \quad (E4)
$$

APPENDIX E

RESOLUTION OF AMBIGUITY BY DIRECTION FINDER TECHNIQUES

One method of resolving the ambiguity of station location is by the use of direction finding techniques in the orbiter. This, of course, means a steerable lobing antenna system on the orbiter or equivalent with the lobes straddling the orbital plane and pointed toward the planet's surface.

Resolution of ambiguity for station positions near the orbital plane will present the greatest problem since the included angle φ between the orbiter and the lines to position points A and B will be small especially when the orbiter is near apoapsis. For example, inability to resolve the ambiguity for $\varphi = 2°$ results in a position uncertainty of approximately *349* km (the distance A to B for $\varphi = 2°$) when the ranging is done at a bus altitude of 10 000 km. The minimum angle φ for which ambiguity resolution can be accomplished is a function of the bus system design and hence is beyond the scope of this preliminary study. However, it is identified as an anticipated problem area. In essence this means that a station located anywhere in a band of possibly several degrees in latitude adjacent (north and south) to the orbital plane cannot be identified as being located at one point or the other by this method.

COORDINATE SYSTEM RELATIONSHIP

This section deals with the relationships of the various coordinate systems used and the derivations of the equations necessary to determine the possible BVS locations on the reference sphere with two pieces of range information from the orbiter.

Referring to figure 53, the relationship between the $\hat{X}'$, $\hat{Y}'$, Z' frame and the $\hat{X}_{EQ}$, $\hat{Y}_{EQ}$, $\hat{Z}_{EQ}$ system is as follows:

$$\begin{bmatrix} \hat{X}' \\ \hat{Y}' \\ \hat{Z}' \end{bmatrix} = \begin{bmatrix} \cos \Omega & \sin \Omega & 0 \\ -\sin \Omega & \cos \Omega & 0 \\ 0 & 0 & 1 \end{bmatrix} \begin{bmatrix} \hat{X}_{EQ} \\ \hat{Y}_{EQ} \\ \hat{Z}_{EQ} \end{bmatrix} \tag{E5}$$

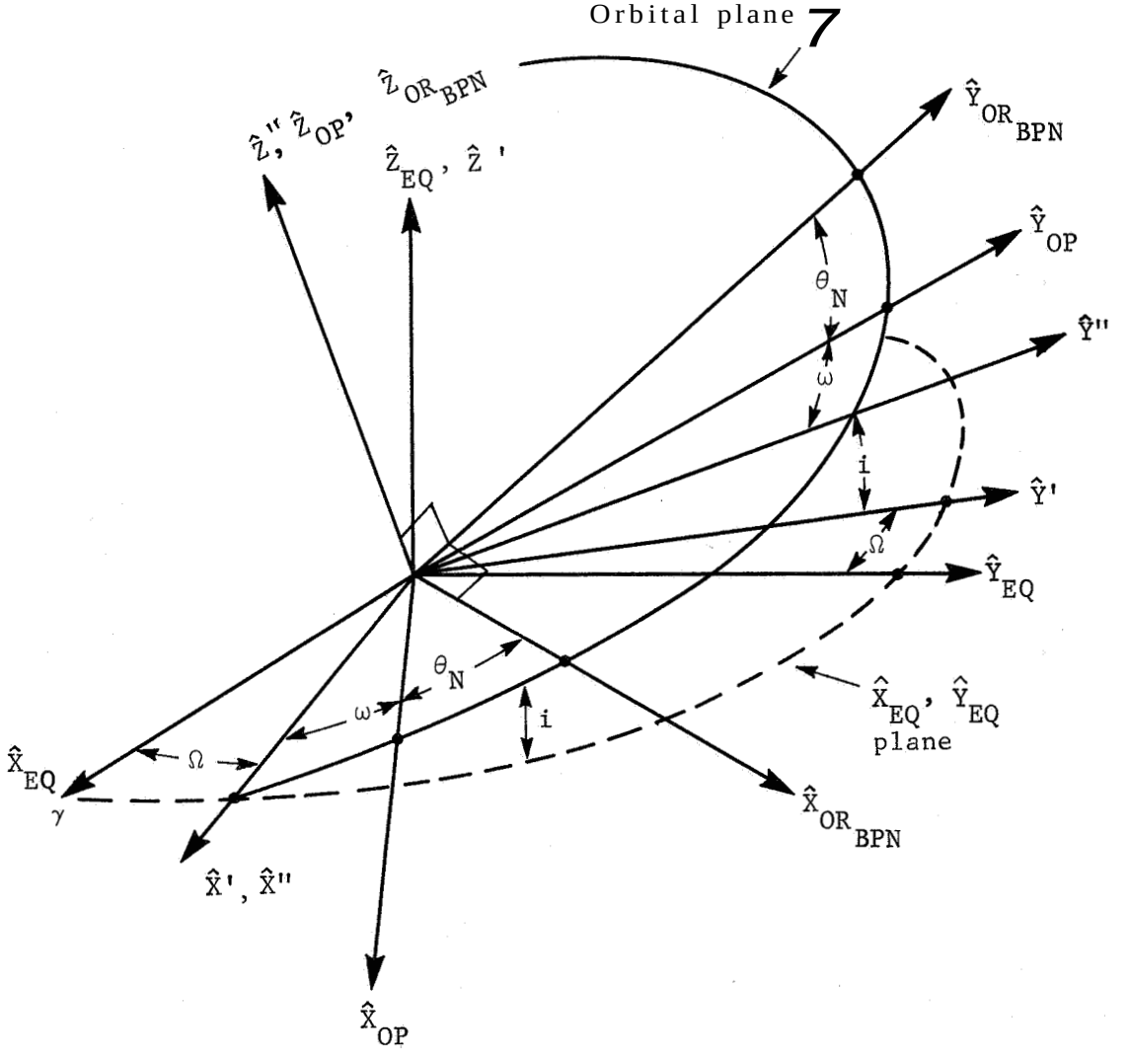

Figure 53. - Determination of Frames Passing through Points on the Orbit Referenced to Inertial System

In similar fashion, the $\hat{X}''$, $\hat{Y}''$, $\hat{Z}''$ relationship to $\hat{X}'$, $\hat{Y}'$, $\hat{Z}'$ is

$$\begin{bmatrix} \hat{X}'' \\ \hat{Y}'' \\ \hat{Z}'' \end{bmatrix} = \begin{bmatrix} 1 & 0 & 0 \\ 0 & \cos i & \sin i \\ 0 & -\sin i & \cos i \end{bmatrix} \begin{bmatrix} \hat{X}' \\ \hat{Y}' \\ \hat{Z}' \end{bmatrix} \tag{E6}$$

and

$$\begin{bmatrix} \hat{X}_{OP} \\ \hat{Y}_{OP} \\ \hat{Z}_{OP} \end{bmatrix} = \begin{bmatrix} \cos w & \sin w & 0 \\ -\sin \omega & \cos \omega & 0 \\ 0 & 0 & 1 \end{bmatrix} \begin{bmatrix} \hat{X}'' \\ \hat{Y}'' \\ \hat{Z}'' \end{bmatrix} \tag{E7}$$

Then combining these to get the relationship between the $\hat{X}_{OP}$, $\hat{Y}_{OP}$, $\hat{Z}_{OP}$ frame and the $\hat{X}_{EQ}$, $\hat{Y}_{EQ}$, $\hat{Z}_{EQ}$ as follows:

$$\begin{bmatrix} \hat{X}_{OP} \\ \hat{Y}_{OP} \\ \hat{Z}_{OP} \end{bmatrix} = \begin{bmatrix} \cos \omega & \sin \omega & 0 \\ -\sin \omega & \cos \omega & 0 \\ 0 & 0 & 1 \end{bmatrix} \begin{bmatrix} 1 & 0 & 0 \\ 0 & \cos i & \sin i \\ 0 & -\sin i & \cos i \end{bmatrix} \begin{bmatrix} \cos \Omega & \sin \Omega & 0 \\ -\sin \Omega & \cos \Omega & 0 \\ 0 & 0 & 1 \end{bmatrix} \begin{bmatrix} \hat{X}_{EQ} \\ \hat{Y}_{EQ} \\ \hat{Z}_{EQ} \end{bmatrix} \tag{E8}$$

yields

$$\begin{bmatrix} \hat{X}_{OP} \\ \hat{Y}_{OP} \\ \hat{Z}_{OP} \end{bmatrix} = \begin{bmatrix} \cos w \cos \Omega - \sin \omega \cos i \sin \Omega & \cos w \sin \Omega + \sin w \cos i \cos \Omega & \sin w \sin i \\ -\sin w \cos \Omega - \cos w \cos i \sin \Omega & -\sin \omega \sin \Omega + \cos w \cos i \cos \Omega & \cos w \sin i \\ \sin i \sin \Omega & -\sin i \cos \Omega & \cos i \end{bmatrix} \begin{bmatrix} \hat{X}_{EQ} \\ \hat{Y}_{EQ} \\ \hat{Z}_{EQ} \end{bmatrix} \tag{E9}$$

APPENDIX E

The frame which includes the point on the orbit at the time a ranging effort is effected is just one rotation in the orbital plane from the $\hat{X}_{OP}$, $\hat{Y}_{OP}$, $\hat{Z}_{OP}$ axis. In this $\hat{X}_{OR_{BPN}}$, $\hat{Y}_{OR_{BPN}}$, $\hat{Z}_{OR_{BPN}}$ frame the $\hat{X}_{OR_{BPN}}$ axis is along the line from the center of the planet to point N along the orbit rotated θ_N about the Z_{OP} axis.

$$\begin{bmatrix} \hat{X}_{OR_{BPN}} \\ \hat{Y}_{OR_{BPN}} \\ \hat{Z}_{OR_{BPN}} \end{bmatrix} = \begin{bmatrix} \cos\theta & \sin\theta & 0 \\ -\sin\theta & \cos\theta & 0 \\ 0 & 0 & 1 \end{bmatrix} \begin{bmatrix} \hat{X}_{OP} \\ \hat{Y}_{OP} \\ \hat{Z}_{OP} \end{bmatrix} \tag{E10}$$

The relationship between this $\hat{X}_{OR_{BPN}}$, $\hat{Y}_{OR_{BPN}}$, $\hat{Z}_{OR_{BPN}}$ frame and the basic equatorial frame is:

$$\begin{bmatrix} \hat{X}_{OR_{BPN}} \\ \hat{Y}_{OR_{BPN}} \\ \hat{Z}_{OR_{BPN}} \end{bmatrix} = \begin{bmatrix} +\cos\ell\cos w\cos\Omega & \cos\theta\cos w\sin\Omega & \cos\theta\sin w\sin i \\ -\sin\theta\cos w\cos i\sin\Omega & +\cos\theta\sin w\cos i\cos\Omega & +\sin\theta\cos\omega\sin i \\ -\sin\theta\cos\Omega\sin w & -\sin\theta\sin w\sin\Omega & \\ -\cos\theta\sin\omega\cos i\sin\Omega & +\sin\theta\cos w\cos i\cos\Omega & \\ -\sin\theta\cos w\cos\Omega & -\sin 0\cos w\sin\Omega & -\sin\theta\sin w\sin i \\ -\cos\theta\sin w\cos\Omega & -\sin\theta\sin w\cos i\cos\Omega & +\cos\theta\cos w\sin i \\ +\sin\theta\sin w\cos i\sin\Omega & -\cos\theta\sin w\sin\Omega & \\ -\cos e\cos w\cos i\sin\Omega & +\cos\theta\cos w\cos i\cos\Omega & \\ \sin i\sin\Omega & -\sin i\cos\Omega & \cos i \end{bmatrix}^{1} \begin{bmatrix} \hat{X}_{EQ} \\ \hat{Y}_{EQ} \\ \hat{Z}_{EQ} \end{bmatrix} \tag{E11}$$

At a time corresponding to the first ranging effort, the orbiter will be at point 1 along the orbit rotated e_1 from periapsis. Knowing the orbital radius of the orbiter at this point as R_1 and the relationship of $\hat{X}_{OR_{BPN}}$ in the equatorial axes as

$$\hat{X}_{OR_{BPN}} = (\cos\theta_1 \cos w \cos\Omega - \cos\theta_1 \sin w \cos i \sin\Omega$$
$$- \sin 8_1 \sin w \cos R - \sin 8_1 \cos w \cos i \sin\Omega)\ \hat{X}_{EQ}$$
$$+ (\cos\theta_1 \cos w \sin\Omega + \cos 8_1 \sin w \cos i \cos\Omega$$
$$- \sin 8_1 \sin w \cos\Omega + \sin 8_1 \cos w \cos i \cos\Omega)\ \hat{Y}_{EQ}$$
$$+ (\cos\theta_1 \sin w \sin i + \sin 8_1 \cos w \sin i\ \hat{Z}_{EQ} \quad \text{(E12)}$$

which can be written as

$$\hat{X}_{OR_{BPN}} = R_{X_1} \hat{X}_{EQ} + R_{Y_1} \hat{Y}_{EQ} + R_{Z_1} \hat{Z}_{EQ} \quad \text{(E13)}$$

where R_{X_1}, R_{Y_1}, R_{Z_1} are the coefficients of $\hat{X}_{EQ}$, $\hat{Y}_{EQ}$, $\hat{Z}_{EQ}$ unit vectors as in equation (E12).

The radius vector is then

$$\bar{R}_1 = \left|\bar{R}_1\right| \left(R_{X_1} \hat{X}_{EQ} + R_{Y_1} \hat{Y}_{EQ} + R_{Z_1} \hat{Z}_{EQ}\right)$$
$$\left|R_1\right| \cdot R_{X_1} = a_1,\ \left|R_1\right| \cdot R_{Y_1} = b_1,\ \left|R_1\right| \cdot R_{Z_1} = c_1 \quad \text{(E14)}$$

The situation is then as shown in figure 54:

1) There is the reference sphere which represents the position of the BVS at radius R from the center of Venus;

2) Spherical shell 1, which is centered at orbiter point 1, with radius G_1 representing the first range data point;

3) Spherical shell 2, which is centered at orbiter point 2, with radius G_2 representing the second range data point.

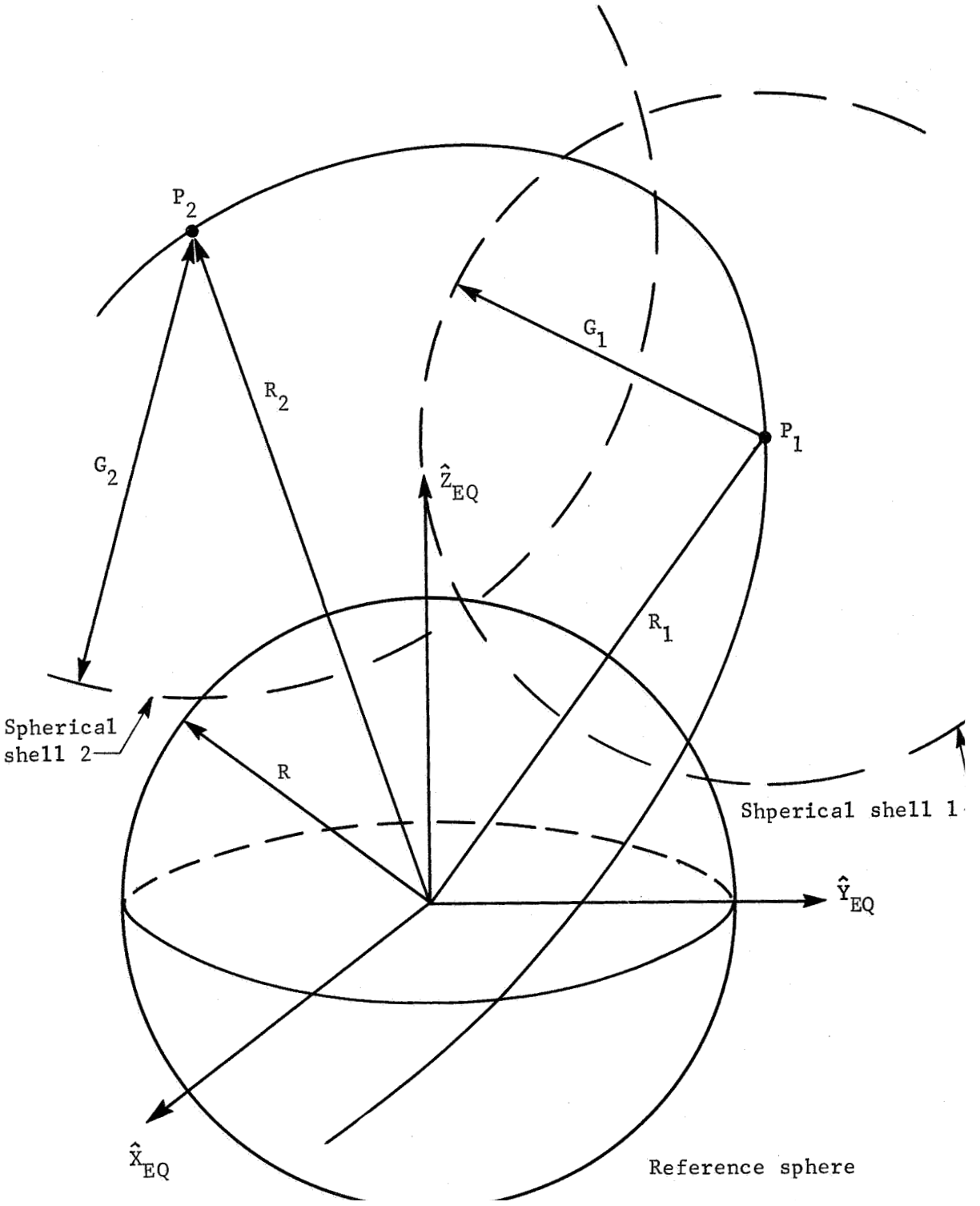

Figure 54. - **Solution** of the Intersection of the Three Spheres

APPENDIX E

The equation of the reference sphere is

$$X^2 + Y^2 + Z2 = R2 \tag{E15}$$

using the $\hat{X}_{EQ}$, $\hat{Y}_{EQ}$, $\hat{Z}_{EQ}$ frame as the basic computational frame.

Orbiter point 1, using θ_1 in equation (E12) can be written as $a_1 \hat{X}_{EO} + b_1 \hat{Y}_{EO} + c_1 \hat{Z}_E$ and this is the origin of spherical shell 1 whose equation is:

$$\left(X - a_1\right)^2 + \left(Y - b_1\right)^2 + \left(Z - c_1\right)^2 = G_1^2 \tag{E16}$$

Orbiter point 2, using θ_2 in equation (E12) can be written as

$$a_2 \hat{X}_{EQ} + b_2 \hat{Y}_{EQ} + c_2 \hat{Z}_{EQ} \tag{E17}$$

The equation of the spherical shell 2 centered at a_2, b_2, c_2 of radius G_2 is

$$(X - a_2)^2 + \left(Y - b_2\right)^2 + \left(Z - c_2\right)^2 = G_2^2 \tag{E18}$$

Solving simultaneous equations (E15), (E16), and (E18) will yield the BVS position in terms of X, Y, and Z in the $\hat{X}_{EQ}$, $\hat{Y}_{EQ}$, $\hat{Z}_{EQ}$ frame.

APPENDIX F

ROTATION RATE, MASS, AND RADIUS OF VENUS

At present, the values for these parameters are in a state of flux. Some recent publications give the values listed below.

Radius of solid globe	6056 ± 1 km (ref. *144)*
Sun-Venus mass ratio	*408 250* ± *120* (Newtonian theory) *408 450* ± *120* (general relativity theory) (ref. *144)* *408 505* ± *6* (ref. *145)*
Sidereal rotation rate (retrograde)	*-244.3* ± *2* days (ref. *146* using R from ref. *144)* *-242.6* ± *0.6* days (ref, *149)* *-250* ± *40* days (ref. 147) *-250* ± *9* days (ref. *148)* -250 *t* 4/-7 days (ref. *59)*

REFERENCES

1. Anon.: Space Research, Directions for the Future. Space Science Board, National Academy of Sciences - National Research Council, Dec. 1965.

2. de Vaucouleurs, G.: Reconnaissance of the Nearer Planets. Technical Report AFOSR/DRA-61-1, Air Force Office of Scientific Research, Nov. 1961. (Available from DDC as AD276833).

3. Briggs, M. H.; and Mamikunian, G.: Venus, A Summary of Present Knowledge, J. Brit. Interplanetary Soc., vol. 19, 1963, pp. 45-52.

4. Evans, D. C.: Physical Properties of the Planet Venus. Report SM-41506, Douglas Aircraft Corporation, Jul. 1962.

5. Kaplan, L. D.: Venus, Recent Physical Data for. Encyclopaedic Dictionary of Physics. Supplement vol. 1, 1966, pp. 366-367.

6. Kellogg, W. W.; and Sagan, C.: The Atmospheres of Mars and Venus. Nat. Acad. Sci. - Nat. Res. Coun., Publ. 944, 1961.

7. Sagan, C.: Planetary Environments and Biology. Astronaut. Aeron., vol. 4, no. 7, Jul. 1966, pp. 12-22.

8. Owen, R. B.: Theoretical Model Atmospheres of Venus. NASA TN D-2527, Jan. 1965.

9. Sagan, C.; and Kellogg, W. W.: The Terrestrial Planets. Annual Review of Astronomy and Astrophysics, 1963, pp. 235-266.

10. Opik, E. J.: The Aelosphere and Atmosphere of Venus. J. Geophys. Res., vol. 66, no. 9, 1961, pp. 2807-2819.

11. Shaw, J. H.; and Bobrovnikoff, N. T.: Natural Environment of the Planet Venus. WADC Phase Technical Note 2, Feb. 1959. (Available from DDC as AD242176).

12. Kaplan, L. D.: A Preliminary Model of the Venus Atmosphere. Technical Report 32-379, Jet Propulsion Laboratory, Dec. 12, 1962.

13. Evans, D. E.; Pitts, D. E.; and Kraus, G. L.: Venus and Mars Nominal Natural Environment for Advanced Manned Planetary Mission Programs. NASA SP-3016, 1965.

14. Brereton, R. G.; et al.: Venus: Preliminary Science Objectives and Experiments for Use in Advanced Mission Studies (rev. 1). Technical Memorandum 33-282, Jet Propulsion Laboratory, Aug. 1, 1966.

15. Dickerman, P.: Scientific Objectives of Deep Space Investigations - Venus. Report P-7, IIT Research Institute, May 1966.

16. Opik, E. J.: Progress in Astronautical Sciences. Vol. I., Chapter VI, Atmosphere and Surface Properties of Mars and Venus. pp. 261-342.

17. Brown, H., et al.: Proceedings of the Caltech-JPL, Lunar and Planetary Conference, Sep. 13-18, 1965, JPL TM33-266,1966, pp. 147-205.

18. Anon.: Voyager Design Studies. Vol. II. Scientific Mission Analysis. RAD-TR-63-34, AVCO Corporation, Oct. 1963.

19. Anon.: Voyager Design Studies. GE 63SD801, General Electric Company, Oct. 1963.

20. de Vaucouleurs, G.: Geometric and Photometric Parameters of the Terrestrial Planets. Icarus, vol. 3, 1964, pp. 187-235.

21. Smith, B. A.: A Photograph Optical Semidiameter of Venus. Astron. J., vol. 69, no. 2, 1964, pp. 201-204.

22. Clark, B. G.; and Kuz'min, A. D.: The Measurement of the Polarization and Brightness Distribution of Venus at 10.6 cm Wavelength. Astrophys. J., vol. 142, 1965, p. 23.

23. Jones, D. E.: The Mariner II Microwave Radiometer Experiment. Technical Report 32-722, Jet Propulsion Laboratory, Jan. 1, 1966.

24. Plummer, W. T.; and Strong, J.: A New Estimate of the Surface Temperatures of Venus. Astronautica Acta, vol. 11, no. 6, 1965, pp. 375-382.

25. Plummer, W. T.; and Strong, J.: A New Estimate of the Surface Temperatures of Venus. Astrophy. J., vol. 144, no. 1, 1966, pp. 422-424.

26. Plummer, W. T.; and Strong, J.: An Answer to F. D. Drake. Astrophys. J., 1966.

27. Spinrad, H.: Spectroscopic Temperature and Pressure Measurements in the Venus Atmosphere. Publications of the Astronomical Society of the Pacific, vol. 74, no. 88, 1962, pp. 187-201.

28. Kaplan, L. D.: The Structure of the Venus Atmosphere. (abstract) Mem. Roy. Soc. Liege, Ser. 5, vol. 7, 1963, pp. 323-324.

29. Sagan, C.: Structure of the Lower Atmosphere of Venus. Icarus, vol. 1, 1962, pp. 151-169.

30. Menzel, D. H.; and de Vaucouleurs, G.: Final Report on the Occultation of Regulus by Venus, July 7, 1959. AFCRL-227, Air Force Cambridge Research Laboratory, 1961.

31. Belton, M. J. S.; and Hunten, D. M.: Water Vapor in the Atmosphere of Venus. Astrophys. J., 1966.

32. Bottema, M.; et al.: The Composition of the Venus Clouds and Implications for Model Atmospheres. J. Geophys. Res., vol 70, no. 17, 1965, pp. 4401-4402.

33. Spinrad, H.: A Search for Water Vapor and Trace Constituents in the Venus Atmosphere. Technical Report 32-256, Jet Propulsion Laboratory, Oct. 1962.

34. Connes, P.; et al.: Traces of HCR and HF in the Atmosphere of Venus. Astrophys. J., vol. 147, no. 3, 1967, pp. 1230-1237.

35. Suess, H.: Remarks Concerning the Chemical Composition of the Atmosphere of Venus. Z. Natur Forschung, vol. 19A, 1964, pp. 84-87.

36. Dollfus, A.: Contributions au Colloque Caltech-JPL sur la lune et les planetes: Venus. Proceedings of the Caltech-JPL Lunar and Planetary Conference, Sep. 13-18, 1965. JPL TM 33-266, 1966, pp. 187-202.

37. Murray, B. C.; Wildey, R. L.; and Westphal, J. A.: Infrared Photometric Mapping of Venus through the 8- to 14-Micron Atmospheric Window. J. Geophys. Res., vol. 68, no. 16, Aug. 1963, pp. 4813-4818.

38. Sagan, C.; and Pollack, J. B.: Properties of the Clouds of Venus. Proceedings of the Caltech-JPL Lunar and Planetary Conference, Sep. 13-18, 1965, JPL TM 33-266, 1966, pp. 155-163.

39. Mayer, C. H.: Radio Astronomy Studies of Venus and Mars. Astronaut. Aeron., vol. 4, no. 4, Apr. 1966, pp. 13-25.

40. Pollack, J. B.; and Sagan, C.: The Microwave Phase Effect of Venus. Icarus, vol. 4, 1965, pp. 62-103.

41. Barrett, A. H.; and Staelin, D. H.: Radio Observations of Venus and the Interpretations. Space Science Reviews, vol. 3, 1964, pp. 109-135.

42. Barath, F. T., ed.: Symposium or Radar and Radiometric Observations of Venus during the 1962 Conjunction. Astron. J., vol. 69, no. 1, Feb. 1964.

43. Staelin, D. H.; and Barrett, A. H.: Spectral Observations of Venus Near 1-Centimeter Wavelength. Astrophys. J., vol. 144, no. 1, 1966, pp. 352-363.

44. Pollack, J. B.; and Sagan, C.: Polarization of Thermal Emission from Venus. Astrophys. J., vol. 141, no. 3, Apr. 1965, pp. 1161-1183.

45. Sinton, W. M.; and Strong, J.: Radiometric Observations of Venus. Astrophys. J., vol. 131, Mar. 1960, pp. 470-490.

46. Pollack, J. B.; and Sagan, C.: The Infrared Limb Darkening of Venus. J. Geophys. Res., vol. 70, no. 18, 1965, pp. 4403-4426.

47. Westphal, J. A.: The 10-micron Limb Darkening of Venus. J. Geophys. Res., vol. 71, no. 11, 1966, pp. 2693-2696.

48. Westphal, J. A.; Wildey, R. L.; and Murray, B. C.: The 8- to 14-micron Appearance of Venus before the 1964 Conjunction. Astrophys. J., vol. 142, no. 2, 1965, pp. 799-802.

49. Low, F. J.: Observations of Venus, Jupiter, and Saturn at $\lambda = 20\mu$. Astron. J., vol. 71, no. 6, Aug. 1966, p. 391.

50. Chamberlain, J. W.: The Atmosphere of Venus near Her Cloud Tops. Astrophys. J., vol. 141, no. 3, 1965, pp. 1184-1205.

51. Mintz, Y.: Temperature and Circulation of the Venus Atmosphere. Planetary and Space Science, vol. 5, 1961, pp. 141-152.

52. Chamberlain, J. W.; and Kuiper, G. P.: Rotational Temperature and Phase Variation of the CO_2 Bands of Venus. Astrophys. J., vol. 124, no. 2, 1956, pp. 399-405.

53. Kaplan, L. D.: A New Interpretation of the Structure and CO_2 Content of the Venus Atmosphere. Planetary and Space Science, vol. 8, 1961, pp. 23-99.

54. Shimizu, M.: Vertical Distribution of Neutral Gases on Venus. Planetary and Space Science, vol. 11, 1963, pp. 269-273.

55. Mueller, R. F.: A Chemical Model for the Lower Atmosphere of Venus. Icarus, vol. 3, 1964, pp. 285-298.

56. Anderson, H. R.: Ionizing Radiation Measured between Earth and Venus by Mariner II. Space Research V, Procedures, Fifth International Space Science Symposium, Florence, Italy, May 8-20, 1964, pp. 521-543.

57. Sagan, C.: The Radiation Balance of Venus. Technical Report 32-34, Jet Propulsion Laboratory, Sep., 1960.

58. Coulson, K. L.; and Lotman, M.: Molecular Optical Thickness of the Atmospheres of Mars and Venus. R62SD71, General Electric Company, Jul. 1962.

59. Carpenter, R. L.: Study of Venus by CW Radar - 1964 Results. Astron. J., vol. 71, no. 2, 1966, pp. 142-152.

60. Staff of JPL: Mariner-Venus 1962 Final Project Report. NASA SP-59, 1965.

61. Barnes, F. L., et al.: Mariner II Flight to Venus. Astronautics, Dec. 1962, pp. 67-72.

62. Wyckoff, R. C.: Scientific Experiments for Mariner R-1 and R-2. Technical Report 32-315, Jet Propulsion Laboratory, Jul. 15, 1962.

63. James, J. N.: The Voyage of Mariner 11. Scientific American, vol. 209, no. 1, Jul. 1963, pp. 70-84.

64. Frank, L. A.; et al.: Mariner II: Preliminary Reports on Measurements of Venus. Technical Report 32-420, Jet Propulsion Laboratory, Mar. 1963.

65. Sonett, C. P.: A Summary Review of the Scientific Finding of the Mariner Venus Mission. Space Science Reviews, vol. 2, Dec. 1963, pp. 751-777.

66. Barrett, A. H.; et al.: Objectives of the Mariner Venus Microwave Radiometer Experiment. Technical Report 32-156, Jet Propulsion Laboratory, Aug. 22, 1961.

67. Barath, F. T.; Barrett, A. H.; Copeland, J.; Jones, D. E.; and Lilley, A. E.: Mariner 2 Microwave Radiometer Experiment and Results. Astron. J., vol. 69, no. 1, Feb. 1964 (also Technical Report 32-533, Jet Propulsion Laboratory, Feb. 1964).

68, Pollack, J. B.; and Sagan, C.: An Analysis of the Mariner 2 Microwave Observations of Venus, Semiannual Progress Report 1, Grant No, NGR-09-015-023, Smithsonian Institution Astrophysical Observatory. Jun. 1966 (NASA CR-76106).

69. Sagan, C.: Planetary Environments and Biology. Astronaut. Aeron., vol. 4, no. 7, Jul. 1966, pp. 12-22.

70. Chase, S. C.; Kaplan, L. D.; and Neugebauer, G.: The Mariner 2 Infrared Radiometer Experiment. J. Geophys. Res., vol. 68, no. 22, Nov. 1963, pp. 6157-6169.

71. Smith, E. J.; et al.: Magnetic Measurements near Venus. J. Geophys. Res., vol. 70, no. 7, Apr. 1, 1965, pp. 1571-1586.

72. Anderson, H. R.: Ionizing Radiation Measured between Earth and Venus by Mariner 11. Space Research V, Proceedings of the Fifth International Space Science Symposium, Florence, Italy, May 8-20, 1964. Edited by P. Muller, North-Holland Pub. Co., 1965, pp. 521-543.

73. Neugebauer, M.; and Snyder, C. W.: Solar-Wind Measurements near Venus. J. Geophys. Res., vol. 70, no. 7, Apr. 1, 1965, pp. 1587-1591.

74. Neugebauer, M.; and Snyder, C. W.: Average Properties of the Solar Wind as Determined by Mariner 11. Technical Report 32-991, Jet Propulsion Laboratory, Nov. 1, 1966.

75. Anderson, J. D.: The Evaluation of Certain Astronomical Constants from the Radio Tracking of Mariner 11. Progress in Astronautics and Aeronautics, vol. 14, 1964, Academic Press, pp. 131-155.

76. Anon.: Space Programs Summary No. 37-39, vol. VI, Jet Propulsion Laboratory, May 1966, pp. 9-11.

77. Fjeldbo, G.; and Eshleman, V. R.: The Bistatic Radar Occultation Method for the Study of Planetary Atmospheres. J. Geophys. Res., vol. 70, no. 13, Jul. 1, 1965, pp. 3217-3225.

78. Fjeldbo, G.; Eshleman, V. R.; Garriott, O. K.; and Smith, F. L.: The Two-Frequency, Bistatic, Radar-Occultation Method for the Study of Planetary Ionospheres. J. Geophys. Res., vol. 70, no. 15, Aug. 1, 1965, pp. 3701-3710.

79. Stoney, W. E.: Collection of Zero-Lift Drag Data on Bodies of Revolution from Free-Flight Investigations. NACA TN-4201, Jan. 1958.

80. Hanel, R. A.: Exploration of the Atmopshere of Venus by a Simple Capsule. NASA TN D-1909, Jan. 1964.

81. Seiff, A.: Some Possibilities for Determining the Characteristics of the Atmospheres of Mars and Venus from Gas-Dynamic Behavior of a Probe Vehicle. NASA TN D-1770, Apr. 1963.

82. Peterson, V. L.: A Technique for Determining Planetary Atmosphere Structure from Measured Accelerations of an Entry Vehicle. NASA TN D-2669.

83. Peterson, V. L.: Analysis of the Errors Associated with the Determination of Planetary Atmosphere Structure from Measured Accelerations of an Entry Vehicle. NASA TR R-225, Jul. 1965.

84. Evans, J. W.: Development of Gun Probe Payloads and a 1750 MC/S Telemetry System. Memo Report 1749, USAMC, Ballistic Research Laboratories, May 1966 (Available from DDC as AD 637747).

85. Chase, S. C.; et al.: The Mariner II Infrared Radiometer Experiment. J. Geophys. Res., vol. 63, no. 22, Nov. 1963, pp. 6157-6169.

86. Jones, D. E.: The Mariner II Microwave Radiometer Experiment. Technical Report 32-722, Jet Propulsion Laboratory, Jan. 1, 1966.

87. Brereton, R. G.; et al.: Venus/Mercury Swing-By with Venus Capsule. EPD-409, Jet Propulsion Laboratory, Jul. 14, 1966. pp. 5-12,

88. Brereton, R. G.; et al.: Venus: Preliminary Science Objectives and Experiments for Use in Advanced Mission Studies. Technical Memoranda 33-282, Jet Propulsion Laboratory, Aug. 1, 1966.

89. Hanel, R. A.; and Strange, M. G.: An Acoustic Experiment to Determine the Composition of an Unknown Planetary Atmosphere, NASA, Goddard Space Flight Center, Greenbelt, Maryland.

90. Hanel, R. A.: Exploration of the Atmosphere of Venus by a Simple Capsule, NASA TN D-1909.

91. Corliss, W. R.: Space Probes and Planetary Exploration. Van Nostrand Co., 1965.

92. Anon.: Introduction to Mass Spectrometry with Applications in Space Technology. Systems Engineering Bulletin 3228, Consolidated Systems Corporation, Oct. 21, 1963.

93. Schaefer, E. J.; and Nichols, M. H.: Mass Spectrometer for Upper Air Measurements. ARS J., vol. 31, Dec. 1961, pp. 1773-1776.

94. Schaefer, E. J.; and Nichols, M. H.: Neutral Composition Obtained from a Rocket-Borne Mass Spectrometer. In-Space Research IV, P. Muller, ed., Interscience Publishers, New York, 1964.

95. Schaefer, E. J.: Neutral Composition, Scientific Report 05627-3-5, University of Michigan, College of Engineering, Feb. 1966 (NASA CR-70523).

96. Nier, A. O.; et al.: Neutral Composition of the Atmosphere in the 100- to 200-Kilometer Range. J. Geophys. Res., vol. 69, Mar. 1, 1964, p. 979.

97. Wilhite, W. F.: The Development of the Surveyor Gas Chromatograph. Technical Report 32-425, Jet Propulsion Laboratory, May 15, 1963.

98. Oyama, V. I.; et al.: Applications of Gas Chromatography to the Analyses of Organics, Water, and Adsorbed Gases in the Lunar Crust. Technical Report 32-107, Jet Propulsion Laboratory, Apr. 25, 1961.

99. Wilhite, W. F.; Burnell, M. R.: Lunar Gas Chromatograph. ISA J., Sep. 1963.

100. Wilhite, W. F.: Developments in Micro Gas Chromatography. J. Gas Chromatography, Feb. 1966, pp. 47-50.

101. Wilhite, W. F.: A Gas Chromatograph for the Analysis of the Martian Atmosphere. SPS 37-29, Vol. IV, Jet Propulsion Laboratory, Oct. 31, 1964, pp. 185-188.

102. Josias, C.; Bowman, L.; and Mertz, H.: A Gas Chromatograph for the Analysis of the Martian Atmosphere. SPS 37-27, Vol. IV, Jet Propulsion Laboratory, Jun. 30, 1964, pp. 85-91.

103. Chaudet, J. H.: Gas Chromatographic Instrumentation for Gas Analysis of the Martian Atmosphere, Final Report, Vol. I, NASA CR-59769; Vol. 11, NASA CR-59773; Vol. 111, NASA CR-59772); Sep. 25, 1962.

104. Bollin, E. M.: Micro-Analytical Gas Pyrolysis Instrumentation for Lunar and Planetary Investigation. SPS-37-31, Vol. IV, Jet Propulsion Laboratory, Feb. 28, 1965, pp. 255-261.

105. Adams, J. L.: The JPL High Impact Program - 1965. TR 32-844, Jet Propulsion Laboratory, Feb. 1, 1966, pp. 10-13.

106. Drummond D.; and Magistrale, V.: JPL Spacecraft Sterilization Technology Program: A Status Report. TR 32-853, Jet Propulsion Laboratory, Dec. 31, 1965, pp. 58-61.

107. Marshall, J. H.; and Franzgrote, E. J.: Analysis of the Martian Atmosphere by α-Particle Bombardment -- The Rutherford Experiment. SPS 37-26, Vol. IV, Jet Propulsion Laboratory, Apr. 30, 1964, pp. 148-154.

108. Anon.: Determination of Oxygen in the Martian Atmosphere via Kryptonates. Final Report, JPL Contract 950279, Parametrics, Inc., Oct. 1962.

109. Anon.: Potential Planetary Atmosphere Sensors. Final Report, JPL Contract 950684, Parametrics, Inc., Dec. 1964.

110. Hoenig, S. A.; and Abramowitz, J.: Detection Techniques for Tenuous Planetary Atmospheres. Fifth Six-Month Report, July 1, 1965-Dec. 30, 1965. NsG-458, Engineering Research Laboratories, University of Arizona.

111. Brereton, R. G.: Venus: Preliminary Scientific Objectives and Experiments for Use in Advanced Mission Studies. EPD-328, Jet Propulsion Laboratory, Dec. 22, 1965.

112. Sukalo, L. H., ed.: Proceedings of the Atmospheric Biology Conference, Apr. 13-15, 1964, University of Minnesota (under NASA grant NsG-461).

113. Pittendrigh, C. S.; et al., eds.: Biology and the Exploration of Mars. Publication 1296, National Academy of Sciences National Research Council, Washington, D.C., 1966.

114. Shneour, E. A.; and Otteson, E. A., eds.: Extraterrestrial Life: An Anthology and Bibliography. Publication 1296A, National Academy of Sciences National Research Council, Washington, D.C., 1966.

115. Young, R. S.; Painter, R. B.; and Johnson, R. D.: An Analysis of the Extraterrestrial Life Detection Problem. NASA SP-75, 1965.

116. Bently, K. E.; et al.: Detection of Life-Related Compounds on Planetary Surfaces by Gas Chromatography-Mass Spectrometry Techniques. Technical Report TR 32- , Jet Propulsion Laboratory.

117. Oyama, V. I.,: Mars Biological Analysis by Gas Chromatography. Proceedings of the Lunar and Planetary Exploration Colloquium. vol III, no. 2, May 5, 1963, pp. 29-36.

118. Corliss, W. R.: Space Probes and Planetary Exploration. Van Nostrand, New York, 1965, pp. 477-502.

119. Quimby, F. H., ed.: Concepts for Detection of Extraterrestrial Life. NASA SP-56, 1964.

120. Soffen, G. A.; and Sloan, R. K.: Life Detection by Visual Imaging. Paper presented at 12th Annual Meeting of AAS, "The Search for Extraterrestrial Life," Anaheim, California, May 23-25, 1966.

121. Loomis, A. A.: A Lunar and Planetary Petrography Experiment. Technical Report 32-785, Jet Propulsion Laboratory, Sep. 1, 1965.

122. Loomis, A. A.: Petrographic Microscope (Breadboard Development). Space Programs Summary 37-30, Vol. IV, Jet Propulsion Laboratory, Dec. 31, 1964, pp. 172-178.

123. Levin, G. V.; and Perez, G. R.: Life Detection by Means of Metabolic Experiments. Paper presented at 12th Annual Meeting of AAS. "The Search for Extraterrestrial Life," Anaheim, California, May 23-25, 1966.

124. Anon.: Space Measurement Survey, Instruments and Spacecraft. NASA SP-3028, Electro Optical Systems Inc, 1966, pp. 902-925.

125. Corliss, W.: Space Probes and Planetary Exploration. D. Van Nostrand Company, Inc, 1965, pp. 297-312.

126. Heyck, H. E.: Magnetometers, Direction and Attitude Sensors for Vehicular Use. RM-213, Martin Company, Baltimore, Maryland, Dec. 1961.

127. Bell, W. E.; and Bloom, A. L.: Optical Detection of Magnetic Resonance in Alkali Metal Vapor. Phys. Rev., vol. 107, 1957, pp. 1559-1565.

128. Bloom, A. L.: Optical Pumping. Scientific American, vol. 203, no. 4, Oct. 1960, pp. 72-80.

129. Smith, E. J.; Coleman, P. J., Jr.; Judge, D. L.; and Sonett, C. P.: Characteristics of the Extraterrestrial Current System: Explorer VI and Pioneer V. J. Geophys. Res., vol. 65, 1960, pp. 1858-1861.

130. Bloom, A. L.: Principles of Operation of the Rubidium Vapor Magnetometer. Applied Optics, vol. 1, Jan. 1962, pp. 61-68.

131. Ness, N. F., Searce, C. S.; and Seek, J. B.: Initial Results of the IMP-1 Magnetic Field Measurements. J. Geophys. Res., vol. 69, Sep. 1964, pp. 3531-3570.

132. Cahill, L. J., Jr.: A Study of the Outer Geomagnetic Field. IEEE Trans. Nucl. Sci, Vol. NS-10, Jul. 1963, pp. 10-19.

133. Heppner; Ness; Searce; and Skillman: J. Geophys. Res., vol. 68, Jan. 1, 1963, pp. 1-46.

134. Smith, E. J.; Davis, L., Jr.; Coleman, P. J., Jr.; and Jones, D. E.: Magnetic Field Measurements near Mars. Science, vol. 149, Sep. 10, 1965, pp. 1242-1243.

135. Schutz, F. L.; et al.: Mariner Science Subsystem. Technical Report 32-813, Jet Propulsion Laboratory, Aug. 15, 1966, pp. 45-57.

136. Barath, F. T.: Symposium on Radar and Radiometric Observations of Venus during the 1962 Conjunction. Astron. J., vol. 69, 1964, pp. 1-2.

137. Kaplan, L. D.: 1964: Recent Physical Data for Venus. NASA CR-56851, Jet Propulsion Laboratory, 1964.

138. Owen, R. B.: Theoretical Model Atmospheres of Venus. Proceedings of Institute of Environmental Sciences, Annual Technical Meetings, Chicago, Ill., Apr. 21-23, 1965, pp. 113-122.

139. Haurwitz, B.: Thermally Driven Circulation Beitr. Phys. Atm., vol. 35, 1962, pp. 145-159.

140. Mintz, Y.: The Energy Budget and Atmospheric Circulation on a Synchronously Rotating Planet. Icarus, vol. 1, 1962, pp. 172-173.

141. Ohring, G.; W. Tang; and J. Mariano: Planetary Meteorology. NASA CR-280. GCA Corporation, 1965.

142. Tang, W.: Meteorological Variables Critical to Geometry of Hurricane Spiral Bands. Technical Report 66-17-G. GCA Corporation, 1966.

143. Kuo, H. L.: Perturbation of Plane Couette Flow in Stratified Fluid and Origin of Cloud Streets. Phys Fluids, vol. 6, 1963, pp. 195-211.

144. Ash, M. E., et al.: Astronomical Constants and Planetary Emphenerides Deduced from Radar and Optical Observations. Astron. J., vol. 72, no. 3, 1967, pp. 338-350.

145. Anderson, J. D.: Determination of the Masses of the Moon and Venus and the A.U. from Radio Tracking Data of the Mariner II Spacecraft, Technical Report 32-816, Jet Propulsion Laboratory. Jul. 1, 1967.

146. Dyce, R. B. and Pettengill, G. H.: Radar Determination of the Rotations of Venus and Mercury. Astron. J., vol. 72, no. 3, 1967, pp. 351-359.

147. Carpenter, R. L.: Study of Venus by CW Radar. Astron. J., vol. 69, no. 1, 1964, pp. 2-11.

148. Goldstein, R. M.: Preliminary Venus Radar Results. J. Res. Natl. Bur. Stds., Radio Sci. vol. 69D, 1965, p. 1623.

149. Goldstein, R. M.: Radar Studies of Venus, COSPAR, Internatl. Space Sci, Symp., Vienna, May 1966.

150. Brereton, R. G., et al.: Venus: Preliminary Science Objectives and Experiments for Use in Advanced Mission Studies. EPD-328, Jet Propulsion Lab, 22 Dec. 1965.